Reconstructing Southeast Iberian Copper Age Mobility:

a strontium isotope analysis of the Camino del Molino mass burial

by © Courtney Merner A Thesis submitted to the School of Graduate Studies in partial fulfillment of the requirements for the degree of

Master of Arts

Department of Archaeology

Memorial University of Newfoundland

September 2017

St. John's Newfoundland

ABSTRACT

This study is the first application of strontium ($^{87}Sr/^{86}Sr$) isotope analysis to identify human mobility patterns during the southeast Iberian Copper Age (3100-2200 BCE). Human (n = 93) and faunal (n = 23) tooth enamel were sampled from the site of Camino del Molino (Caravaca de la Cruz, Murcia, Spain), a dense communal burial pit in continuous use during cal. 2800-2400 BCE. Results show twelve human individuals and two of the fauna, an ovicaprid and a canid, are likely migrants to the burial area, exhibiting $^{87}Sr/^{86}Sr$ values higher than the fauna-defined local biologically available Sr isotope range (0.7064-0.7107). The identified non-locals were all adults and included both females and males. These migrant individuals were found throughout the burial, however, the number of migrants were highest in the upper most levels. The local male population had a greater Sr isotope variation in comparison to the local female population, which supports a gendered division of mobility. Inter-site comparison within the Iberian Peninsula showed the local biologically available $^{87}Sr/^{86}Sr$ values at the sites La Pijotilla and Perdigões from the Ossa-Morena Zone had comparable $^{87}Sr/^{86}Sr$ ratios with the majority of non-local Camino del Molino individuals and, potentially, reflect a transhumant pastoral orbit between these two regions. The Sr isotope results endorse transhumance as an important economic practice at Camino del Molino. Overall, this research supports potential wide ranging networks between Iberian Copper Age communities.

ACKNOWLEDGEMENTS

I would like to first express my thanks to my two supervisors, Dr. Vaughan Grimes and Dr Domingo Carlos Salazar García, for their knowledge, motivational words, and most of all their patience. I would like to express my further gratitude to Dr. Grimes who assisted me every step of this process and taught me all the theories and techniques needed for this thesis to be successful. Domingo for always assisting me in knowledge and reports from Spain.

I am grateful for the generous funding for my graduate studies provided by the Graduate Students Union and Vaughan Grimes.

Rebecca Lam for her assistance with the MC-ICP-MS Neptune and allowing free reign over the lab. I apologize for constantly bombarding her collectors. Donna for use of the conservation lab and putting up with the continuous cutting of dental tissue.

The Camino del Molino research project. I am indebted to the professors and students of the Camino del Molino excavation team. Their meticulous work allowed this study to have appropriate and individualized samples from a large commingled mess. The excavating team, the supervising professors. As this is one part of a larger research goal, I would like to acknowledge the work of the other members and for all the archaeological and anthropological information provided about this site. Special thanks to Joaquín Lomba, María Haber, and Azucena Avilés

My deepest gratitude goes to my family, for their encouragement and supporting words. A tremendous thanks to my three fellow graduate students that helped to complete this thesis: Chelsea, Corina, and Hilary. Through encouraging words, comments, editing, or simply being a person to complain to, they helped me through this process and got me to the other side.

Table of Contents

ABSTRACT ii
ACKNOWLEDGEMENTS iii
Table of Contents v
List of Tables viii
List of Figures ix
List of Appendices xii

Chapter 1 - Introduction 1

Chapter 2 - Site Context: Southeast Spanish Copper Age and Camino del Molino 4
2.1 - Introduction 4
2.2 - The Study Region 5
    2.2.1 - The geology of Spain 7
2.3 - Southeast Spanish Copper Age 9
    2.3.1 - Neolithic 9
    2.3.2 - Copper Age 10
    2.3.3 - Bronze Age 13
2.4 - Camino del Molino 14
    2.4.1 - The burial site 14
    2.4.2 - The osteological record 16
    2.4.3 - Grave goods 20
    2.4.4 - Los Molinos de Papel 21
2.5 - Conclusion 23

Chapter 3 - Strontium Isotope Analysis in Studies of Human Mobility 24
3.1 - Introduction 24
3.2 - Strontium Isotopes 24
    3.2.1 - Strontium isotopes in geology 25
    3.2.2 - Strontium isotopes in the biosphere 26
3.3 - Strontium in Human Skeletal Tissue 27

3.3.1 - Bone ... 28
3.3.2 - Teeth ... 29
3.4 - Diagenesis ... 37
3.4.1 - Diagenesis in bone, dentine, and enamel ... 38
3.4.2 - Methods to identify diagenetic material ... 40
3.4.3 - Methods for removing diagenetic material ... 42
3.5 - Bioavailable Strontium ... 43
3.5.1 - Geology ... 43
3.5.2 - Determining the local bioavailable Sr ... 46
3.6 - Conclusion ... 45

Chapter 4 - Analytical Methods ... 49
4.1 - Introduction ... 49
4.2 - Sample Selection ... 49
4.2.1 - Human samples ... 49
4.2.2 - Sample material ... 52
4.2.3 - Faunal samples ... 52
4.3 - Strontium Isotope Analysis: Sample Preparation ... 53
4.3.1 - Human samples ... 53
4.3.2 - Faunal samples ... 54
4.4 - Strontium Chemical Preparation ... 55
4.5 - Strontium Isotope Measurement ... 56
4.6 - Conclusion ... 58

Chapter 5 - Strontium Isotope Results ... 59
5.1 - Introduction ... 59
5.2 - Strontium Isotope Results: Human ... 59
5.2.1 - Enamel Samples ... 59
5.2.2 - Diagenesis ... 64
5.3 - Establishing the Local Bioavailable Sr Limits ... 69
5.3.1 - Faunal Results ... 69
5.3.2 - $^{87}Sr/^{86}Sr$ range for Camino del Molino ... 72

5.3.3 - Concerns with the Camino del Molino local limit 75
5.4 - Conclusion 76

Chapter 6 - Discussion 77
6.1 - Introduction 77
6.2 - Human Mobility Patterns 77
6.2.1 - Sex-based patterns 77
6.2.2 - Age-specific patterns 81
6.2.3 - Temporal Trends 84
6.3 - Faunal Migration Patterns 87
6.4 - Non-Local Mobility 89
6.4.1 - Migrant Patterns 89
6.4.2 - Potential origins of the non-local individuals 91
6.4.3 - 'Local' male mobility 98
6.4.4 - A transhumance model for Camino del Molino mobility 103
6.5 - Conclusion 108

Chapter 7 - Conclusions 109
7.1 - Summary of Results 109
7.2 - Limitations of the Study 111
7.3 - Future Considerations 112

References 115
Appendix I 148

List of Tables

Chapter 3

Table 3.1. – Deciduous tooth denomination and mineralization timing 35

Table 3.2. – Permanent tooth demonination and mineralization timing 36

Chapter 4

Table 4.1. – Sample population age-at-death and sex demography 51

Chapter 5

Table 5.1. – Camino del Molino human enamel $^{87}Sr/^{86}Sr$ and Sr concentration results 60

Table 5.2. – Dentine $^{87}Sr/^{86}Sr$ ratio and Sr concentration results with enamel pairing 66

Table 5.3. – Faunal $^{87}Sr/^{86}Sr$ ratio and Sr concentration results 70

Table 5.4. – The identified non-local individuals 73

List of Figures

Chapter 2

Figure 2.1. – Map of southeast Spain, including major archaeological sites....................... 6

Figure 2.2. – Major components of Iberian geology 8

Figure 2.3. – Photograph of the Camino del Molino site during excavation 15

Figure 2.4. – The primary burial position at Camino del Molino 19

Figure 2.5. – Photograph of the articulated individuals next to the perimeter wall........... 19

Figure 2.6. – Photograph of the preservation of the crania on the perimeter wall 19

Chapter 3

Figure 3.1. – Premolar cross-section 30

Figure 3.2. – Geology underlying Camino del Molino and surrounding area 45

Chapter 5

Figure 5.1. – Human enamel $^{87}Sr/^{86}Sr$ and Sr concentration (ppm) results 63

Figure 5.2. – Histogram of enamel/dentine paired $^{87}Sr/^{86}Sr$ ratios 67

Figure 5.3. – Histogram of enamel/dentine paired Sr concentrations (ppm) 68

Figure 5.4. – Faunal $^{87}Sr/^{86}Sr$ ratio and Sr concentration (ppm) results 71

Figure 5.5. – Human enamel results with local limit 74

Chapter 6

Figure 6.1. – Human enamel $^{87}Sr/^{86}Sr$ results separated by sex 79

Figure 6.2. – Local human enamel $^{87}Sr/^{86}Sr$ restults separated by sex 80

Figure 6.3. – Human enamel $^{87}Sr/^{86}Sr$ results separated by age categories 83

Figure 6.4. – Human $^{87}Sr/^{86}Sr$ results separated by layer number 85

Figure 6.5. – Faunal $^{87}Sr/^{86}Sr$ results separated by species 88

Figure 6.6. – Geological map showing potential origins for the non-local individuals.....94

Figure 6.7. – Fauna and local human $^{87}Sr/^{86}Sr$ results separated by species and sex 100

List of Appendices

Appendix I Data Tables

Introduction

Migration is a dynamic, multilayered process that is fundamental to all human activity and affects how individuals, communities, and cultures spread, expand, and change (Anthony 1997; Burmeister 2000). Archaeologists use a variety of methods to identify and understand mobility, including artifact provenance, mortuary practices, grave goods, and historical documents. Starting in the late 1980s, biochemical analyses of skeletons were able to identify migrant individuals in burial populations. Ericson (1985) and Sealy (1989) were the first to apply strontium isotope analysis to answer questions on archaeological human migration practices. Strontium isotope analysis uses direct evidence from skeletal tissue to help determine if an individual is local to the area of their burial site or of non-local origin. Over the last 30 years, studies using strontium isotopes have demonstrated its utility in understanding the mobility patterns of humans and animals in the past (e.g. Bentley et al. 2003; Bentley et al. 2004; Britton et al. 2009; Evans et al. 2006; Knudson and Price 2007; Montgomery et al. 2000; Nehlich et al. 2009; Price et al. 1994a; Price et al. 1994b; Price et al. 2001; Price et al. 2004; Wright 2005).

The purpose of this thesis is to investigate the provenance and possible mobility patterns of the individuals interred at the Camino del Molino burial through strontium isotope analysis. It will be the first application of this analysis to investigate mobility at a southeast Iberian Copper Age site. Camino del Molino was a unique mass burial discovered in Caravaca de la Cruz (Murcia, Spain) and excavated in a salvage operation. The burial contained approximately 1300 individuals and was in use from the mid- to late-Copper Age (cal. 2800-2400 BCE). Studies of movement during the Copper Age in southeast Iberia have focused on the provenance of copper metallurgy, pottery shards, and grave goods. However, these particular approaches only provide indirect evidence of human mobility and cannot assess movement on an individual human scale.

This study's primary aim is to establish if non-local individuals can be identified at Camino del Molino. Furthermore, as this is the first strontium isotope analysis of a southeast Iberian Copper Age population, it will serve as a base study to build an understanding of mobility within this region. Consequently, the main questions this thesis aims to answer are as follows. How mobile were the individuals interred at Camino del Molino? What are the demographic and temporal based mobility patterns within the sample population? Where are the potential origins of those non-local individuals? What does this mobility signify for the social and economic interpretations of Camino del Molino and the southeast Iberian region?

This thesis is organized into seven chapters. Chapter two provides the archaeological background to establish the cultural context for this study. It presents a concise history of the southeast Iberian Neolithic, Copper Age, and Bronze Age as well as a summary of the region's climate and geology. Then, an overview of the study site of Camino del Molino, including the osteological material, grave goods, and information on the associated settlement site of Los Molinos de Papel is given. Chapter three provides a theoretical background of the approach to strontium isotope analysis and how strontium is used as a correlate for human mobility. There is a brief summary of the natural strontium isotope variation within geology and how this variation transitions into the biosphere, eventually becoming part of human skeletal tissue. The chapter will also further describe the geological substrate underlying Camino del Molino and the expected local Sr isotope signature for the area. Additionally, the problems and limitations associated with this analysis will be discussed. Chapter four outlines the specific analytical techniques employed to obtain strontium isotope values for the human and faunal remains. This includes the sample selection process, mechanical and chemical preparation of the tissue, and the isotope ratio measurement from the mass spectrometer. Chapter five presents the results of this isotopic analysis. It establishes a local strontium isotope range for the Camino del Molino site using the faunal isotope results and identifies the non-local individuals. Chapter six interprets the strontium isotope results of the identified non-local and local individuals to discern mobility patterns within the data. This chapter also discusses faunal mobility, the potential origins for the non-local individuals, and the implications this movement might have had on the broader cultural framework of the Iberian Peninsula Copper Age. Chapter seven summarizes the conclusions of this study and provides considerations for future research on mobility during the southeast Iberian Copper Age.

Site Context: Southeast Iberian Copper Age and Camino del Molino

2.1 Introduction

The region of southeast Spain has a long tradition of archaeological research that began in the 1880s with the work of Louis and Henri Siret (1887). The Siret brothers focused much of their research on metals and grave goods of southeast Spanish archaeology. The richness and often foreign origin of the grave goods in the region were theorized to be an indication of a wide-reaching, stratified society (Chapman 1990). Therefore, it was considered one of the key regions in the West Mediterranean for understanding the emergence of cultures with greater social complexity (Chapman 1990, 2003). However, the sites and, in particular, the graves excavated by the Sirets' and their contemporaries were not done with anthropological supervision and much of the contextual information concerning the osteology and funerary practices was lost (Díaz-Zorita Bonilla et al. 2012). More recent fieldwork has focused on the stratigraphic excavations of major sites, such as El Malagón (Arribas et al. 1974; de la Torre and Sáez 1986), Cerro de la Encina (Arribas et al. 1974), Los Millares (Almagro Basch and Arribas 1963; Gilman 1987), and Almizaraque (Almagro Gorbea 1973; Micó 1991) (Figure 2.1).

This chapter presents the geological and archaeological context for the burial site of Camino del Molino. A brief summary focused on southeast Spain's development during the Neolithic, Copper, and Bronze Ages provides information of common cultural, economic, and funerary practices. Studies of the movement and trade of goods has been a focus for this region and provides indirect evidence of human mobility practices (Chapman 1990, 2008).

2.2 The Study Region

Southeast Iberia refers to the coastal lowlands of the modern provinces of Almería and Murcia, as well as part of eastern Granada (Chapman 2008; Gilman and Thornes 1985) (Figure 2.1). The region has a typical Mediterranean climate with warm, dry summers in June-September and mild, wet winters (Gilman and Thornes 1985). The lowland coastal areas are the most arid with low, unpredictable precipitation (less than 400 mm annually on average) and high evapotranspiration rates. Low scrubland vegetation including thorny scrubs, esparto grass, and aromatic shrubs (i.e. rosemary) dominate the landscape and become denser further inland within less arid, mountainous areas. The climate of southeast Spain has remained stable over the past 6000 years allowing current environmental conditions and vegetation patterns to be used in prehistoric reconstructions of the area (Gilman and Thornes 1985).

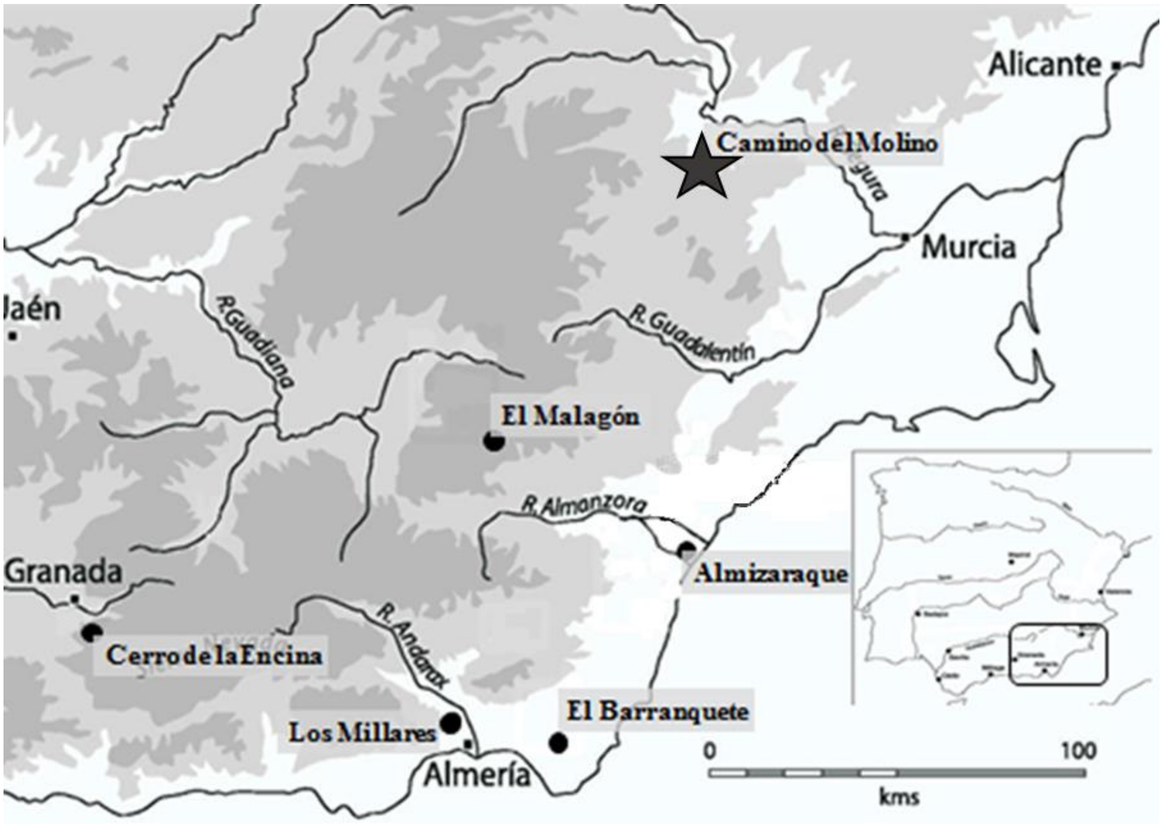

Figure 2.1 Simplified map of major southeast Spanish Copper Age archaeological sites: Cerro de la Encina (Arribas et al. 1974), Los Millares (Almagro Basch and Arribas 1963; Gilman 1987), El Barranquete (Almagro Gorbea 1973; Micó 1993), Almizaraque (Almagro Gorbea 1973; Micó 1991), and El Malagón (Arribas et al. 1974; de la Torre and Saez 1986). The map also shows the study site, Camino del Molino (Lomba et al. 2009), indicated by a star.
Adapted from Chapman 2003

2.2.1 The geology of southeast Iberia

Southeast Iberia is dominated by the Betic Cordillera geological formation just south of the Iberian Massif (Gibbons and Moreno 2002) (Figure 2.2). The Betic Cordillera is the westernmost section of the European Alpine Belt and forms an arc shaped mountain range connected to the Rif Cordillera in Africa through the Straits of Gilbraltar. The Betic Cordillera began its formation in the Mesozoic Era (252-66 Ma) and consists of four main areas: the Guadalquivir River Basin, the flysch unit of the Gibraltar, the Internal Betics on the coast, and inland External Betics (Sanz de Galdeado 2000). The majority of southeast Spanish Copper Age sites, including the site in this study, are located on the Internal and External Betics Zone.

The Betic Cordillera formed in part as a reaction to both the extension and then convergence of Iberia and Africa (Gibbons and Moreno 2002; Sanz de Galbreado 2000). During the Triassic (252-200 Ma), the Iberian plate began moving eastward as a result of the western Mediterranean extending and forming oceanic crust, gradually opening the area to the Atlantic Ocean and displacing the African plate to the east (Sanz de Galdeano 2000). In the Cretaceous (145-66 Ma), this opening eventually caused the Iberian plate to rotate anticlockwise and begin convergence with the northern part of the African plate. The area of the Internal Betics was separated from both plates during the first convergence, which created a passive margin between itself and the Iberian plate. A

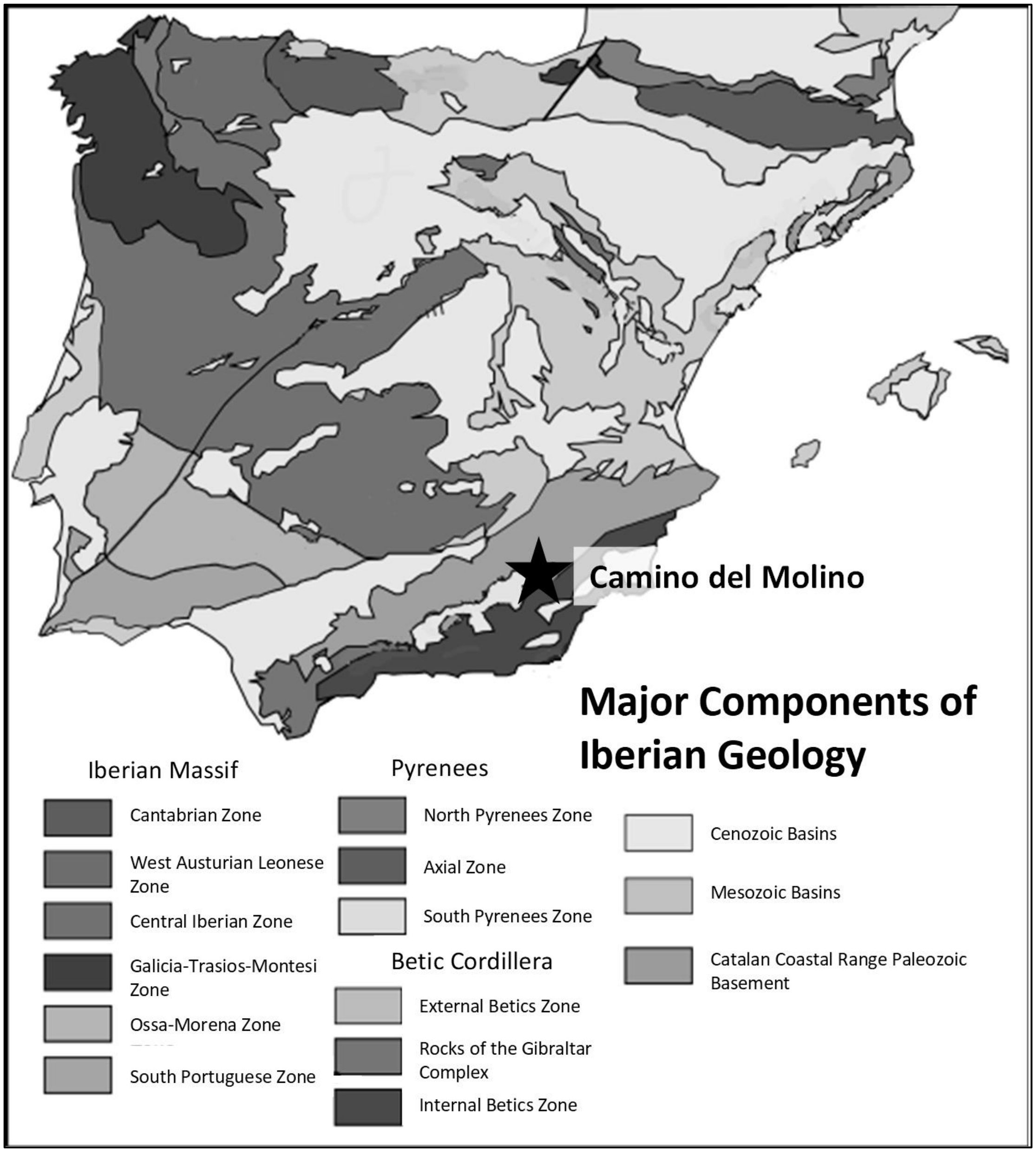

Figure 2.2 Simplified geology map of the Iberian Peninsula showing the major components and age of the geology. The study site, Camino del Molino, is indicated by the star.
Adapted from Vera 2004

passive margin is a place of transition between the continental and oceanic crust formed by the deposition of sedimentation (Gibbons and Moreno 2002). Subsequent compression events, especially during the Neogene (23.03-2.588 Ma), joined the Internal Betics with the Iberian Massif, folding the passive margin between them into what is now known as the External Betics. Despite a more recent formation, the External Betic is comprised of Mesozoic age sedimentation deposited through the passive margin and gradually formed sedimentary rock. Both the Internal and External zones are primarily comprised of Triassic-Miocene sedimentary rocks, including limestone, marlstone, lutite, and sandstone (Aguirre et al. 2007; Geel et al. 1992; Martín et al. 2009).

2.3 Southeast Spanish Copper Age

The chronology of southeast Spain since the arrival of farming communities is traditionally divided into three periods based on technological and social changes: Neolithic (5600-3200 BCE), Copper Age (3200-2250 BCE), and Early Bronze Age (or El Argar culture) (2250-1550 BCE). Although, this current chronological framework is not fixed between the Neolithic and Copper Age periods. This section summarizes the major characteristics of each period and the common burial practices. An emphasis is placed on the Copper Age, rather than the Neolithic or El Argar, as the site examined in this study, Camino del Molino, was in use during this time period.

2.3.1 Neolithic

The Neolithic of southeast Spain (c. 5600-3200 BCE) is commonly characterized by small, ephemeral sites of a highly mobile population (Chapman 1990). Archaeological surveys of the southeast area show a low density of Neolithic sites, approximately 1 per 165 km^2, and provide little evidence of standing structures or agricultural production (Chapman 2008). Similarly, there is scarce information concerning Neolithic burial practices (Díaz-Zorita et al. 2012; García Sanjuán 2009). The known burial sites are communal and located in extra-mural stone tombs or natural caves. The stone tombs mark the first known appearance of the megalithic tomb funerary practice in southeast Spain (Leisner and Leisner 1943). The scarcity of modern excavations of Neolithic grave sites makes it difficult to infer common funerary practices or demographic information during this time period. Grave sites that have been excavated and dated include Cerro Virtud (Montero Ruiz et al. 1999), Cueva de Nerja (Aura et al. 2006; Jordá and Aura 2008), and Cueva de Murciélagos de Alnuñol (Cacho et al. 1996). Overall, the Neolithic has not been as well-researched and few larger-scale excavations or artifact analyses have been undertaken to provide more accurate data on the mobility patterns, agricultural production, and social relations during this period (Chapman 2008).

2.3.2 Copper Age

The archaeological record of the Iberian Copper Age is more clearly defined than the Neolithic. The transition to the Copper Age is seen through increases in settlement size, the production of copper metallurgy and an intensification of labour investment in the construction of domestic structures, megalithic tombs, and site fortifications (Chapman 1990, 2008). Major Copper Age sites that have contributed to the knowledge of this time period include La Pijotilla (Hurtado et al. 2000), El Malagón (Arribas et al. 1974; de la Torre and Saez 1986), El Barranquete (Almagro Gorbea 1973; Micó 1993), and Los Millares (Almagro Basch and Arribas 1963; Gilman 1987) (Figure 2.1). Radiocarbon dates from these main sites and graves define this period from cal. 3200-2250 BCE.

The number of sites known through both survey and excavation increase significantly during the Copper Age in southeast Spain. Settlements established during this period are generally small at less than one hectare. However, Las Pilas and Los Millares increased greatly in size during the Copper Age, eventually spreading out over five hectares. Many of these Copper Age sites were fortified with enclosing stone walls, external defense forts, and gated entrances (Esquivel and Navas 2007; Molina and Cámara 2002). The extra-mural megalithic tombs were built larger and more complex than during the Neolithic, including false corbelling over the main chambers and added side chambers. Inside the enclosing walls, dome shaped domestic structures were built with stone foundations and timber superstructures. This rise in the number and size of settlements as well as the increase of labour invested into the site structures has been interpreted as evidence of a more sedentary population (Chapman 1990).

There is also evidence for agricultural production at the Copper Age sites based on the presence of domesticated wheat, barley, and legume species (Delibes et al. 1986). Barley, a drought tolerant crop, is the most frequent seed found in excavated storage pits. Instruments of agricultural production such as grinding stones, stone axes and adzes, flint items and storage pots, are also found (Almagro Basch and Arribas 1963; Gilman 1987).

Faunal studies show evidence of animal husbandry of cow, goat and sheep species, which were used for both primary and secondary products (Chapman 1990).

Copper metallurgy increased during this period in southeast Spain and evidence of copper working areas can be found within settlement sites. Surveys of the region place over half of the Copper Age sites within 10 km of a copper deposit (Chapman 2003). Trace element analyses of copper artifacts have found them to be manufactured from locally mined ore, often from a settlement’s closest copper source (Montero 1993). The most common copper artifacts found are axes, awls, saws, chisels, and knives.

Burial and funeral practices have been integral to the understanding of trade networks and social relations during this time period. Copper Age burials are most commonly found in artificial pits and megalithic tombs (Díaz-Zorita et al. 2012). These burials are communal and rarely contain more than fifty individuals. The interred were often repositioned after their initial interment, usually to be relocated to the sides of the pit or tomb chamber walls. The demographic profile of the graves is shown to be generally representative of the population and do not appear to be exclusive based on age or sex of the individuals. However, the extra-mural megalithic tombs at Los Millares are believed to represent kinship groups within the settlement’s population (Chapman 1981, 1990). Proximity to the settlement site, the increase of labour investment put into the tomb structure, and the richness of the grave goods are thought to be indicators of higher ranked kinship groups at Los Millares (Mathers 1984; Chapman 2003). Commonly excavated grave goods in Copper Age communal burials include pottery vessels, copper awls, flint blades and arrowheads, as well as more ornamental objects, such as beads and figurines. Prestige grave goods were often of foreign origin, including ivory and ostrich eggshell from North Africa, jet from Sierra Morena in southern Spain, and chlorite from northeast or northwest Spain (Harrison and Orozco-Kohler 2001). During the later Copper Age, the Beaker material assemblage was introduced to the southeast Spanish region and is commonly found in burial contexts as prestige grave goods (Harrison 1977). The Beaker material culture consists mainly of decorated pottery and styled lithics. This assemblage is found throughout the Iberian Peninsula, England, and the European continent during the late Copper Age and early Bronze Age.

At the end of Copper Age (~2400-2200 BCE), there is evidence of increased fortifications being constructed and a preference to building new structures on more easily defendable locations, such as hilltops (Chapman 2003). It has been inferred that there was an increase of social tension and, potentially, physical conflict in the region. Almost all of the Copper Age settlements were razed or abandoned during the transition to the Bronze Age.

2.3.3 Bronze Age

The transition to the Bronze Age marks a distinct change in the architecture, material culture, and mortuary practices of the southeast Spanish region (Chapman 2003, 2008). It has been hypothesized that this cultural shift was provoked by a foreign culture entering and, possibly, invading the region. The Copper Age settlements were deserted and the area’s population nucleated at new sites. The domestic structures at these new sites were built rectangular instead of circular. Communal burial practices were abandoned in favour of individual interments underneath these domestic structures. The individual burials contained personal items symbolic of one's wealth as well as gendered grave goods. For example, females were buried with awls and daggers, while males are found with halberds, swords, and axes. The Bronze Age also brought standardization in the production of pottery and metal goods, highlighting the regional homogeneity. As expected, there was also a great increase in the manufacture of bronze weapons: halberds, knives, axes, spears, and arrowheads. Many archaeologists believe that these changes of social and production inequalities represent an early state society (Aranda and Molina 2006; Cámara 2001; Chapman 2003; Lull 2000).

2.4 Camino del Molino

2.4.1 The burial site

Camino del Molino is a Copper Age communal burial found in the city of Caravaca de la Cruz, Murcia, southeast Spain (Figure 2.1). The site was discovered during the construction of a modern building and excavated from February to November 2008 in a salvage operation. It is a dense burial pit, roughly 2 m deep, which contained a minimum of 1300 individuals representing a broad demographic profile. Radiocarbon dates from twenty-one bone collagen samples spanning the burial sequence determined that the site was continuously in use from cal. 2800-2400 BCE or the mid-late Copper Age (Lomba et al. 2009).

Figure 2.3 Photograph of the Camino del Molino site during excavation. The dotted line shows the original size and shape of the burial. (Lomba et al. 2009).

The Camino del Molino burial is defined by a bell-shaped cavity with a 7 m circular base (Lomba et al. 2009) (Figure 2.3). The pit is a natural hollow approximately 4 m deep, however, the burial is only found within the lower 2 m. There are clear human modifications to the ground surface and the walls of the cavity. The base had a thin layer (1-2 cm) of spread yellow clay, followed by a layer of charcoal (1-2 cm) upon which ceramic fragments were placed horizontally to make the floor of the burial. The walls were modified in various sections to standardize the natural shape of the cavity and perforated to support an interior structure. The top half of the site was destroyed in the early twentieth century as a result of agricultural terracing but the damage was limited to the upper portion of the cavity, affecting the cover of the burial but not the deposit itself. Within this damaged portion of the cavity, it is believed there was a 2-3 m opening at the top of the cavity where the walls converged. This opening is thought to have been the only access point to the burial based on the natural morphology of the cavity and the placement pattern of the interred.

2.4.2 The osteological analysis of Camino del Molino

The site contained a minimum of 1300 individuals; approximately 30% of the individuals interred are juvenile (under the age of nineteen with mostly undetermined sex), while the remainder are both females and males of all age categories (Lomba et al. 2009). The interred at Camino del Molino were subject to a pattern of repositioning that created a complex skeletal arrangement within the pit. This pattern began by the primary placement of the individual onto the pit bottom alongside the perimeter wall, most often on their side in a flexed position with arms crossed over their chests (Figure 2.4). After a period of time (or coinciding with subsequent burials) the individual was moved towards the center of the pit. The relocated remains were arranged in no apparent order and the majority of the pit's center contained highly fragmented skeletons with little or no anatomical connection (Figure 2.5). The bodies were most likely only partially decomposed during the repositioning because some still maintained partial joint articulation and, in a few cases, are complete skeletons. Only 175 individuals were found fully articulated, the majority of them were the primary and final interments. Repositioning the interred is a common Copper Age burial practice but the movement of bodies to the center rather than the cavity wall is less customary (Díaz-Zorita et al. 2012).

In contrast to the appendicular skeleton, most of the crania were not relocated to the center but, instead, they were placed next to the perimeter walls (Figure 2.6). Lomba et al. (2009) hypothesized that this intentional placement of the crania was to protect them from environmental damage caused by the overhead entrance, which would allow rainwater and sediment to collect in the center during the wet season. This practice of cranial repositioning is not exclusive to Camino del Molino and is also found in the tombs of the Copper Age site El Barranquete (Almagro Gorbea 1973). The majority of the megalithic tombs at El Barranquete display the same pattern of cranial placement against the walls, most notably in Tomb 7 (Almagro Gorbea 1973: 249, *Plano XXIII*). However, there is no evidence of flood damage in the tombs of El Barranquete. Therefore, this particular cranial rearrangement may not be just for protection against nature but also a deliberate symbolic burial practice.

The skeletal repositioning pattern continued throughout the use of the site, altering during its final phase where the level contained unmoved, fully articulated individuals. The intra-tomb movement did cause a significant amount of damage to the interred skeletal remains, particularly those in the center of the pit. However, it allowed for the continual deposition of individuals from the settlement, maintaining a link between the living, the newly deceased and the community's ancestors.

In addition to the anthropological record at Camino del Molino, there were at least fifty canid skeletons found as well as isolated remains of ovicaprids, rabbits, rats/mice, lizards, and pigs. The fauna were subject to the same perimeter-to-center repositioning pattern and were found dispersed throughout the burial sequence. This does not suggest all the fauna movement was on purpose and part of the funerary practice; some of the animals, such as the rats and mice, may have entered accidently. However, the majority of the canid skeletons were found fully articulated despite being relocated within the pit. Burial practices incorporating dogs are present in southeast Spain but are generally found in repurposed storage pits of individual or double canid interments (Díaz-Zorita et al. 2012; Lomba et al. 2009). The presence of dogs within a Copper Age burial site has been interpreted as evidence of animal husbandry or shepherding, an activity that was developed during this time period and which later became a notable economic activity during the Bronze Age (Chapman 1990; Lomba et al. 2009). Canids present in the Camino del Molino burial may indicate the value of this type of economic activity within the surrounding Copper Age community and their inclusion in the tomb could be viewed

Figure 2.4 The primary burial position at Camino del Molino was flexed on their side with arms crossed over the chest.
Photograph courtesy of Joaquin Lomba

Figure 2.5 This photograph shows the articulated individuals located next to the perimeter wall and, as one moves further towards the center of the pit, the remains become unarticulated.
Photograph courtesy of Joaquin Lomba

Figure 2.6 This photograph shows the preservation of the crania on the perimeter wall.
Photograph courtesy of Joaquin Lomba

as a prestige grave good, a personal item, or a symbolic object related to their belief system.

2.4.3 Grave goods

In comparison to other Copper Age communal burials in the region, Camino del Molino contained a low number of grave goods (Lomba et al. 2009). The grave goods followed the same perimeter-to-center movement pattern, making it difficult to discern if an individual was interred with personal items and, if so, which item(s) belonged to which individual(s). Some of the artifacts found that could be personal items include various necklaces, beads, copper punches, and a large flint blade approximately 32 cm in length. Other grave goods identified within the burial were various bone and flint tools, five polished axes, sixty arrowheads, and approximately 200 ceramic vessels.

The majority of the ceramics present were highly fragmented, most likely as a result of the skeletal rearrangement. Among the vessels there was only one decorated ceramic piece, a cup with horizontal incised chevrons and the ocular design of Los Millares. There were several keeled pieces located in the final levels of the burial and are traditionally considered part of the Bronze Age material assemblage, although they can be found in sites from the late Copper Age. The fragmentary flint daggers, blades, scrapers, and flakes are common funerary items in the Murcia region, especially during the late Copper Age, and are believed to have been sourced from the Archivel area west of the site or from Jumilla to the east (Lomba et al. 2009). The flint items also included various tips from concave blades of the Beaker material assemblage found in the final layer of the site.

While the mass extra-mural funerary practice at Camino del Molino was common in this region during the Copper Age, the high number of individuals buried at the site is beyond comparison (Lomba et al. 2009). The closest example on the Iberian Peninsula is the early Copper Age site of San Juan Ante Portam Latinam in the Basque Country where 338 individuals were interred (Vegas 2007). During this period in southeast Iberia, the number of individuals in these communal burials rarely reached over one hundred and was more often less than fifty (Chapman 1990; Díaz-Zorita et al. 2012; Lomba et al. 2009). Furthermore, neither the high number of interred nor the demographic profile of the site follow the interpretation that these communal tombs signified membership to a kin group. As such, Camino del Molino did not represent a select familial group, but rather could be the majority of the inhabitants from an adjacent village site, such as Los Molinos de Papel.

2.4.4 Los Molinos de Papel

Los Molinos de Papel is located approximately 400 m away from Camino del Molino and was partially excavated from September 1999-August 2000 as part of an urban expansion (Martínez 2005). Based on the dates from the stratigraphy and ceramic typology analysis, this settlement was active from the Final Neolithic into the late Copper Age. The site was comprised mainly of stone-based circular houses and many agricultural storage pits. Artifacts from the domestic structures include various ceramics, awls, ivory objects, sickle teeth, scrapers, stone mills, and a weighted loom. Most of these items are typical for a southeast Spanish Copper Age site and are comparable to those found at Camino del Molino (Chapman 1990; Lomba et al. 2009; Martínez 2005). There is also a high frequency of well-developed blades and arrowheads that are thought to be evidence of a small lithic industry at Los Molinos de Papel.

Los Molinos de Papel also contained two double burials dated to the late Copper Age (Martínez 2005). Burial I was a double interment found inside a storage pit near one of the houses. Both individuals were buried in the fetal position with personal items: a bone button with an incised "V" found along the shoulder blades of one individual and a Palmela copper arrow between both skeletons. Burial II was found in a pit beneath one of the houses and was also a double burial. However, the preservation of the skeletons was poor due to the strong acidity of the soil. These individuals were also interred in the fetal position and found with two artifacts: a silver ring and a bone button. Lacking absolute dates from these two burials and without a clear chrono-archaeological attribution, it is unknown whether the Camino del Molino site was still in use when these individuals were buried. If the site was in use, it is not clear why these individuals were buried at the settlement site instead of the communal tomb at Camino del Molino.

During the late Copper Age, the village was razed and abandoned (Martínez 2005). Also around the same time (~2400 BCE), the Camino del Molino burial was closed and the final interments remained fully articulated and unmoved (Lomba et al.

2009). This follows the pattern of destruction and desertion occurring throughout southeast Spain in the transition to the Bronze Age.

2.5 Conclusion

Based on the archaeological evidence of both Camino del Molino and other Copper Age sites in southeast Spain, we know that large exchange networks existed within and beyond the region. Studies of the material assemblages show that objects were very mobile and originated from various places on the Iberian Peninsula and even from North Africa. Less information is known of the mobility of humans during this time period in southeast Spain (Chapman 2008). The aim of this study is to use direct evidence from the bone chemistry of the individuals interred at Camino del Molino to examine human mobility patterns. Strontium isotope analyses were carried out on a sub sample of the skeletal remains recovered from the Camino del Molino site to identify possible migrant individuals. The strontium isotope approach to mobility research and how was it used in this study is discussed in Chapter 3.

Strontium Isotope Analysis in Studies of Human Mobility

3.1 Introduction

Archaeological mobility studies of the southeast Spanish Copper Age have focused on analyses of artifact assemblages and the movement of material goods. Assessing mobility patterns through strontium (Sr) isotope analyses of human skeletal tissue is a more direct approach that has rendered successful results in archaeology (e.g. Bentley et al. 2003; Bentley et al. 2004; Evans et al. 2006; Knudson and Price 2007; Montgomery et al. 2000; Nehlich et al. 2009; Price et al. 1994a; Price et al. 1994b; Wright 2005). Strontium isotopes were first used by Sealy (1989) and Ericson (1985) to answer questions concerning an individual's geographic origin. Since then, strontium isotopes have been a frequently used tool to identify past human and faunal mobility patterns. This chapter explains how strontium isotope ratios are used to identify local and non-local individuals at the site of Camino del Molino. It will provide an understanding of the basic principles behind strontium isotope ratios, their natural variation within geology, and how they become incorporated into human skeletal tissues. Additionally, the chapter will discuss the problems and limitations associated with strontium isotope analysis and how they will be addressed for this study.

3.2 Strontium Isotopes

Strontium (Sr) is an alkaline earth metal (atomic number 38) and has four naturally occurring isotopes with different abundances: ^{84}Sr (0.56%), ^{86}Sr (9.87%), ^{87}Sr

(7.04%), and ^{88}Sr (82.53%) (Capo et al. 1998; Faure 2005). ^{84}Sr, ^{86}Sr, and ^{88}Sr are stable and their abundances do not vary over time. The proportion of ^{87}Sr does continually increase through the radioactive decay of rubidium-87 (^{87}Rb). This decay occurs at an extremely slow rate (^{87}Rb has a half-life of approximately 48.8 billion years) and allows the radioactive isotope ^{87}Sr to be regarded as stable in archaeological studies (Faure 2005; Pollard et al. 2007). The procedure in Sr isotope analysis is to measure ^{87}Sr relative to ^{86}Sr, denoted as the ratio $^{87}Sr/^{86}Sr$. These two isotopes are similar in abundance and atomic mass, thereby reducing measurement errors (Faure 2005).

3.2.1 Strontium isotopes in geology

The $^{87}Sr/^{86}Sr$ isotope ratio in geology is affected by two main factors: the initial composition of the rock and its age (Beard and Johnson 2000; Bentley 2006; Capo et al. 1998; Ericson 1985; Miller et al. 1993; Faure 2005; Montgomery 2002). Rocks composed of minerals abundant in Rb, such as granite, are more enriched in radiogenic ^{87}Sr due to the constant decay of ^{87}Rb. Newly formed rocks will have low $^{87}Sr/^{86}Sr$ isotope ratios because there simply has not been sufficient time for the decay of ^{87}Rb. Generally, geology $^{87}Sr/^{86}Sr$ values range from 0.703 in young, volcanic rock to 0.740 within older, crustal rocks. Sr ratios can also be affected by post-formation alterations, such as metamorphic activity and fluid-mineral interaction that change the amount of strontium or rubidium within the rock.

3.2.2 Strontium isotopes in the biosphere

Strontium isotopes are released from the geological substrate into the environment through weathering (Bentley 2006; Faure 2005). The strontium isotopic signature of an area will *reflect* the geological substrate Sr values but will not be an *exact replication* of them. A local area will contain a wide range of $^{87}Sr/^{86}Sr$ values and Sr concentrations as a result of diverse geology and differential weathering rates.

The Sr isotopic signature of a local area can be further modified through the incorporation of non-local Sr source(s) (Åberg 1995; Andersson et al. 1990; Bacon and Bain 1995; Bentley 2006; Blum et al. 2000; Capo et al. 1998; Land et al. 2000; Miller et al. 1993). Surface waters, precipitation, and wind-blown dust contain strontium from different geological substrates that mix with the local Sr signature. Strontium isotopes from rivers generally have a high $^{87}Sr/^{86}Sr$ as a result of weathering and erosion of the more radiogenic, crustal rocks of the continents (Capo et al. 1998; Graustein 1989; Wadleigh et al. 1985). The varying Sr isotope ratios from rivers enter the ocean, effectively being mixed and homogenized by ocean currents and the long residence time of Sr (~20 million years) (Åberg 1995). The ocean Sr isotope ratio has remained constant at 0.7092 during the Holocene (the last 10,000 years) but has varied between 0.707-0.709 during the Paleozoic, Mesozoic, and Cenozoic eras (Bentley 2006; Faure 2005; White et al. 2007). Coastal terrestrial environments can be affected by the contribution of strontium from sea spray and rainwater modifying the geological Sr isotopic value to reflect the current $^{87}Sr/^{86}Sr$ seawater ratio of 0.7092 (Bentley 2006; Hartman & Richards 2014).

Strontium released from soil, water, and atmospheric sources are incorporated into both flora and fauna when it substitutes for calcium (Ca) (Blum et al. 2000; Elias et al. 1982). Plants contain high concentrations of Sr for use in cell wall development. These plants are ingested by animals and the Sr isotopes are integrated into the organism's skeletal structure. The isotopic composition of strontium, as it moves through the food chain, is not altered by biological processes or by changes in trophic level, and reflects the $^{87}Sr/^{86}Sr$ signature within the local geology where the food originated (Beard and Johnson 2000; Bentley 2006; Blum et al. 2000; Capo et al. 1998; Graustein 1989; Miller et al. 1993). Strontium concentrations are, however, generally higher in herbivores because plants contain more strontium than meat (Bocherens et al. 1994; Tuross et al. 1989). The Sr isotopes within the local flora and fauna represent the biologically available Sr from the area's geological substrate (Bentley 2006; Price et al. 2002; Schwarcz et al. 2010).

3.3 Strontium in Human Skeletal Tissue

Humans obtain trace amounts of strontium primarily from their diet and should have a Sr signature characteristic of the bedrock, soil, and water in which their food items were living (Bentley 2006; Bentley et al. 2004; Capo et al. 1998; Price et al. 2002). The majority of the Sr in the human body is found in the skeletal tissues of bone and teeth (Underwood and Mertz 1977). Strontium is incorporated into the skeletal tissue by replacing Ca in the carbonated hydroxyapatite [(**Ca,Sr**)$_5$(PO_4,CO_3)$_3$(OH)] (Boivin et al. 1996; Brudevold and Söremark 1967; Capo et al. 1998). Carbonated hydroxyapatite is also known as biogenic apatite because it is found almost exclusively in skeletal tissue. Bone, dentine, and enamel mineralize at different stages in life and reflect the local geological ^{87}Sr/^{86}Sr ratio during these periods of formation, mineralization, and remodelling. The Sr uptake and turnover processes between the skeletal tissues of bone, dentine, and enamel differ greatly. Understanding the formation, mineralization, and remodelling processes of each of these skeletal tissues are essential to selecting an appropriate material for analysing and interpreting Sr isotope data.

3.3.1 Bone

Bone in humans begins to form in utero and continuously remodels throughout an individual's lifetime. Strontium is homogeneously distributed into bioapatite structure of bone tissue during formation and subsequent remodelling. Bone does not have a defined chronological pattern of remodelling and turnover rates are highly variable between individual bones, the type of bone, and the age of the individual. In infants and children, bone turnover can exceed 100% per year as a result of growth spurts (Aufderheide and Wittmers 1992; Stamoulis et al. 1999). The turnover of old bone tissue results in the removal of the bioapatite and the previously incorporated strontium isotopes (Priest and Van de Vyver 1990). Consequently, bone tissue does not maintain the Sr signature obtained during its initial formation and instead records a composite of Sr isotopes that could reflect one or multiple geological residences.

The great individual variability in bone remodelling rates, and a lack of clear-cut remodelling chronology, means unconnected movement events or multiple migrations between geological regions and their corresponding Sr signatures would be amalgamated, and, therefore, indistinguishable from one another. As a result, bone tissue is not suitable sample material for strontium isotope studies of mobility patterns (see section 3.4 Diagenesis). Therefore, despite the availability of bone from the Camino del Molino site, no strontium isotope analyses of bone tissue were attempted in this study.

3.3.2 Teeth

Teeth are the most durable part of the human skeleton and can potentially provide extensive biological information on an individual, including age at death, ancestry, diet, and health. Human teeth are formed and begin mineralization within the mandible and maxilla bones during gestation (Hillson 2005). It is during this mineralization that strontium isotopes become incorporated into the hydroxyapatite structure of dental tissue. Teeth are composed of four tissues: enamel, dentine, pulp, and cementum (Figure 3.1). A layer of enamel covers and protects the crown – the visible part of the tooth that erupts through the gum tissue. Below the gums, the tooth root is covered by cementum and attaches to the alveolar bone within the mandible and maxilla. Dentine composes the majority of the tooth core and surrounds the pulp chamber. Pulp tissue within that chamber connects the tooth to the bloodstream and nervous system. Strontium isotope

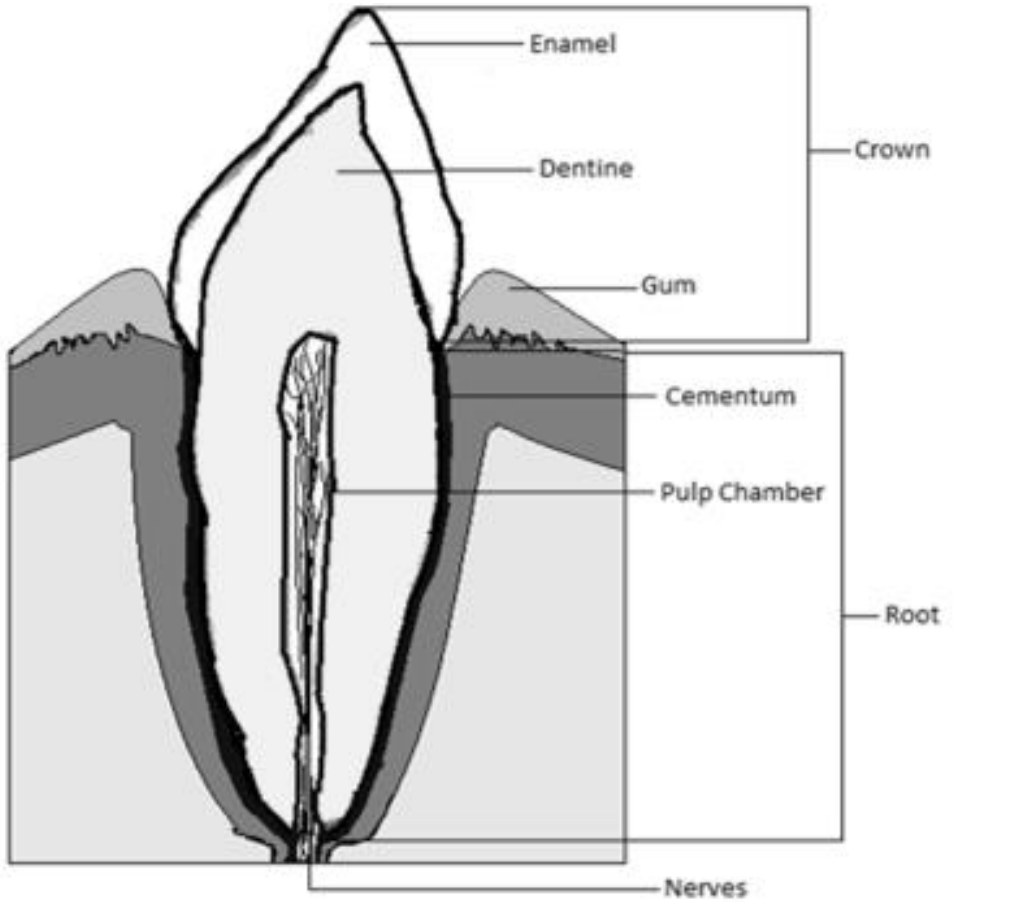

Figure 3.1 Longitudinal cross section of a human pre-molar with anatomical terms.
Adapted from Hillson 2005 and drawn by Author

studies have often focused on enamel and dentine tissue in their analyses because of their physical and chemical formation processes.

The tooth crown is covered by a layer of enamel, the hardest and most mineralized tissue in the human body (Hillson 2005; Fincham et al. 1999; Mann 1997). It has < 3% organic material and, unlike other skeletal tissues, does not contain collagen. Enamel is formed by two unique proteins, amelogenin and enamelin, secreted by specialized cells, called ameloblasts (Hillson 2005). Its formation and mineralization, called amelogenesis, develops in a roughly sequential pattern from the top of the crown down to the cementum-enamel junction. This sequential pattern does vary slightly between species with humans having a less precise formation sequence than other fauna.

Amelogenesis occurs through the following phases: secretion, assembly, formation, transition/resorption, and maturation (Hillson 2005). In the first stage, an amelogenin-enamelin protein matrix is secreted by ameloblasts as they pull away from the mineralized dentine at the enamel-dentine junction (EDJ). Crystallites form and nucleate within this matrix. In the second stage, the ameloblasts assemble these crystallites from the EDJ extending out to create a curved pattern, in which the amelogenins are able to move through. In the formation stage, the crystallites are then elongated into extremely thin, long ribbons that spread from the EDJ to the enamel surface (Fincham and Simmer 1997; Mann 1997). As the ameloblasts approach the enamel surface, the temporary protein matrix is resorbed by enzymes and tissue fluid floods the empty space left by the matrix removal (Robinson et al. 1995). The crystallites resume growth, expanding from the EDJ to the enamel surface and gather to form densely packed and organized mature enamel tissue (Simmer and Fincham 1995). Once enamel mineralization is complete, the ameloblasts perish and the tissue becomes isolated from the tooth's blood supply located in the pulp chamber (Brudevold et al. 1977; Veis 1989). Any organic protein content remaining is located primarily near the EDJ with negligible amounts closer to the enamel surface. Without access to the bloodstream, enamel is unable to remodel after mineralization and retains the strontium isotopic signature ingested during its mineralization (Brudevold et al. 1977; Koch et al. 1997; Underwood and Mertz 1977).

Dentine composes the bulk of a tooth and provides support for the enamel crown as well as the pulp chamber. It has an organic content of ~20%, higher than that of enamel, but it is harder and more mineralized than bone (Hillson 2005). Initial dentine formation precedes enamel, however, the subsequent growth of both tissues occurs simultaneously (Arsenault and Robinson 1989; Boyde et al. 1988; Diekwisch et al. 1995; Fincham and Simmer 1997; Sasaki et al. 1997).

There are three forms of dentine: primary, secondary, and tertiary. Primary dentine is located between the enamel-dentine junction and the pulp chamber. It is formed before and during tooth eruption through the secretion of a pre-dentine collagen fibre matrix by odontoblasts. As the odontoblasts retreat from the matrix, short carbonate hydroxyapatite crystals are deposited and mineralized within this pre-dentine matrix (Hillson 2005). After the completion of the tooth root, secondary dentine is continuously formed throughout the lifetime of an individual. The new dentine is produced around the pulp chamber but the previously mineralized dentine is not resorbed. Its development is similar to primary dentine but occurs at a much slower rate. Tertiary dentine is the least common type, formed as a reaction to an external stimulus, such as caries. Only the odontoblasts that are directly affected by the stimulus will form tertiary dentine. In general, the majority of a tooth's dentine does not significantly remodel during its lifetime and its $^{87}Sr/^{86}Sr$ ratios and Sr concentrations remain relatively consistent in life with enamel Sr values from the same tooth (Brudevold and Söremark 1967).

Human teeth are preferred to bone in strontium isotope studies for two reasons. First, dental development occurs in a predictable sequence over a finite period of time. Humans are diphyodonts, growing a primary and secondary set of teeth (Tables 3.1 and 3.2). The first set, called deciduous or milk teeth, begin formation in utero and erupt through the gums at around 6 months of age. There are 20 deciduous teeth in total (8 incisors, 4 canines, and 8 molars) and their eruption occurs in a relatively fixed sequence (Table 3.1) (Hillson 2005). Deciduous tooth mineralization is not fully complete until the individual is around the age of one year. The deciduous teeth begin to shed at age six and are replaced by 32 permanent teeth: 8 incisors, 4 canines, 8 premolars, and 12 molars. The first permanent molar (M1) forms in utero at approximately 30 weeks in gestation but all other permanent dentition are produced after birth. The normal sequence of permanent tooth eruption is found in Table 3.2 (Hillson 2005). The M1 is fully mineralized by age 5, the rest complete mineralization by age 9. The third molar (M3) or wisdom tooth is more irregular in its development with some individuals never developing them at all. However, in general, M3 enamel develops between ages 9 and 17 (Hillson 2005).

The second reason teeth are the preferred material in Sr isotope studies is the resiliency of enamel and dentine tissue. Unlike the constant remodelling of bone, teeth are relatively inert. Enamel and primary dentine do not remodel after mineralization and can only be physically modified during life by attrition, breakage, or an external stimulus such as caries. Without new dental tissue being produced or old tissue being resorbed, enamel and primary dentine will maintain the Sr isotopic signature incorporated during their initial mineralization. As described above, tooth enamel and primary dentine are only formed in a fixed pattern during childhood. Using knowledge of dental mineralization timings, enamel and dentine provide a reliable isotopic snapshot that reflects the bioavailable Sr signature of the individual’s residence during this mineralization period (Brudevold and Söremark 1967). For example, a permanent premolar mineralizes from age 6-9 and integrates only strontium ingested during this 3 year period (Hillson 2005). After age 9, if no physical modification occurs, the premolar enamel and primary dentine preserve the original Sr throughout the individual’s lifetime.

Table 3.1 Deciduous tooth denomination, initial formation, and complete mineralization timing. Adapted from Hillson (2005) and Montgomery (2002)

Deciduous Dentition	**Abbreviation**		**Initial Formation (weeks in gestation)**		**Crown Complete (months after birth)**	
Tooth	**Maxillary**	**Mandibular**	**Maxillary**	**Mandibular**	**Maxillary**	**Mandibular**
First Incisor	di^1	di_1	13-16	13-16	1.5	2.5
Second Incisor	di^2	di_2	14.7-16.5	14.7-16.5	2.5	**3**
Canine/Cuspid	dc^1	dc_1	15-18	16-18	9	9
First Molar	dm^1	dm_1	14.5-17	14.5-17	6	5.5
Second Molar	dm^2	dm_2	16-23.5	17-19.5	11	10

Table 3.2 Permanent tooth denomination, initial formation, and complete mineralization timing. The formation and crown completion are shown in years unless otherwise specified. Adapted from Hillson (2005) and Montgomery (2002)

Permanent Dentition	**Abbreviation**		**Initial Formation**		**Crown Complete**	
Tooth	**Maxillary**	**Mandibular**	**Maxillary**	**Mandibular**	**Maxillary**	**Mandibular**
First Incisor	I^1	I_1	3-4 months	3-4 months	4-5.25	3.5-5
Second Incisor	I^2	I_2	10-12 months	3-4 months	4-5.75	4-5
Canine/ Cuspid	C^1	C_1	4-5 months	4-5 months	5.5-7	4.5-7
First Premolar	P^1	P_1	1.5-2	1.5-2	5-7.5	4.5-7
Second Premolar	P^2	P_2	2-2.5	2-2.5	6-8.5	6-8
First Molar	M^1	M_1	peri-natal	peri-natal	2.5-4.25	2.5-4
Second Molar	M^2	M_2	2.5-3	2.5-3	7-8	6.25-8
Third Molar	M^3	M_3	~9	~9	17-25	17-25

3.4 Diagenesis

The use of skeletal tissue in archaeological isotopic studies can be further complicated by the post-depositional process called diagenesis. Diagenesis is the combined physical, chemical, and biological processes in the burial context that transform and break down skeletal tissue's original chemical and physical structure. After death, the Sr composition of bone, dentine, and enamel tissue can be diagenetically altered to become isotopically equilibrated with the burial environment (Beard and Johnson 2000; Budd et al. 2000; Kohn et al. 1999; Pate and Brown 1985; Pate and Hutton 1988). Isotopic alteration of the mineral phase occurs through the deterioration of the skeletal tissue's organic matter. As the organic matter decomposes, the tissue becomes more susceptible to infiltration and incorporation of the labile Sr ions in groundwater. This is a highly variable and environment-specific process that has an impact on the preservation of the original Sr isotopic composition in bone and teeth.

In general, skeletal tissue Sr chemical diagenesis occurs on three different scales: (1) permeation into the pores, (2) ionic exchange, and (3) recrystallization (Pate and Hutton 1988). The first is the accumulation of strontium ions within the pore spaces of the tissue. These ions enter through the porous tissue but do not incorporate into the chemical structure of the hydroxyapatite. These separate strontium isotopes can be removed through a weak acetic acid wash (Grupe et al. 1997; Price et al. 1992; Sealy et al. 1991; Sillen and Sealy 1995). The second involves ionic exchanges between the groundwater solution and the transitory Ca phosphate segments. Those transitory segments can be converted to hydroxyapatite by exchanging ions from the burial environment. As with living skeletal tissue, Sr can substitute for Ca in these exchanges. This type of diagenetic alteration can be difficult to identify and separate from the original hydroxyapatite structure (Pate and Hutton 1988). At the third scale, diagenetic alteration causes a recrystallization of the bioapatite structure (LeGeros 1991; Sillen 1989). This leads to an increase in crystallinity to form larger, more structurally perfect crystals. These newly formed crystals can be differentiated from the in vivo structure through Fourier Transform Infrared spectroscopy (FT-IR) or X-ray Diffraction (XRD) techniques that determine crystal formation. Factors such as soil composition, site hydrology, pH, and temperature can all affect chemical preservation of the skeletal tissue; however, there is no clear correlation between any of these factors and the degree of diagenetic Sr replacement (Pate and Hutton 1988). In vivo Sr values of the skeletal tissue can be partially or even completely replaced to, ultimately, reflect the isotopic composition of the burial environment (Beard and Johnson 2000; Budd et al. 2000; Pate and Hutton 1988).

3.4.1 Diagenesis in bone, dentine, and enamel

Diagenesis occurs most frequently in bone and dentine because of their physical and chemical structure. Both of these tissues contain higher organic content than enamel and increase in porosity as they decompose (Beeley and Lunt 1980; Hanson and Buikstra 1987). This porosity allows Sr ions from the burial environment to filter in and can potentially elevate the Sr concentration. Bone and dentine in their mineral phase are structured with smaller crystals than enamel, giving them a greater surface area and increase the opportunity for ionic exchanges between the burial environment and the apatite (Parker and Toots 1980; Pate and Hutton 1988). Bone and dentine Sr values are more susceptible to diagenetic alteration and are, therefore, considered to be an unreliable material to use in isotopic studies of migration (Bentley et al. 2004; Budd et al. 2000; Kohn et al. 1999; Price et al. 2004; Sponheimer and Lee-Thorp 1999; Vuorinen et al. 1996).

Enamel, in comparison, is not as susceptible to diagenesis and has a greater chance of retaining its *in vivo* Sr isotopic composition. Enamel tissue is more resistant to diagenetic alteration than dentine and bone as a result of its lower organic content, larger crystal size, structurally small pore space, and formation pattern. The minute amount of organic matter (< 3% of the enamel tissue) lost during diagenetic decay limits the increase in porosity and leaves little room for the Sr ions from the burial environment to accumulate in. Furthermore, the enamel hydroxyapatite crystal is much larger and has less surface area than bone and dentine (Neuman and Neuman 1953; Parker and Toots 1980). The lower surface area of the crystal reduces the potential for ionic exchange between the apatite surface and the labile Sr that can lead to the incorporation of Sr from the burial environment into the apatite structure of the enamel. By weight, 97% of tooth enamel is composed of a dense hydroxyapatite structure with little porosity. The density greatly reduces gaps in the surface enamel and helps to prevent the infiltration of labile Sr ions from the groundwater. Additionally, after the initial mineralization, enamel does not remodel and the hydroxyapatite crystals present are fully matured. As a result, enamel is more kinetically stable and resistant to the incorporation of Sr ions into its structure (Budd et al. 2000; Kohn et al. 1999; Pate and Brown 1985; Price 1989).

Overall, the fundamental characteristics of enamel make it a more reliable sample material in isotopic studies than bone and dentine (Budd et al. 2000; Elias et al. 1982; Koch et al. 1997; Lee-Thorp and van der Merwe 1991; Montgomery et al. 2000; Nielsen-Marsh and Hedges 2000; Price et al. 2002; Price et al. 1994a; Robinson et al. 1986). However, enamel is not impervious to diagenetic alteration. Mineralization, porosity, and crystal size of enamel tissue will vary slightly depending on the age at death, sex, and pathology of the individual, which can affect the preservation of the strontium isotopic signature.

3.4.2 Methods to identify diagenetic material

Diagenetically contaminated samples of bone, dentine, and enamel should be identified and taken into consideration during the interpretation of the Sr isotope data. Several methods have been developed to identify markers that signify diagenetic change in skeletal tissue such as increased crystallinity (Shemesh 1990), changes in the calcium/phosphate (Ca/P) ratio (Sillen 1989), and the uptake of uranium (Millard and Hedges 1996). Natural skeletal tissue will have fairly heterogeneous crystal structure but through diagenetic alteration, and as a result of an increase in crystallization, the structure becomes more uniform. This structural homogeneity is measured by infrared spectroscopy, which registers the degree of homogeneity through the infra-red splitting factor (IRSF) (Shemesh 1990; Wright and Schwarcz 1996). A crystallinity index was developed from IRSF measurements (Shemesh 1990); the higher the index score, the more homogeneous the crystal structure is. Therefore, diagenetically altered skeletal tissue will score higher on the index.

In the burial environment, skeletal tissues do not just absorb strontium from the groundwater but uptake other detectable ions of elements, such as uranium and calcium. Uranium (U) ions are absorbed into bone, dentine, and enamel from the groundwater and the amount of U present within these tissues generally increases with the duration of interment (Millard and Hedges 1996). Higher concentrations of uranium will indicate a diagenetically altered tissue. Regarding Ca/P, the *in vivo* Ca/P ratio of skeletal tissue is 2.1:1 (Sillen 1989). Calcium from the burial environment permeate and saturate the decomposing skeletal tissue, thereby altering the Ca/P ratio. An abnormal Ca/P ratio will, therefore, also signify skeletal tissue that has been modified by diagenesis.

Overall, it is uncertain how useful these indicators are in determining the presence or degree of Sr isotopic changes (Burton et al. 1999; Hedges 2002). However, they do provide further confirmation of the susceptibility of bone and dentine tissue as well as the resiliency of enamel to diagenetic alteration. Bone and dentine in a burial context will contain diagenetically modified Sr isotopic values as a result of their physical and chemical composition. In tooth enamel, there is less porosity, organic matter, and labile apatite structures. Therefore, enamel is less likely to uptake uranium or calcium in significant quantities (Kohn et al. 1999; Millard and Hedges 1996; Sillen 1989) and its crystallinity index value remains constant (Sponheimer and Lee-Thorp 1999). Another established method to check for contaminated enamel samples, and the one employed for this study, is to compare the $^{87}Sr/^{86}Sr$ ratios and Sr concentrations between the enamel and primary dentine from the same tooth (Budd et al. 2000). Both tissues are formed at the same time and should contain very similar *in vivo* Sr ratios and concentrations (Brudevold and Söremark 1967). Contaminated dentine will often contain greater Sr concentrations because of the addition and exchange of Sr within the tissue. It may also have altered Sr isotope ratios that reflect a systematic shift towards the burial environment Sr values (Budd et al. 2000).

3.4.3 Methods for removing diagenetic material

Currently, there is no proven physical or chemical method that will remove all diagenetic Sr (Budd et al. 2000; Nielson-Marsh and Hedges 2000; Trickett et al. 2003). A skeletal sample (bone, dentine, or enamel) can be pre-treated prior to analysis by washing or leaching in a weak acetic acid to remove the accumulated Sr (Grupe et al. 1997; Price et al. 1992; Sealy et al. 1991; Sillen and Sealy 1995), but these washings can remove as little as 5% or as much as 40% of its total Sr concentration (Horn et al. 1994; Koch et al. 1992; Sillen and Legeros 1991). Furthermore, these treatments do not discern between biogenic Sr and diagenetic Sr during the removal, compromising the *in vivo* Sr isotopic signature of the sample in the process and are, therefore, not advisable to use. To mitigate the effect of diagenesis, tissues more likely to have been altered in the burial environment, such as bone or dentine, should be discarded and, in the case of dentine, removed from the enamel sample prior to analysis.

3.5 Local Bioavailable Strontium Signatures

Enamel, as a sample material, provides a potentially robust $^{87}Sr/^{86}Sr$ ratio that reflects the geological residence during an individual's different stages of childhood. Strontium isotope analysis identifies migrant individuals by distinguishing samples deemed 'local' (residents of the area around the burial) from those that are 'non-local' (individuals who were not from the burial environment). This 'local' Sr signature is reported as a range of $^{87}Sr/^{86}Sr$ ratios that reflect the burial environment's biologically available, or bioavailable, strontium. Correspondingly, a 'non-local' is any individual that does not have $^{87}Sr/^{86}Sr$ values within this 'local' range. An enamel sample that is interpreted as non-local signifies the individual resided in at least two different geological regions (the burial area and the childhood residence) and migrated sometime after the mineralization of the tissue. There are several methods that are used to analytically separate the local individuals from the non-local. Knowledge of the Sr isotope cycle and the geology of the burial environment will provide a rough estimate of the local $^{87}Sr/^{86}Sr$ range. However, this estimate can be further defined by understanding the local bioavailable strontium signature. Analyses of faunal remains from the archaeological context will provide the local bioavailable Sr signature to establish the local limit that can be compared to the enamel Sr values.

3.5.1 Geology

As described in Chapter 2 (Section 2.2.1), Camino del Molino is situated in the anterior of the Subbetic region within the External Betics (Figure 2.2) (Gibbons and Moreno 2002; Hoedemaeker and Leereveld 1995; McArthur et al. 2007; Moiroud et al.

2012). During the late Jurassic to the early Cretaceous, the area was a passive margin where Triassic-Cretaceous sedimentation and marine organisms were deposited over the course of millions of years. Limestone beds alternating with marlstone interbeds comprise the area surrounding Camino del Molino (Figure 3.2) (Hoedemaeker and Leereveld 1995). It is additionally noted that the geology present is well-preserved and was not significantly metamorphosed after formation. Marine sedimentary rocks, such as marlstone and limestone, have an expected $^{87}Sr/^{86}Sr$ isotopic range between 0.707-0.709 that is dependent on the Sr composition of seawater during its formation (Bentley 2006; Sealy et al. 1991; Wright 2005). During the Mesozoic era, seawater Sr isotope values ranged from ~ 0.707-0.708 (Bentley 2006; White et al. 2007). MacArthur et al. (2007) conducted a study measuring the $^{87}Sr/^{86}Sr$ values of three Subbetic sampling areas surrounding Caravaca de la Cruz. One of these sites is on the Río Argos, which is the river directly next to the site of Camino del Molino. The $^{87}Sr/^{86}Sr$ ratios at the Río Argos range from 0.7072-0.7074 and averaged 0.70726. This strontium value, taken directly from the geology, provides a baseline Sr isotope ratio to help determine the local Sr range at the site of Camino del Molino. Geological baselines, however, are limited. Sr isotope ratios in bedrock and soil do not always accurately reflect the range of biologically available Sr within the local area and, generally, can only distinguish non-locals if they exhibit extreme $^{87}Sr/^{86}Sr$ values (Price et al. 2002).

Figure 3.2 Detailed map of the geological substrates underlying Camino del Molino, indicated by a star, and the surrounding area. Note the geological substrate for the region is predominantly Mesozoic.
Adapted from Gibbons and Moreno 2002.

3.5.2 Determining the bioavailable Sr isotope signature

The primary method to create a local Sr range that is reflective of the bioavailable Sr is to use the average enamel $^{87}Sr/^{86}Sr$ (± 2 σ) values of fauna from the archaeological context. It has been determined that archaeological fauna provide a homogeneous, local Sr isotopic range and are a good proxy for assessing the Sr sources that are biologically available to the human population (Bentley et al. 2004; Blum et al. 2000; Price et al. 2002). Faunal remains from the archaeological site are preferred over modern samples because they reduce the effect of modern imported food sources and anthropogenic pollution on the local Sr ratios (Bentley et al. 2004).

The Sr isotope signature of any fauna will always be dependent on the geological variability of the area within their home range. Therefore, the species and their natural home range should be taken into consideration when using fauna as proxy for the local bioavailable Sr. In general, large herbivores will have larger home ranges and will be more likely to graze on a variety of geological substrates. As a result, these species will record a $^{87}Sr/^{86}Sr$ ratio representative of the broader area. Smaller animals, such as mice and snails, exploit much smaller areas and will usually provide a correspondingly more defined Sr isotope ratio range.

Price et al. (2002, 2004) have obtained successful results using herbivorous species that eat a range of plant material from their small home range, such as mice, guinea pigs, rabbits, squirrels, and snails. As diet is the main source of strontium in humans, testing an omnivorous species with a moderate home range can also provide a picture of the Sr available to the local population. Bentley et al. (2004) investigated the use of domestic pig samples from archaeological contexts to define the local Sr limit. The advantage of using domestic pigs centers on the assumption that it will ingest a very similar diet to the human owners. However, domesticated animals can be highly mobile, as a result of trading or herding practices, and their Sr isotope values may not correspond to the ‘local’ bioavailable Sr signature (Pellegrini et al. 2008; Towers et al. 2010). To define a robust local limit, it is recommended to use a variety of animal species with small and large home ranges to accurately reflect the local Sr isotope ratio range within the human populations. Enamel tissue as sample material is preferred over bone and dentine because, like human remains, fauna are also subject to diagenetic alteration in the burial environment.

3.6 Conclusion

Sr isotope analysis is an established method in archaeology to determine possible migrant individuals. The radioactive decay of ^{87}Sr allows for geological areas to have specific Sr isotope signatures that are absorbed and reflected in the local flora and fauna. This bioavailable Sr is then absorbed into human skeletal and dental tissue through food and water sources. Bone, dentine, and enamel will contain Sr isotope ratios that are reflective of local Sr signature where these tissues formed and mineralized. Dental enamel, because of its inert properties and predictable formation schedule, is the preferred material in archaeological Sr analyses. To determine whether an individual is local or non-local to a burial site, a local Sr range for this site must be found. In this study, combined published information on the geology of southeast Iberia as well as Sr isotope analysis of the archaeological fauna from the site of Camino del Molino help to create a robust local Sr range. Chapter 4 will describe the exact analytical methods used to obtain the $^{87}Sr/^{86}Sr$ ratios from the Camino del Molino human and faunal dental tissue.

Analytical Methods

4.1 Introduction

A subset of the human (n = 93) and animal (n = 25) teeth uncovered during the excavation at Camino del Molino were collected and mailed to St. John’s, Newfoundland, Canada. This subset served as the material basis for the Sr isotope study conducted. The methods used to sample, prepare, and measure strontium isotopes from the dental tissue are discussed in this chapter.

4.2 Sample Selection

4.2.1 Human samples

Of the thirteen hundred humans buried at the site of Camino del Molino, ninety-three individuals were selected for this study. These ninety-three subjects were well preserved and could be clearly identified as separate individuals. They were also chosen to represent both the temporal and demographic span of the site. The osteological study of the ninety-three sampled individuals from Camino del Molino was undertaken by Maria Haber Uriarte (Haber Uriarte et al. 2012) at the University of Murcia (Murcia, Spain). The basic demographic information collected from these skeletons included individual age-at-death estimates, the sex of the adult individuals, stature estimation, and paleopathology. These data are used to identify the demographic profile of the human population at Camino del Molino.

Table 4.1 presents the estimated age at death of the ninety-three individuals from Camino del Molino selected for strontium isotope analysis. The biological age categories were used in the osteological study of Camino del Molino individuals and applied here for continuity (Haber Uriarte et al. 2012). The categories are defined as: Infant (0-2 years), Child (3-12 years), Adolescent (13-19 years), Young Adult (20-35 years), Mature Adult (36-50 years), and Elderly (>51). The individuals that were identified as adult but not further classified into more defined age categories were placed into the category of Adult ($\geq$20 years).

Of the ninety-three individuals examined, forty-five were estimated for sex (48% of the sample population) (Table 4.1). The remainder were in poor or incomplete condition and no sex estimate was possible. Individuals identified as female form 42% of the ‘sexed’ sample population (nineteen individuals) and are most often categorized as Young Adult (20-35 years). Females comprise the majority (60%) of the Adolescent age category (13-19 years). The number of identified males is twenty-six (58% of the ‘sexed’ sample population) and the majority are classified as Young Adults. Males are well represented in the Mature Adult (36-50 years) and Elderly (<51) categories, comprising 67% and 100% of these age categories, respectively.

Table 4.1 The age-at-death and sex demography of this study's sample population. Note the age categories and ranges were used in the Camino del Molino osteological study by Haber Uriarte et al. (2012).

Age Category	**Male**	**Female**	**Indeterminate or Unknown**	**Total**
Infant (0-2)	*	*	*	0
Child (2-12years)	*	*	7 (Indet.)	7
Adolescent (13-19)	*	3	2 (Indet.)	5
Young Adult (20-35)	15	12	0	27
Mature Adult (36-45)	8	4	0	12
Elderly (> 51)	2	0	0	2
Adult (≥20)	1	0	39 (unknown)	40
Total	26	19	48	93

4.2.2 Sample material

From each selected sample individual, one first premolar (P1) or second premolar (P2) from the maxilla was mechanically extracted. However, if P1 or P2 were not present, P1 or P2 were too damaged (as a result of carious lesions or poor preservation) or the selection of another tooth from the individual would cause less damage to the maxilla/mandible, then another tooth was selected. The total number of tooth samples was ninety-three; sixty-five were premolars, eight were first molars, six incisors, four canines, three third molars, two molars, and six deciduous teeth (see Table 5.1).

As stated in Chapter 3, dental enamel is the primary material used in this study. Dentine samples from the ninety-three tooth samples were also analyzed to check for possible diagenetic alteration. Due to a limited budget, only ten dentine samples, selected at random, were analyzed. The ten selected dentine samples are listed in Table 5.2.

4.2.3 Faunal samples

Various archaeological fauna were also sampled from the site of Camino del Molino in order to establish the local isotope signature for the area. A total of twenty-five faunal tooth samples were selected from throughout the burial sequence and analyzed for $^{87}Sr/^{86}Sr$ ratios: one pig, three lizards, three rabbits, five small rodents (i.e. mice), five ovicaprids, and eight dogs (see Table 5.3). Due to the fragmentary nature of the majority of the teeth, as well as a lack of zooarchaeological identifications, the type of tooth/teeth or the age of the animal from which the sample was taken were not identified. As with the human samples, tooth enamel was the primary material analyzed.

4.3 Strontium Isotope Analysis: Sample Preparation

4.3.1 Human samples

The mechanical preparation of the samples took place in the Archaeology Conservation Lab at Queen's College, Memorial University (St. John's, Newfoundland, Canada). A wedge sample of both the enamel and dentine from each tooth were required for this study. The section of enamel sampled was dependent on its preservation and the presence of caries, fractures, and other dental anomalies on the tooth surface. Overall, the teeth were well preserved and contained few caries or fractures (< 5% of the teeth sampled).

The external surface of each tooth was mechanically abraded using a hand-held dental drill (Grobet USA™) equipped with a 3 mm spherical diamond-tipped grinding burr to remove external debris and surficial enamel. A wedge of enamel was cut along the length of the tooth using a small diamond-cut wheel. Each enamel sample weighed ~ 10-15 mg. The wedge was cut lengthwise to obtain an average of the strontium isotopic composition over the course of the tooth's growth. The interior surface of the enamel wedge was abraded using a 1 mm diamond-tipped burr to remove any adhering surface enamel and dentine from the dentine-enamel junction (Evans et al. 2006).

This process was repeated to obtain a sample of each tooth's primary dentine. The external tooth surface was abraded to remove the enamel and a portion of dentine was cut. Care was taken to avoid cutting into the secondary dentine closer to the pulp chamber or the root as these tissues do modify after their initial formation. This portion was then abraded to remove any remaining enamel. Each wedge sample of enamel and dentine was sonicated in deionized (DI) water (18.0 MΩ) for 3 minutes to remove enamel/dentine powder then rinsed three times with the deionized water. The samples were placed into individual 2 mL plastic centrifuge tubes, rinsed with acetone, and left covered on the lab countertop to dry.

The dental burr and wheel used during each sample extraction were rinsed with deionized water, placed in an ultrasonic bath for 5 minutes, dipped three times in 2M nitric acid and then deionized water. The lab area where the sampling occurred was cleaned after each individual sample preparation by washing the work surface with deionized water and acetone.

4.3.2 Faunal samples

The mechanical sampling of the faunal teeth was approached with the same method as the human teeth (Evans et al. 2006). However, this method had to be slightly altered for a number of faunal samples to address issues of tooth fragmentation and sample amount. The small rodent, lizard, and rabbit teeth samples (CM 94-103, 116, and 117) were small in size and it was not possible to manually separate the enamel from the dentine. The entire tooth, or several teeth if more tissue was needed, was/were used to ensure there would be sufficient Sr to analyze. The whole teeth sampled were mechanically abraded using the same hand-held drill equipped with a 1 mm spherical diamond-tipped grinding burr to remove external debris and, if possible, surficial enamel.

CM 97 (a small rodent) was too fragmented and did not have sufficient intact enamel tissue to be used for this study. The remainder of the faunal teeth (CM 104-115, 118, and 119) were from larger species and could be mechanically sampled in the same manner as the human teeth. All of the faunal tissue samples, including the whole teeth from the smaller species, were cleaned by the method used for the human samples (see section *4.3.1 Human samples*).

4.4 Strontium Chemical Preparation

Each enamel, dentine, and whole tooth sample was weighed into a clean 3 mL Savillex™ (Minnetonka, MN, USA) vial on a Sartorius R200S scale in the Radiogenic Isotope Laboratory at the Earth Sciences Department, Memorial University (St. John's, Newfoundland, Canada). The weighed samples were dissolved in 1 mL of single distilled 8M nitric acid (HNO_3) and placed onto a hot plate (approximately 120°C) in closed vials to digest. While the samples dissolved, the columns used for the strontium elution process were prepared.

Modified plastic pipette tips (1 mL) served as micro-columns for the strontium separation process. The bottom of each pipette tip was cut on an angle to assist the movement of the liquids and a porous polyethylene frit was positioned into the column at the base. The columns were rinsed with one column volume (~1 mL) of deionized water and then washed with one column volume of 6M HCl. A small amount of Sr-Spec resin suspended in deionized water was loaded into the columns to make a bed volume of approximately 0.15 mL. The pipette, now with the Sr-Spec resin in place, was again rinsed with two column volumes (~ 2 mL) of 6M HCl, followed by one column volume of deionized water, and two column volumes of 8M HNO_3. The columns were then ready to receive the human and faunal samples that were digested in the Savillex™ vials.

The human and faunal samples were removed from the hot plate to cool. Once cooled, the 1 mL sample was loaded directly into the pre-conditioned Sr-Spec resin column and then collected into the Savillex™ vial the sample was in during its digestion on the hot plate. The collected strontium sample was then re-loaded by pipette into the column to ensure the maximum retention of Sr ions. To remove the matrix elements, three successive column volumes of 8M HNO_3 (~ 3 mL) were passed through the column. The sample was then eluted with 1 mL of deionized water into a clean 2 mL plastic centrifuge tube. An additional 1 mL of water and 75 µL of 8M HNO_3 was pipetted into the centrifuge tube (1:2 dilution) to acidify the sample to 0.3M, the required concentration used for introduction to the Thermo-Finnigan Neptune mass spectrometer.

4.5 Strontium Isotope Measurement

The $^{87}Sr/^{86}Sr$ isotope ratios were measured on a Thermo-Finnigan Neptune multi-collector inductively coupled plasma mass spectrometer (MC-ICP-MS) located in the Bruneau Center at Memorial University. The Neptune is a high-resolution, double-focusing MC-ICP-MS, containing 9 Faraday collectors and ion counting detectors to allow for the simultaneously high precision measurement of multiple isotopes. Samples were introduced using a semi-automated sampler into the plasma source of the MC-ICP-MS through a self-aspiring capillary, using a 100 mL PFA (perfluoroalkoxy) nebulizer.

The Camino del Molino human and faunal samples were first run on the Neptune over the course of twenty-four hours, February 2nd-3rd, 2012. All samples were measured in reference to the lab standard NBS 987 (200 ppb) (strontium carbonate isotope standard dissolved in 3% HNO_3), which was run once for every 10 samples. A list of the sequence of samples, procedural blanks, and the NBS 987 standard can be found in Appendix I. During each analysis, the acquisition of the sample data was in one block of 50 cycles with 2 sec integration. Procedural blanks taken throughout the Sr chemical preparation (to ensure no procedural introduction of Sr to the samples) were measured and considered negligible; Sample ^{88}Sr = 8.6 V (on average), Blank ^{88}Sr = 0.007 V (or <0.01% of sample ^{88}Sr intensity).

Some of the ^{88}Sr signal intensities measured from the samples were relatively low, at less than 5V. Though they were above the level considered acceptable (Richards et al 2007), a re-run of all the samples with signal intensities below 5V was deemed appropriate to corroborate the results from the first run. The second run took place on February 13, 2012 and the data were acquired in one block of 30 cycles with 2 sec integration. Results from the sample re-run measured closely with those taken during the first run. The difference of the ^{87}Sr/^{86}Sr sample ratios between the two runs was insignificant with a mean of -0.000010. The list of samples in the re-run and the differences between the two runs are listed in Appendix I. The results from the first sample run on the Neptune are the ^{87}Sr/^{86}Sr ratios and Sr concentrations used for the results of this study.

All the $^{87}Sr/^{86}Sr$ ratios and Sr concentrations of the samples were corrected to the NBS 987 standard ($^{87}Sr/^{86}Sr$ = 0.710240, Sr conc = 200 ppb) (See Appendix I). The average $^{87}Sr/^{86}Sr$ value for the SRM 987 standard was 0.710279 during the run and all of the sample $^{87}Sr/^{86}Sr$ data were corrected by 0.000039. Sample Sr concentrations (ppm) were determined through the sample's ^{88}Sr signal intensity (V) and mass (mg) corrected by a factor of 18.2 (NBS 987 standard concentration = 200 ppb/NBS 987 standard average ^{88}Sr intensity = 11.0 V).

4.6 Conclusion

A subset of the human and faunal teeth uncovered at Camino del Molino were used as the material to conduct the Sr isotope study. The teeth were selected to represent the temporal and demographic span of the site. The mechanical and chemical preparation for this study was completed by the author under the supervision of Dr. Vaughan Grimes. A wedge of enamel and dentine from each tooth was extracted, abraded, and rinsed with deionized water. Each sample wedge was dissolved in nitric acid, loaded into preconditioned Sr Spec resin columns, and eluted with deionized water. The samples Sr isotopes ratios were measured on a Thermo Finnigan Neptune mass spectrometer and corrected to NBS 987 standard. The measurement of the strontium isotopes by the Neptune was completed by the author under the supervision of Rebecca Lim, the Neptune's assigned technician, and Dr. Vaughan Grimes. The human and faunal sample Sr isotope results and the establishment of the local Camino del Molino Sr range are presented in Chapter 5.

Strontium Isotope Results

5.1 Introduction

The human and faunal Sr isotope analysis results are presented in this chapter. Migrant individuals are identified by comparing the enamel $^{87}Sr/^{86}Sr$ ratio to the local Sr isotope range. This range is defined by the average faunal enamel $^{87}Sr/^{86}Sr$ within two standard deviations. Statistical analyses were conducted using the statistical program SPSS.

5.2 Strontium Isotope Results: Humans

5.2.1 Enamel Samples

The measured $^{87}Sr/^{86}Sr$ ratios and Sr concentrations from human enamel samples are presented in Table 5.1 and displayed in Figure 5.1. The $^{87}Sr/^{86}Sr$ results are not normally distributed and have a positive skew (Kurtosis = 13.568, s.d. = .495; Skewness = 3.198, s.d. = .495). The average $^{87}Sr/^{86}Sr$ ratio of the human enamel samples is 0.709141 (n = 93) with a standard deviation of 0.001992. The lowest value is 0.707625 and the highest is 0.720961 with a range of 0.13336. Strontium concentrations were varied, ranging from 24 to 397 ppm with an average of 131 ppm. Typically, enamel Sr concentrations range from 50 to 300 ppm but can vary depending on the Sr concentrations of the geology and drinking water (Brudevold and Söremark 1967; Curzon and Cutress 1983; Losee et al. 1974).

Table 5.1 Camino del Molino human enamel $^{87}Sr/^{86}Sr$ ratio and Sr concentration results. The sample's code, sex, age, and tooth type are also included.

Sample	Sex	Age	Tooth	$^{87}Sr/^{86}Sr$	Sr conc. (ppm)
CM-1	Unknown	Adult	P^2	0.707830	242
CM-2	Unknown	Adult	P_1	0.708884	162
CM-3	Female	Young Adult	P^1	0.712937	122
CM-4	Male	Young Adult	I^2	0.708264	348
CM-5	Unknown	Adult	M^1	0.708594	125
CM-6	Unknown	Adult	P^1	0.710639	148
CM-7	Indet.	Adolescent	M_1	0.708730	98
CM-8	Unknown	Adult	P^2	0.713135	296
CM-9	Male	Mature Adult	C^1	0.713027	103
CM-10	Female	Young Adult	P^1	0.708967	115
CM-11	Male	Mature Adult	I_2	0.709895	117
CM-12	Unknown	Adult	P^1	0.715012	74
CM-13	Male	Mature Adult	P^2	0.709715	214
CM-14	Unknown	Adult	P^2	0.708340	305
CM-15	Unknown	Adult	P^2	0.707857	102
CM-16	Unknown	Adult	M_1	0.708307	114
CM-17	Unknown	Adult	P^1	0.708494	52
CM-18	Male	Young Adult	I^2	0.713301	107
CM-19	Indet.	Child	I^1	0.708364	98
CM-20	Unknown	Adult	P_1	0.707922	244
CM-21	Unknown	Adult	P^2	0.707961	55
CM-22	Unknown	Adult	P^1	0.709103	52
CM-23	Unknown	Adult	P_1	0.712275	231
CM-24	Indet.	Child	dm^1	0.707904	109
CM-25	Male	Young Adult	P^2	0.708487	293
CM-26	Unknown	Adult	P^1	0.708409	128
CM-27	Unknown	Adult	P^2	0.707810	326
CM-28	Indet.	Child	dm_1	0.708060	68
CM-29	Unknown	Adult	P^2	0.707960	154
CM-30	Unknown	Adult	P^1	0.708280	86
CM-31	Unknown	Adult	P^1	0.708970	59
CM-32	Unknown	Adult	P^2	0.708794	133

CM-33	Unknown	Adult	P	0.710323	88
CM-34	Unknown	Adult	C^1	0.710004	75
CM-35	Unknown	Adult	P^1	0.713483	98
CM-36	Unknown	Adult	P^1	0.708293	184
CM-37	Male	Mature Adult	P^1	0.712812	59
CM-38	Unknown	Adult	P^1	0.711212	86
CM-39	Male	Mature Adult	P^1	0.708077	154
CM-40	Female	Young Adult	P_1	0.708153	97
CM-41	Unknown	Adult	P^1	0.708369	203
CM-42	Male	Young Adult	P^1	0.709486	87
CM-43	Unknown	Adult	M^1	0.709007	48
CM-44	Unknown	Adult	I^1	0.708105	220
CM-45	Indet.	Child	di^1	0.707946	151
CM-46	Male	Young Adult	P^1	0.708497	397
CM-47	Indet.	Child	dm^1	0.708463	120
CM-48	Indet.	Child	dm^1	0.707865	96
CM-49	Male	Adult	P^1	0.708459	371
CM-50	Male	Young Adult	P^1	0.708236	330
CM-51	Unknown	Adult	P^1	0.710343	104
CM-52	Male	Mature Adult	P^1	0.708140	197
CM-53	Female	Mature Adult	P^2	0.708042	123
CM-54	Female	Mature Adult	P^2	0.708074	62
CM-55	Female	Young Adult	P^1	0.708400	104
CM-56	Female	Young Adult	P_1	0.708950	24
CM-57	Unknown	Adult	P^1	0.708376	132
CM-58	Male	Elderly	P_1	0.708565	34
CM-59	Female	Young Adult	P^1	0.707625	311
CM-60	Male	Young Adult	M^3	0.709547	271
CM-61	Unknown	Adult	C^1	0.708421	31
CM-62	Unknown	Adult	P^2	0.708721	30
CM-63	Indet.	Adolescent	P^1	0.708430	164
CM-64	Indet.	Child	M_1	0.708009	80
CM-65	Female	Young Adult	P_1	0.707979	95
CM-66	Female	Young Adult	P^2	0.720961	117
CM-67	Male	Mature Adult	M^3	0.707870	117
CM-68	Female	Young Adult	M^3	0.707967	108
CM-69	Male	Young Adult	P^1	0.709487	63

CM-70	Male	Young Adult	C^1	0.708860	45
CM-71	Female	Adolescent	P^1	0.708148	184
CM-72	Female	Young Adult	P_1	0.708098	58
CM-73	Male	Mature Adult	P^1	0.707894	214
CM-74	Indet.	Child	M^1	0.707972	163
CM-75	Unknown	Adult	P^2	0.708173	269
CM-76	Male	Young Adult	P_1	0.708590	86
CM-77	Male	Young Adult	I^1	0.708425	99
CM-78	Male	Young Adult	P^1	0.709198	47
CM-79	Female	Mature Adult	P^1	0.712914	44
CM-80	Indet.	Child	P^1	0.708229	50
CM-81	Unknown	Adult	P^1	0.708346	43
CM-82	Female	Young Adult	P^2	0.708504	69
CM-83	Indet.	Child	dm_2	0.708195	62
CM-84	Male	Elderly	P^2	0.709007	91
CM-85	Male	Young Adult	P^2	0.710586	40
CM-86	Male	Young Adult	P^2	0.709037	13
CM-87	Unknown	Adult	M^1	0.708793	42
CM-88	Female	Adolescent	M^2	0.707959	147
CM-89	Female	Mature Adult	P^1	0.707871	115
CM-90	Male	Mature Adult	P^2	0.708634	78
CM-91	Female	Adolescent	P^1	0.707917	143
CM-92	Indet.	Child	M_2	0.707982	96
CM-93	Female	Young Adult	M^1	0.708153	107

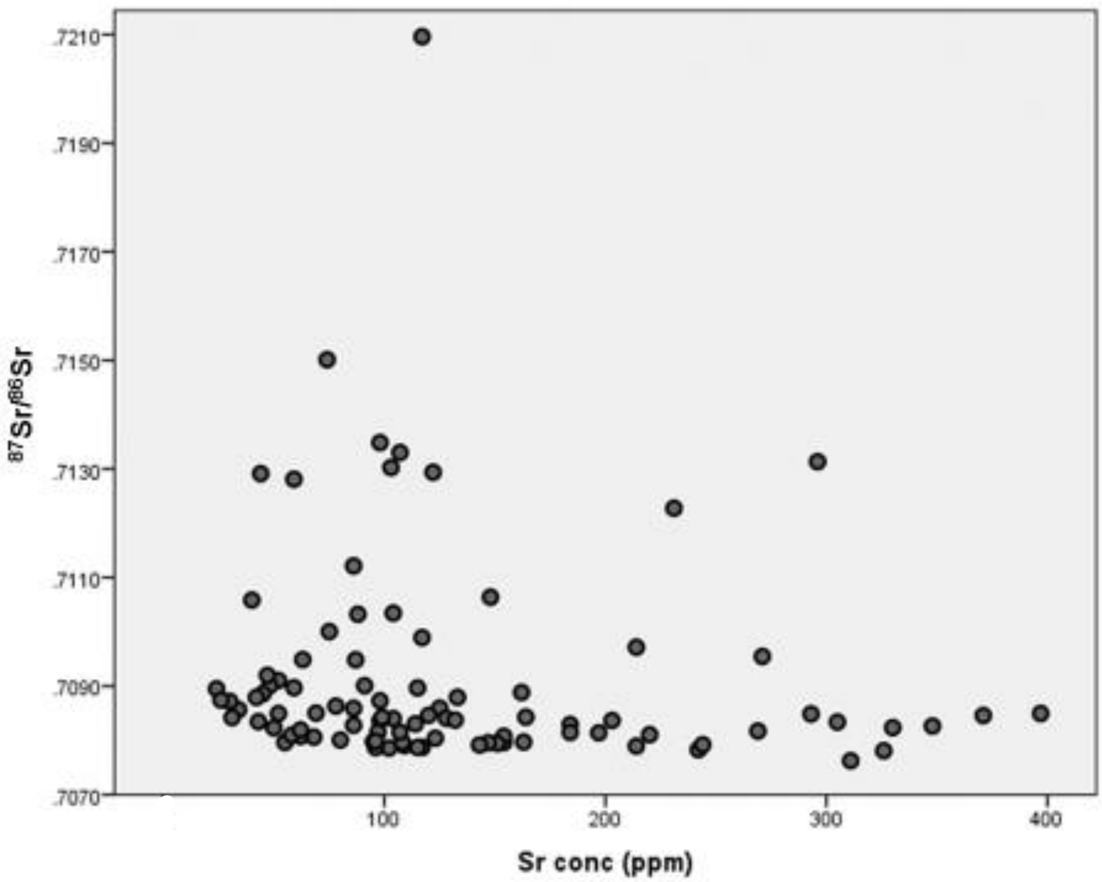

Figure 5.1 Plot of $^{87}Sr/^{86}Sr$ ratio versus Sr concentration (ppm) for the Camino del Molino human enamel results. The majority of the $^{87}Sr/^{86}Sr$ ratio results cluster between .7080 and .7090. There are no human $^{87}Sr/^{86}Sr$ ratio results below 0.7070.

5.2.2 Diagenesis

Strontium isotope ratios and concentrations are relatively homogeneous within dental tissues from a single tooth unless one of the tissues is diagenetically altered (Brudevold and Söremark 1967; Hillson 2005; Parker and Toots 1980; Underwood and Mertz 1977). Dentine tissue, due to its physical and chemical structure, will uptake Sr ions from the burial environment. As a result, dentine Sr isotopic composition will shift towards the Sr signature of the burial environment. Human enamel that is not diagenetically altered does not display this systematic shift in Sr values towards the isotopic composition of the burial environment. Therefore, relatively unaltered enamel samples should have different Sr ratios and concentrations to the dentine tissue from the same tooth.

Ten randomly selected dentine samples were analyzed to indicate if the enamel samples were diagenetically altered or not. The dentine-enamel pairs $^{87}Sr/^{86}Sr$ ratio and Sr concentration results are presented in Table 5.2 and displayed in Figures 5.2 ($^{87}Sr/^{86}Sr$ ratios) and 5.3 (Sr concentrations). The dentine samples have a mean Sr ratio of 0.708063 (s.d. = 0.000179) with a high value of 0.708483 and a low value of 0.707908. The data are relatively normally distributed (Kurtosis = 2.941, s.d. = 1.334) but have a slight positive skew (Skewness = 1.812, s.d. = 0.687). The dentine Sr concentrations are more varied than the enamel samples but display a normal distribution (Kurtosis = -0.132, s.d. = 1.334). The results range from 27 to 466 ppm with an average of 242 ppm (s.d. = 124).

The dentine tissues sampled in this study show an increase in the Sr concentrations with a decrease in the $^{87}Sr/^{86}Sr$ ratios when compared to their enamel pairs. Figure 5.2 and Figure 5.3 present the $^{87}Sr/^{86}Sr$ ratios and Sr concentrations of the dentine-enamel pairs, respectively. All but one of the sample pairs tested produced a decrease in the Sr ratio from the enamel to the dentine tissues. One sample (CM89) did see a minimal increase (+0.000136). The majority of the paired samples (seven out of ten) had an increase in the Sr concentrations between the enamel and dentine tissues, indicating that diagenetic accumulation of Sr from the burial environment may have occurred in the dentine (Figure 5.3). The other three samples had a decrease in the concentrations of strontium: CM 13 (-69 ppm), CM 25 (-20 ppm), and CM 89 (-88 ppm).

The dentine samples all contained similar $^{87}Sr/^{86}Sr$ ratios to each other as well as distinct $^{87}Sr/^{86}Sr$ ratio and Sr concentration from their paired enamel. Therefore, the enamel samples do not appear to have been greatly altered by diagenesis and, consequently, are likely to contain reliable strontium isotopic data. Using this subset, it is assumed that all of the human enamel Sr values used for this study have not been significantly affected by the burial environment and can be used as correlates of human mobility. It is understood that this is a generalization based on a small subset and only a complete analysis of all the dentine samples will ensure no significant diagenetic alteration occurred in the enamel samples.

Table 5.2 Dentine $^{87}Sr/^{86}Sr$ ratio and Sr concentration results with their tooth's enamel sample

				Dentine		Enamel	
Sample	**Sex**	**Age**	**Tooth**	**$^{87}Sr/^{86}Sr$**	**Sr conc. (ppm)**	**$^{87}Sr/^{86}Sr$**	**Sr conc. (ppm)**
CM-2	Unknown	Adult	P_1	0.708074	208	0.708884	162
CM-13	Male	30-40	P^2	0.708269	145	0.709715	214
CM-25	Male	24-28	P^2	0.708000	273	0.708487	293
CM-38	Unknown	Adult	P^1	0.708483	223	0.711212	86
CM-42	Male	20-28	P^1	0.707986	466	0.709486	87
CM-53	Female	33-42	P^2	0.707908	368	0.708042	123
CM-63	Juvenile	14-18	P^1	0.707966	360	0.708430	164
CM-78	Male	22-24	P^1	0.708012	140	0.709198	47
CM-83	Juvenile	Juvenile	dm_2	0.707922	217	0.708195	62
CM-89	Female	40-55	P^1	0.708007	27	0.707871	115

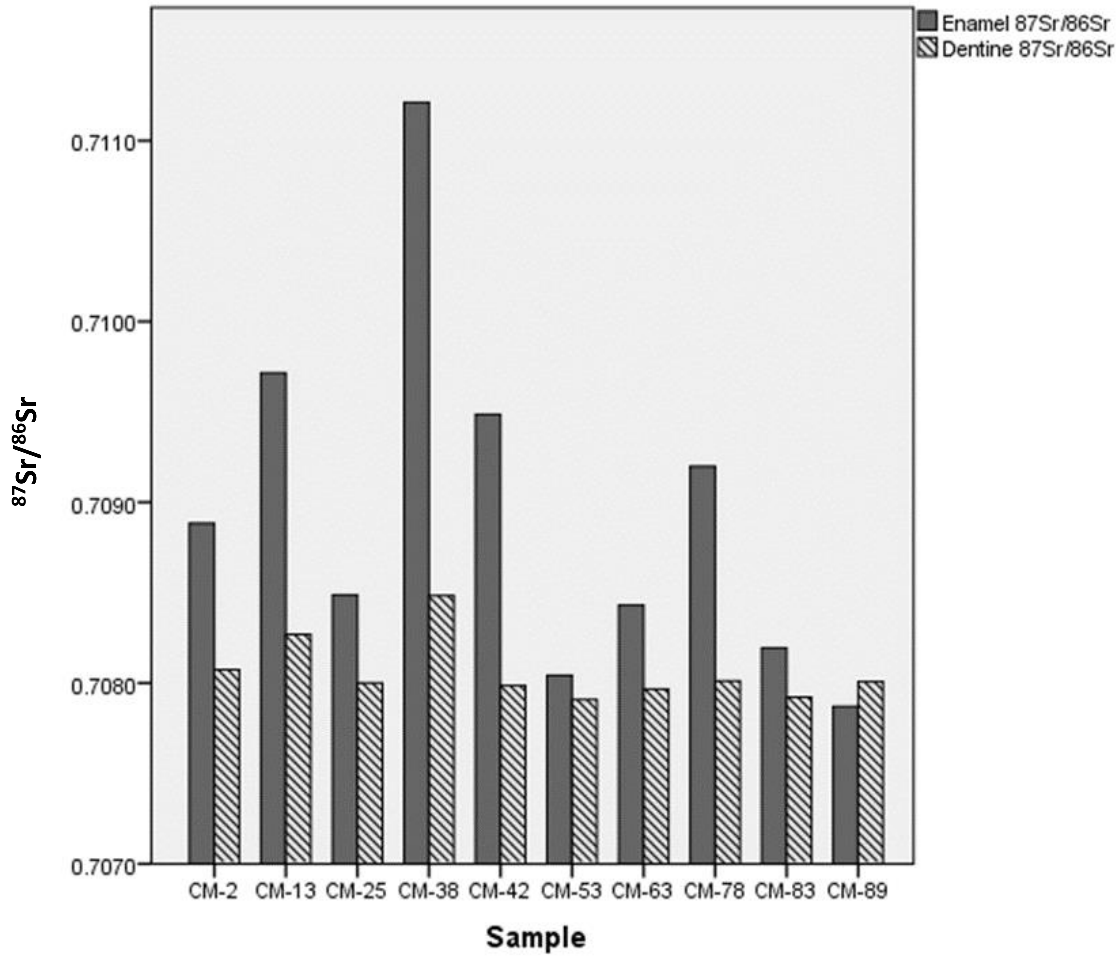

Figure 5.2 Histogram illustrating the relationship between the $^{87}Sr/^{86}Sr$ ratios of the enamel and dentine from the same tooth. Note the dentine samples show similar $^{87}Sr/^{86}Sr$ ratio results, whereas the enamel $^{87}Sr/^{86}Sr$ ratio results vary greatly among the samples.

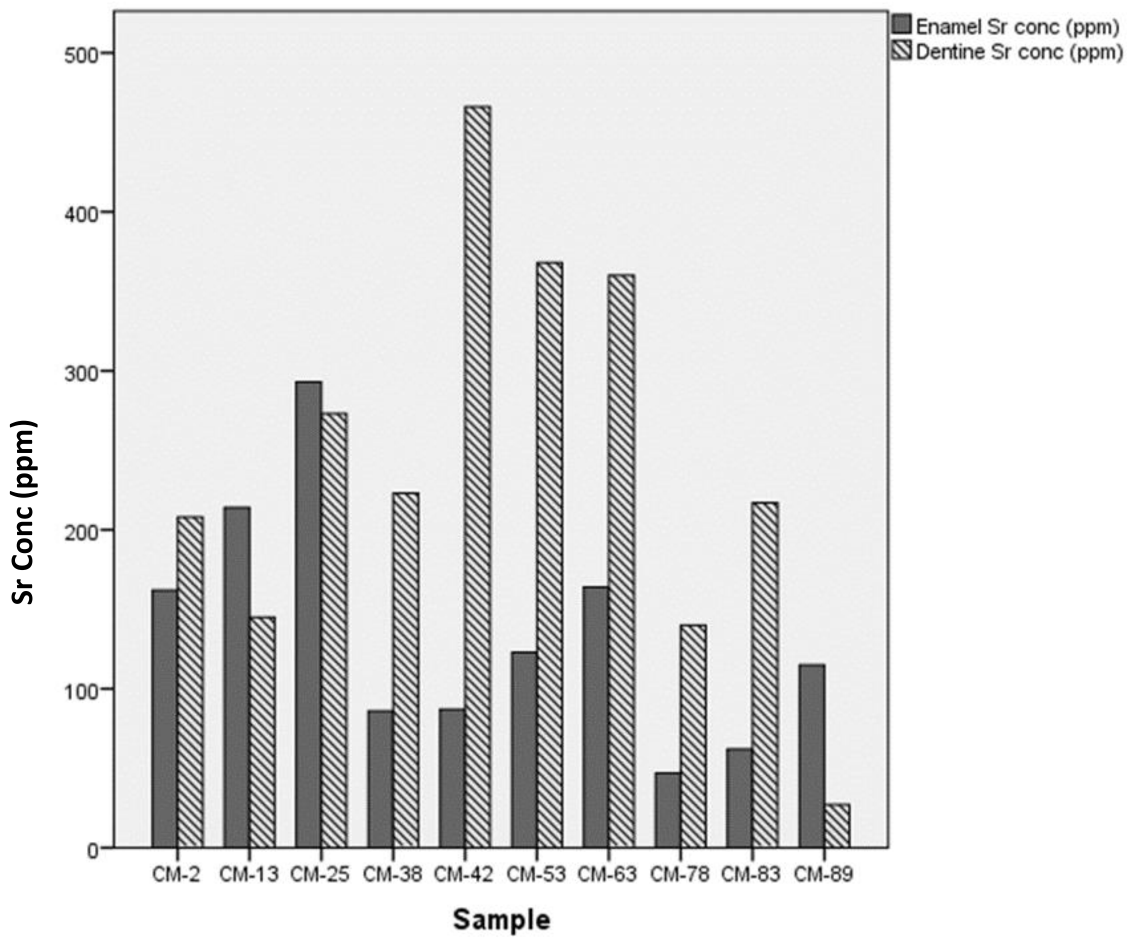

Figure 5.3 Histogram illustrating the relationship between the Sr concentrations (ppm) of the enamel and dentine from the same tooth. Note the Sr concentrations of the dentine results are generally much greater than the enamel results.

5.3 Establishing the Local Bioavailable Sr Limit

5.3.1 Faunal results

The results of the strontium analysis of twenty-five teeth from the archaeologically recovered fauna are presented in Table 5.3 and displayed in Figure 5.4. The $^{87}Sr/^{86}Sr$ ratios range from 0.707846 to 0.711588 with a mean of 0.708481 (s.d. = 0.001065). Similar to the human enamel results, the faunal data are not normally distributed (Kurtosis = 3.149, s.d. = 0.902) and have a slight positive skew (Skewness = 1.989, s.d. = 0.464). The Sr concentrations were normally distributed (Kurtosis = 0.687, s.d. = 0.902) and are on average higher than the human enamel, which is expected since herbivorous species uptake more Sr from vegetation (Bocherens et al. 1994; Tuross et al. 1989). The mean faunal Sr concentration is 236 ppm (s.d. = 205) with a range between 21-789 ppm.

Table 5.3 Faunal $^{87}Sr/^{86}Sr$ ratio and Sr concentration results, including the sample code and animal.

Sample	**Animal**	**$^{87}Sr/^{86}Sr$**	**Sr conc. (ppm)**
CM-94	Rabbit	0.707869	120
CM-95	Small Rodent	0.707870	540
CM-96	Rabbit	0.707871	538
CM-98	Rabbit	0.707913	438
CM-99	Small Rodent	0.707897	380
CM-100	Small Rodent	0.707897	574
CM-101	Lizard	0.707898	415
CM-102	Small Rodent	0.707867	789
CM-103	Small Rodent	0.707878	175
CM-104	Ovicaprid	0.711588	99
CM-105	Ovicaprid	0.707925	21
CM-106	Ovicaprid	0.708583	196
CM-107	Ovicaprid	0.708161	61
CM-108	Dog	0.708174	109
CM-109	Dog	0.709559	29
CM-110	Dog	0.708188	96
CM-111	Ovicaprid	0.708590	238
CM-112	Dog	0.710062	87
CM-113	Dog	0.708043	188
CM-114	Dog	0.709512	52
CM-115	Dog	0.711190	91
CM-116	Lizard	0.707863	153
CM-117	Lizard	0.707895	148
CM-118	Dog	0.707887	279
CM-119	Pig	0.707846	88

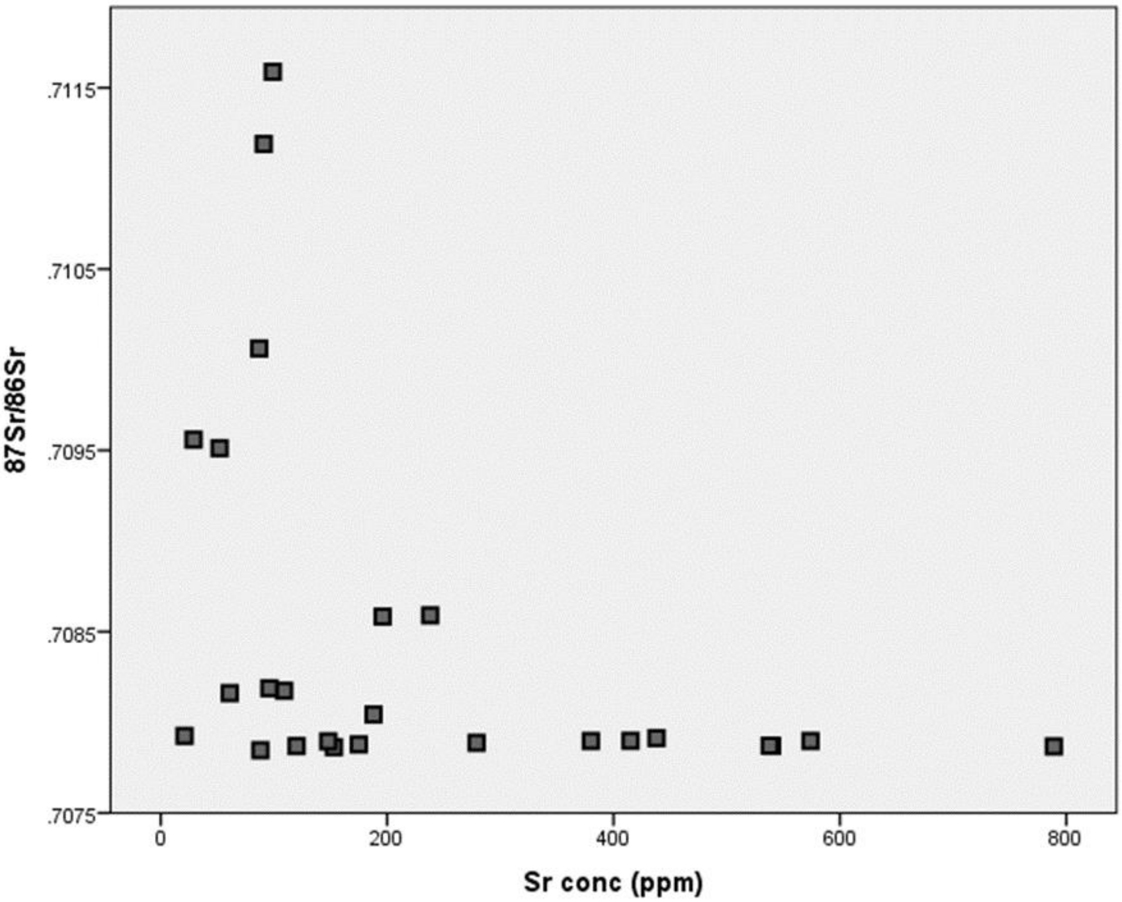

Figure 5.4 Plot of $^{87}Sr/^{86}Sr$ ratio versus Sr concentration (ppm) for the Camino del Molino faunal results. Note, similar to the human Sr results, the majority of the faunal $^{87}Sr/^{86}Sr$ ratios concentrate around .7080 and none are below 0.7075.

5.3.2 Local $^{87}Sr/^{86}Sr$ range for Camino del Molino

Camino del Molino is located within the Subbetic region of the External Betics comprised mainly of marine sedimentary rock. The region's sedimentary geology gives a broad baseline local Sr range of 0.707-0.709 (Bentley 2006; Sealy et al. 1991; Wright 2005) and the local area around Camino del Molino has an average $^{87}Sr/^{86}Sr$ value of 0.70726 (MacArthur 2007) (see section *3.5.1 Geology)*. To better define this local range, archaeological fauna from the burial context was also analyzed as a proxy for the bioavailable strontium (Price et al. 2002). The mean faunal $^{87}Sr/^{86}Sr$ ratio $\pm 2\sigma$ defines the local $^{87}Sr/^{86}Sr$ limit of 0.706351-0.710611 for Camino del Molino. This range is displayed with the human enamel $^{87}Sr/^{86}Sr$ results in Figure 5.5. With the local range of Sr values established there are twelve individuals (13% of the sample population) that fall above this boundary: CM 3, 6, 8, 9, 12, 18, 23, 35, 37, 38, 66, and 79 (Table 5.4). None of the individuals were found below the Sr local limit. The majority of the samples from Camino del Molino are identified as 'local' to the Camino del Molino area (81 individuals, 87% of the sample population). Although, several of the individuals identified as 'local' (CM 6, 34, 33, 51, and 85) have $^{87}Sr/^{86}Sr$ ratios that place them just inside the local Sr range.

Table 5.4 The identified non-local Camino del Molino individuals

Sample	Layer	Sex	Age	Tooth	$^{87}Sr/^{86}Sr$	Sr conc. (ppm)
CM-3	1106	Female	Young Adult	P^1	0.712937	122
CM-6	1106	Unknown	Adult	P^1	0.710639	148
CM-8	1106	Unknown	Adult	P^2	0.713135	296
CM-9	1106	Male	Young Adult	C^1	0.713027	103
CM-12	1106	Unknown	Adult	P^1	0.715012	74
CM-18	1107	Male	Young Adult	I^2	0.713301	107
CM-23	1107	Unknown	Adult	P_1	0.712275	231
CM-35	1108	Unknown	Adult	P^1	0.713483	98
CM-37	1108	Male	Mature Adult	P^1	0.712812	59
CM-38	1108	Unknown	Adult	P^1	0.711212	86
CM-66	1109	Female	Young Adult	P^2	0.720961	117
CM-79	1109	Female	Mature Adult	P^1	0.712914	44

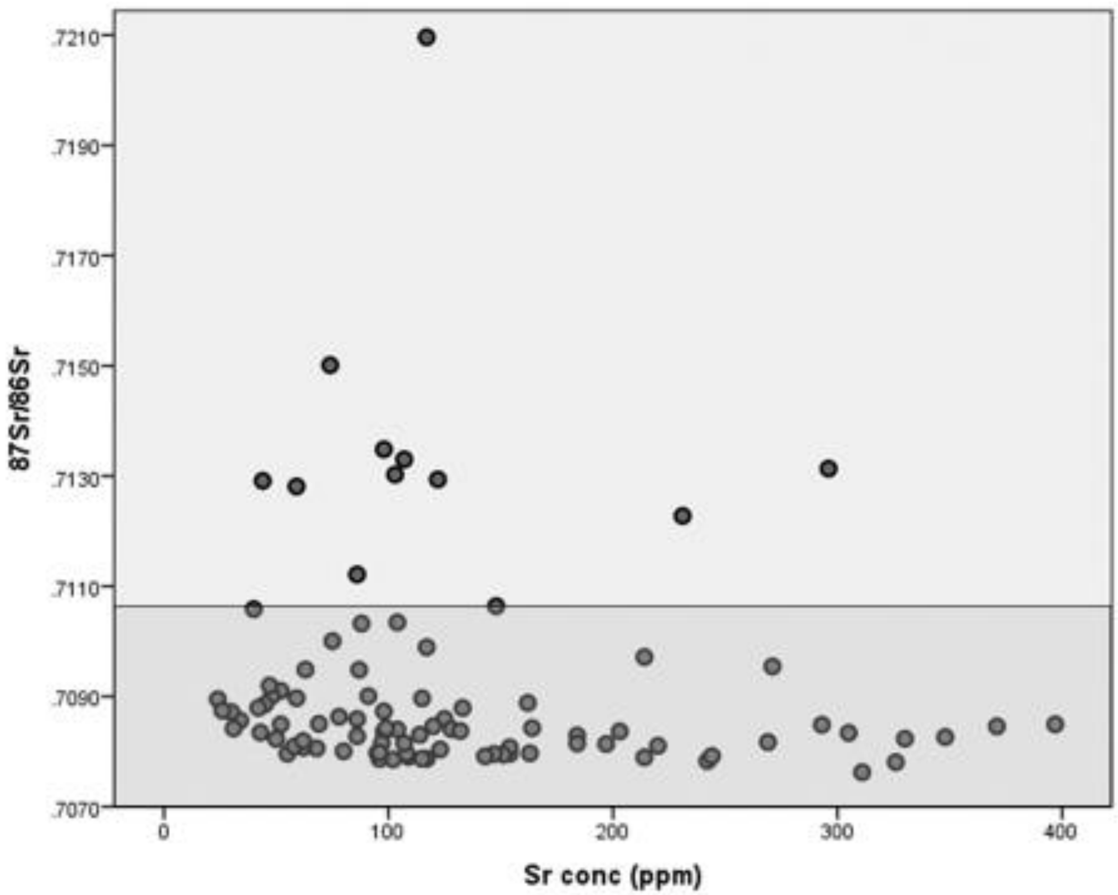

Figure 5.5 Plot of $^{87}Sr/^{86}Sr$ ratio versus Sr concentration (ppm) for the Camino del Molino human enamel results with the local Sr limit (0.706351-0.710610), calculated from the average faunal $^{87}Sr/^{86}Sr$ ratio (±2σ). Note that there are 12 human individuals above the local Sr limit.

5.3.3 Concerns with the Camino del Molino local limit

Two of the Camino del Molino fauna samples were identified as non-local: a dog (CM 115) at 0.711190 and an ovicaprid (CM 104) at 0.711588 (Table 5.3 & Figure 5.4). These two samples had $^{87}Sr/^{86}Sr$ ratios that were much higher than the geological Sr signature of the region (~0.707-0.709) and above the local Sr limit (0.706351-0.710611). The presence of non-local animals at Camino del Molino does affect the validity of the local limit used to define the non-local human samples. Omitting the animal species that have greater potential to be non-local from the establishment of the Camino del Molino Sr limit could provide a more precise local Sr range as well as distinguish other possible non-locals. Some faunal species have larger home ranges or are part of a shepherding/trading network, such as ovicaprid or canine species, making them more likely to have non-local Sr ratio values (see section *3.5.2 Determining the bioavailable Sr isotope signature*). Removing the ovicaprid and dog samples from the local Camino del Molino Sr limit creation greatly narrows the local Sr limit to 0.707850-0.707917 and the number of identified non-locals dramatically increases to 90 (~97% of the sample population). Although it is possible that the entire sample population of Camino del Molino are non-locals, it is improbable. Therefore, it is acknowledged that the Camino de Molino $^{87}Sr/^{86}Sr$ local limit that includes the identified non-local fauna and the potentially more mobile species created a larger local Sr range and could have identified possible non-local humans as local. However, in this study, including non-local animals produced a more conservative but still valid estimate of the human migrant population. A better defined local Sr signature for Camino del Molino through the addition of a larger fauna sample population could reveal more migrant individuals or different mobility patterns.

5.4 Conclusion

Migrant individuals are identified by comparing the $^{87}Sr/^{86}Sr$ ratio to the local Sr isotope range, which was defined by the average faunal enamel $^{87}Sr/^{86}Sr$ within two standard deviations. Results from the human and faunal analysis determine there are at least twelve non-local human individuals (13% of the sample population) as well as two non-local fauna, a dog and an ovicaprid, present at Camino del Molino. Chapter 6 discusses the detectable temporal and demographic patterns of mobility as well as explores the possible origins of these non-local individuals and motivations for their movement.

Discussion

6.1 Introduction

Results from the human and faunal Sr isotope analyses show there are non-local individuals present at the Camino del Molino burial site. The local $^{87}Sr/^{86}Sr$ range defines a group of twelve migrant human individuals, who at some point after childhood moved near to the burial site. The following sections will compare the non-local individuals based on their sex and age at death to identify any demographic based mobility patterns. Trends between the migrant individuals and their layer number will also be examined to observe how migration changed over the course of the burial. The hypothetical origins for the twelve ‘non-local’ individuals are considered as well as the possible motivations for their migration to the Camino del Molino area. This chapter also explores the possibility of mobility occurring within the identified ‘local’ population and what that could signify for the individuals from Camino del Molino and their society. The final section considers the broader social and economic implications of the mobility and migration identified at this site as well as its links to other parts of the Iberian Peninsula.

6.2 Human Mobility Patterns

6.2.1 Sex-based patterns

In the sample population, there are 19 identified females, 26 males, and 35 unsexed adults. For all three of these categories, the $^{87}Sr/^{86}Sr$ data are normally distributed and have a positive skew. The male, female, and unsexed $^{87}Sr/^{86}Sr$ averages are very similar at 0.709300 (s.d. = 0.001529), 0.709348 (s.d. = 0.003201), and 0.709273 (s.d. = 0.001774), respectively. The female results had a higher Sr isotope variance (σ^2 = 0.00001, range = 0.13336) compared with the males (σ^2 = 0.000002, range = 0.005432) or unsexed individuals (σ^2 = 0.000003, range = 0.007202). Based on the defined local range, three females (16% of the sample female population), three males (12% of the sample male population), and six unsexed individuals (17% of the sample unsexed population) are identified as migrant individuals (Table 5.4 and displayed in Figure 6.1). A non-local female (CM 66) produced the highest $^{87}Sr/^{86}Sr$ ratio (0.720961) of the sample population, well above the upper limit of the local Sr range. There is no definite pattern of migrant individuals based on their identified sex. However, this could be affected by the future sex identification of the five unsexed individuals.

Looking at the Sr isotope values of only the individuals within the local limit (Figure 6.2), identified male individuals have a greater variability of Sr ratios than the females or sub-adults. The local male average is 0.708824 with a range of 0.002716 (0.707870-0.710586). Local female individuals have a similar $^{87}Sr/^{86}Sr$ average of 0.708175 but exhibit a more finite range of 0.001342 (0.707625-0.708967). A simple F-test to compare the variances between the sexes found that the local male Sr ratio variation is statistically greater than that of the local females ($F_{22,15} = 3.66$, $p < 0.01$). Part of the identified 'local' male population, therefore, had access to more diverse geological terrain and/or food sources that would produce the sex-specific difference in strontium isotope values. Either they have been misidentified as local due to a broad Sr local limit or there is a sex-specific form of local mobility/food procurement occurring within the

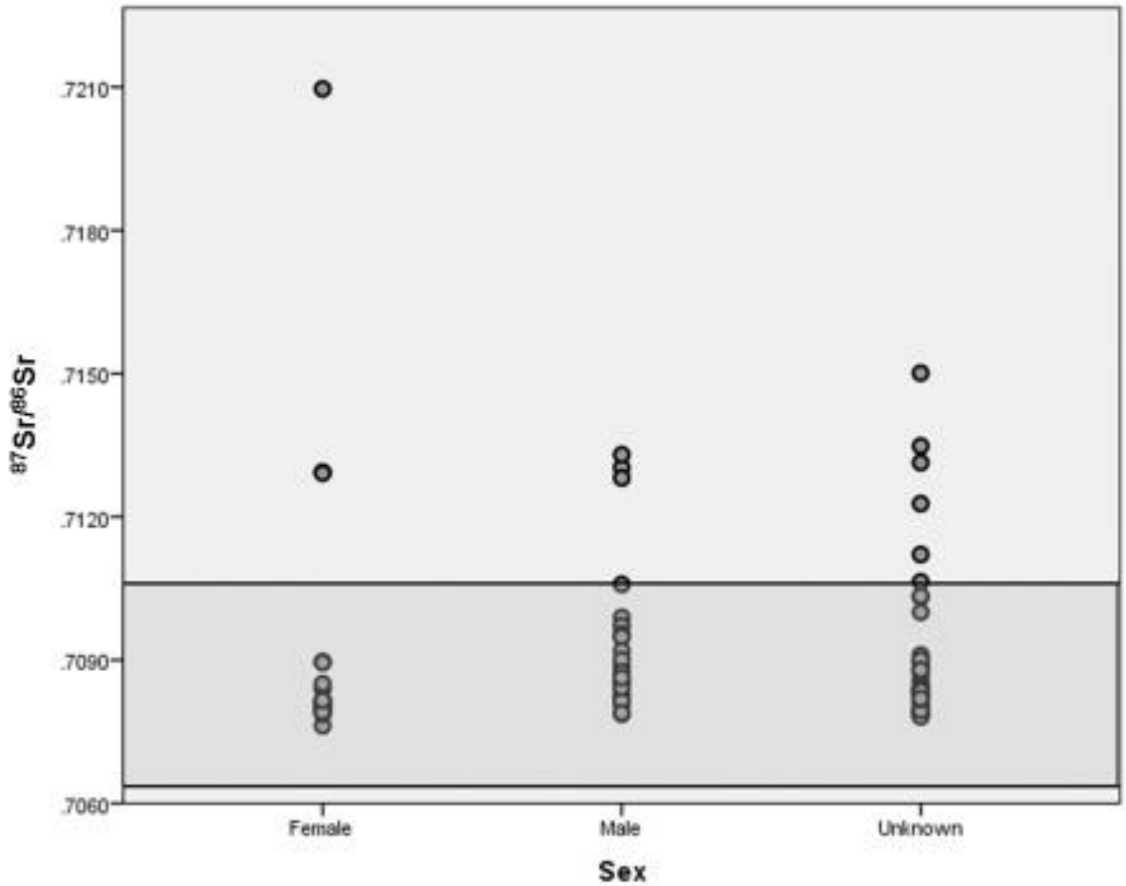

Figure 6.1 Plot of $^{87}Sr/^{86}Sr$ ratio versus sex categories for the Camino del Molino human enamel results, including the Sr local limit of 0.706351-0.710610 to demonstrate the possible sex differences with the identified local and non-local population. Sub-adult samples were not included in this plot. Note that while both female and males are represented in the non-local population, the majority of the non-local population are of unknown sex.

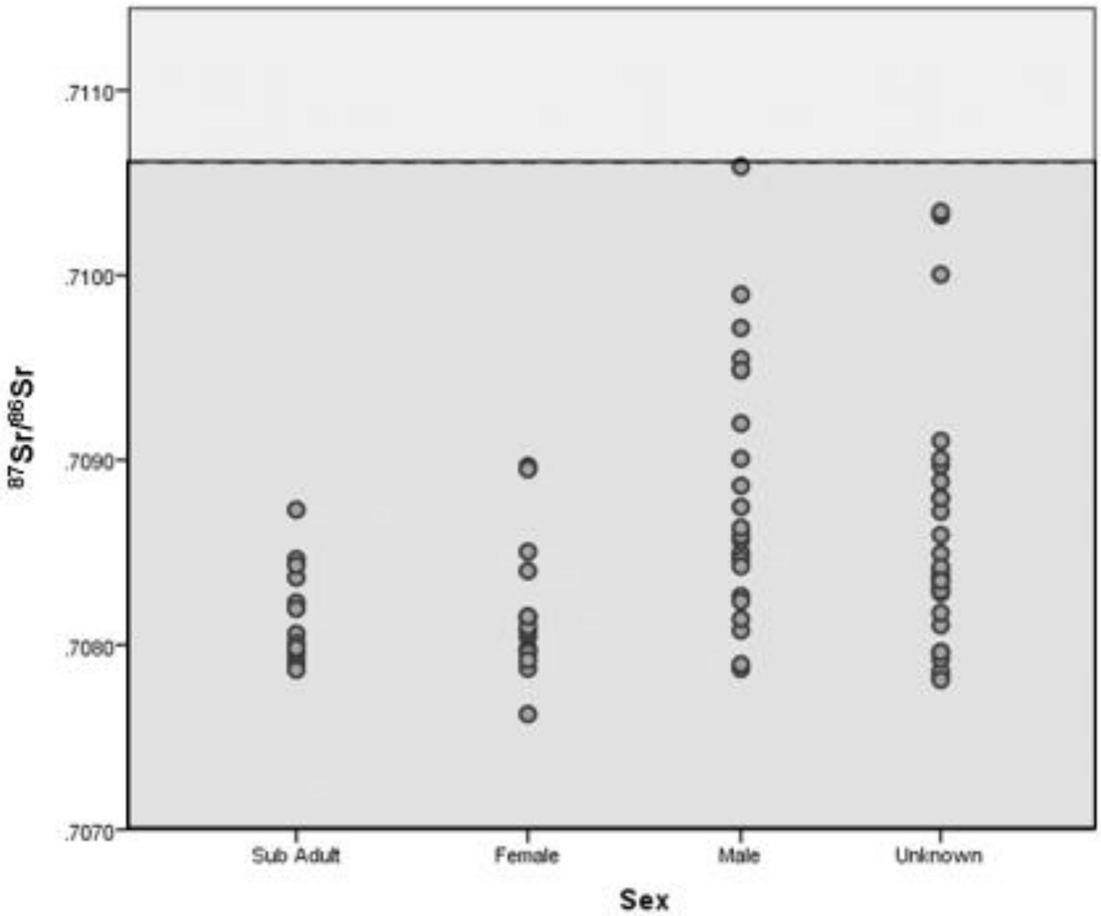

Figure 6.2 Plot of $^{87}Sr/^{86}Sr$ ratio versus sex categories with sub-adult individuals included for only the local Camino del Molino human enamel results. Note the male individuals have more varied $^{87}Sr/^{86}Sr$ results compared with the sub-adult, female, and unknown sex individuals.

population of Camino del Molino. However, this interpretation could vary on the future sex identification of those unsexed individuals.

6.2.2 Age-specific patterns

The sample population was separated into six age categories: child (3-12 years), adolescent (13-19), young adult (20-35), mature adult (36-50), elderly (>51), and adult (20-50). These age-at-death categories are broad for the purpose of showing general demographic trends in the burial. The strontium analyses with age categories are displayed in Figure 6.3.

The child and adolescent groups were underrepresented in the sample population. They contained eleven and five individuals, respectively. The child group had an average $^{87}Sr/^{86}Sr$ ratio of 0.708090 (s.d. = 0.000196). This group had a low variance (σ^2 = 0.00000007) and a small range (0.000598). The adolescents were similar to the child category with an average $^{87}Sr/^{86}Sr$ ratio of 0.708237 (s.d. = 0.000342), but had a more limited range of 0.000813. None of the individuals in these two age categories were found outside of the local limit. This, as well as the limited amount of the $^{87}Sr/^{86}Sr$ variability, suggests that the younger individuals were not highly mobile.

The individuals aged above twenty years are classified as adults. There are twenty-six young adults (fourteen male, ten female), thirteen mature adults (nine male, four female), and two elderly individuals (both male). Thirty-six of the individuals were identified as adults but their ages at death were not defined further. The young adult, mature adult, and adult categories had similar $^{87}Sr/^{86}Sr$ ratio averages of 0.709477 (s.d. = 0.002710), 0.709459 (s.d. = 0.002080), and 0.709250 (s.d. = 0.001753), respectively. The Sr concentration averages of these three categories were also comparable at 136 ppm (young adult), 125 ppm (mature adult), and 142 ppm (adult). The two elderly men both fall within the local range containing Sr ratios of 0.708565 (CM 58) and 0.709007 (CM 84).

All twelve of the identified migrants were adult aged: three were classified as young adults (12% of the sample young adult age category), three as mature adults (23% of the sample mature adult category), and six were adults (17% of the sample adult category). There is no apparent correlation between age at death and sex identity for adults. All three of the young adult migrants (two female, one male) were between the ages of 20-25. This implies that after the age of 8, when the premolar crown is fully mineralized, and before the age of 20-25 these three individuals migrated from their childhood home to the Camino del Molino area. Additionally, despite their identity as new young immigrants, these three were buried in the same location as the local individuals. The three mature adult migrants (two male, one female) ranged in age from 33-51. Their movement from their childhood residence could have been during adolescence, as seen with the young adult group, or later in their adult life. Overall, the only obvious correlation between the $^{87}Sr/^{86}Sr$ ratios and the age of the individuals is that adults are more likely than sub-adults to be non-local.

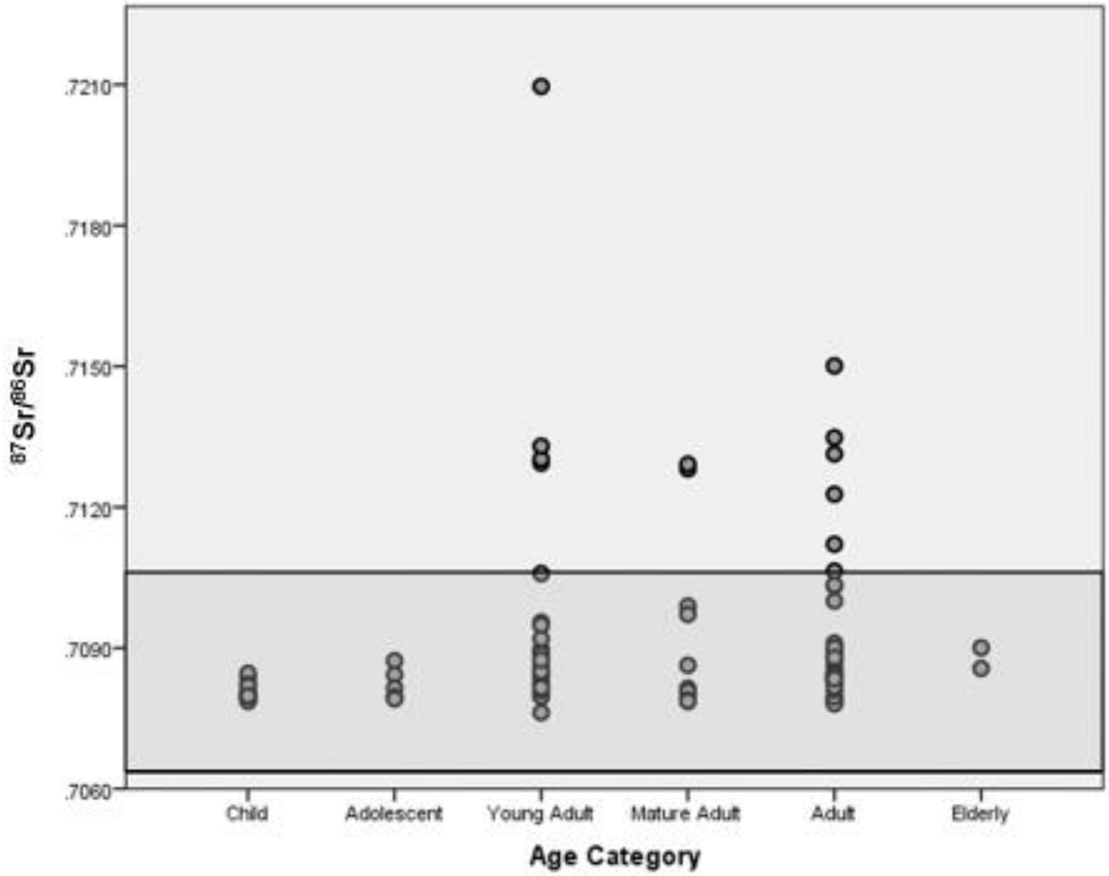

Figure 6.3 Plot of $^{87}Sr/^{86}Sr$ ratio versus age categories for the Camino del Molino human enamel results, including the Sr local limit of 0.706351-0.710610 to demonstrate the identified local and non-local population. Note that only the young adult, mature adult, and adult population are found in the 'non-local' population.

6.2.3 Temporal trends

The burial of Camino del Molino covers roughly 400 years from the mid- to late-Copper Age (2800-2400 BCE). These dates are represented in the layer numbers given during excavation. The oldest at the site is layer 1110, radiocarbon dated to cal. 2800 BCE, and the most recent layer is 1106, dating to cal. 2400 BCE. The Camino del Molino samples in this study were chosen specifically to represent the entire span of the burial.

The human enamel $^{87}Sr/^{86}Sr$ results separated by layer number are plotted in Figure 6.4. The identified migrants are found in almost every layer of the burial: two individuals in layer 1109, three in layer 1108, two in layer 1107, and five in layer 1106. None of the migrant individuals were discovered to be from layer 1110, the earliest interments at the site.

Layer 1109 was the most represented in the sample population (n = 39). There were two female non-locals identified, comprising 5% of this layer. One of these females (CM 66), a young adult, had the highest $^{87}Sr/^{86}Sr$ value within the entire sample population at 0.720961. This Sr ratio is very high for the geology of southeast Spain (Gibbons and Moreno 2002; Hoedemaeker and Leereveld 1995; McArthur et al. 2007; Moiroud et al. 2012), suggesting this individual travelled a great distance to come to the Camino del Molino site. The complete lack of migrants in layer 1110 indicates that migration to Camino del Molino was perhaps not as prevalent during the early stages of the burial. The lack of identified male migrants in layer 1109 may suggest a female-specific migratory pattern then.

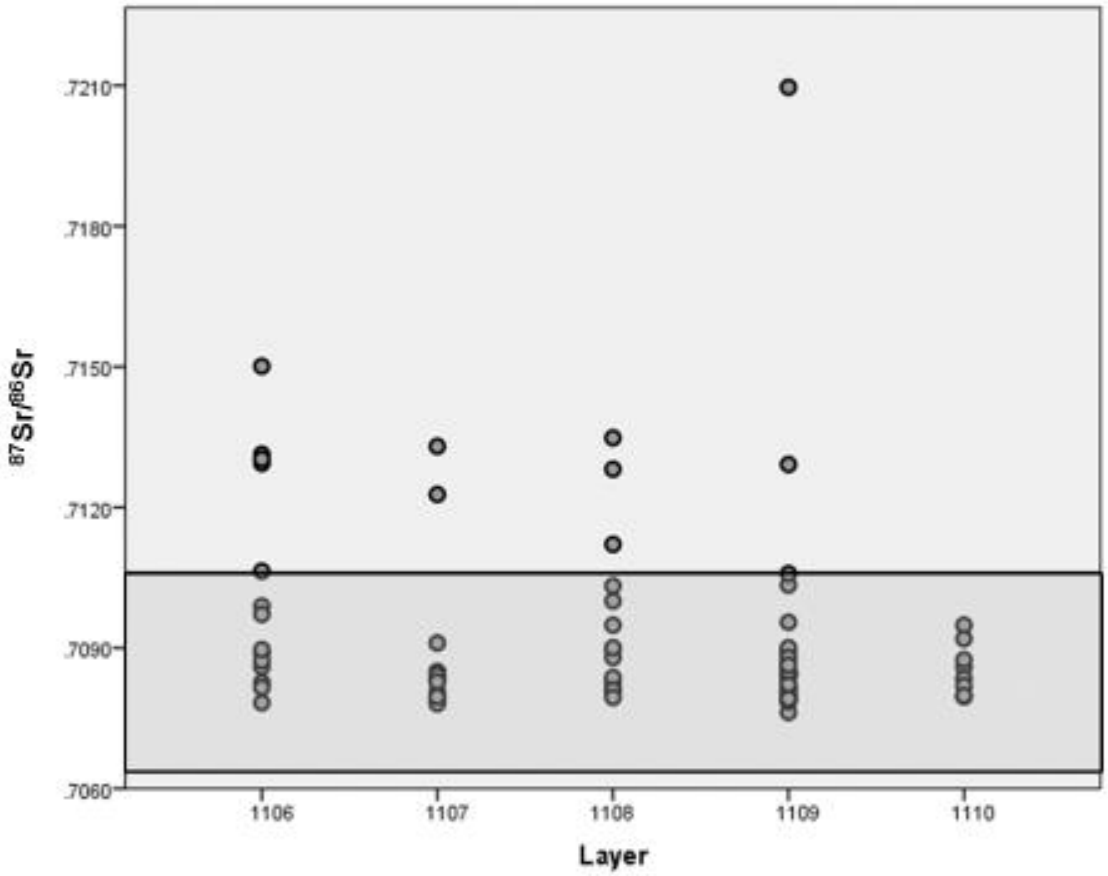

Figure 6.4 Plot of $^{87}Sr/^{86}Sr$ ratio versus the layer number in which the sample was found for the Camino del Molino human enamel results, including the Sr local limit of 0.706351-0.710610 to demonstrate the identified local and non-local population. Layer 1110 is the earliest interments (the oldest layer) and layer 1106 are the final interments (the newest layer). Note that non-local individuals are found present in almost every layer of the site.

In the middle phase of the burial (layer 1108 and 1107), the number and proportion of non-locals identified increase. Two unsexed adults and one mature male adult were found in layer 1108, comprising 20% of the layer's subset. Layer 1107 contained two non-locals (12% of the subset sample): one unsexed adult and one young male adult. This middle phase marks the first presence of identified male non-locals. The absence of identified female migrants in these layers may suggest a male-specific migratory pattern then. However, the lack of sex identification of three of the five identified migrant individuals as well as the low number of male non-locals do not confirm a sex-specific migration pattern during the middle phase of the burial.

The final stages of the burial, layer 1106, contained the majority of the non-local individuals: three unsexed adults, one mature male adult, and one young female adult. There is a large increase in both the number and proportion (36% of the subset) of non-local individuals compared to the previous layers. There are no obvious age- or sex-defined patterns of migration in this layer, but this could be altered by the sex/age identification of the three adults.

Based on these results, migration at Camino del Molino appears to increase as the burial progresses, with the greatest proportion of non-locals found in the final phase, layer 1106. However, there are non-locals identified in almost every layer of the burial (except the initial interments in layer 1110), indicating that migration to Camino del Molino was not just a one-time event. Throughout the layers, there is no strong correlation between the sex of an individual and their identification as a non-local. Female migration was more prevalent during the earlier stages and male more in the middle stages, but without more data, specifically the sex identification of the unsexed ‘non-local’ individuals, this pattern cannot be substantiated.

6.3 Faunal Migration

Animal husbandry is believed to be a present economic practice in southeast Spain during the Copper Age (Chapman 2008; Greenfield 2001; Manzano and Casas 2010; Murrieta-Flores 2014). Canine and ovicaprid (goat/sheep) skeletons present within the Camino del Molino burial are inferred as further evidence of shepherding in the region (Lomba et al. 2009). Strontium isotopic analysis of faunal enamel can provide information on the animals’ seasonal migration patterns (using serial sampling, which was not undertaken in this study) (Britton et al. 2009; Pellegrini et al. 2008; Thornton et al. 2011), their effect on hunting strategies (Britton et al. 2011), or evidence of long-distance exchange networks (Towers et al. 2010). Interpreting the mobility patterns of the Camino del Molino fauna from the Sr isotopic results can lead to a better understanding of the economic and social significance of these animals as well as a potential explanation for the human mobility patterns. The faunal Sr isotope results are separated by species and displayed in Figure 6.5.

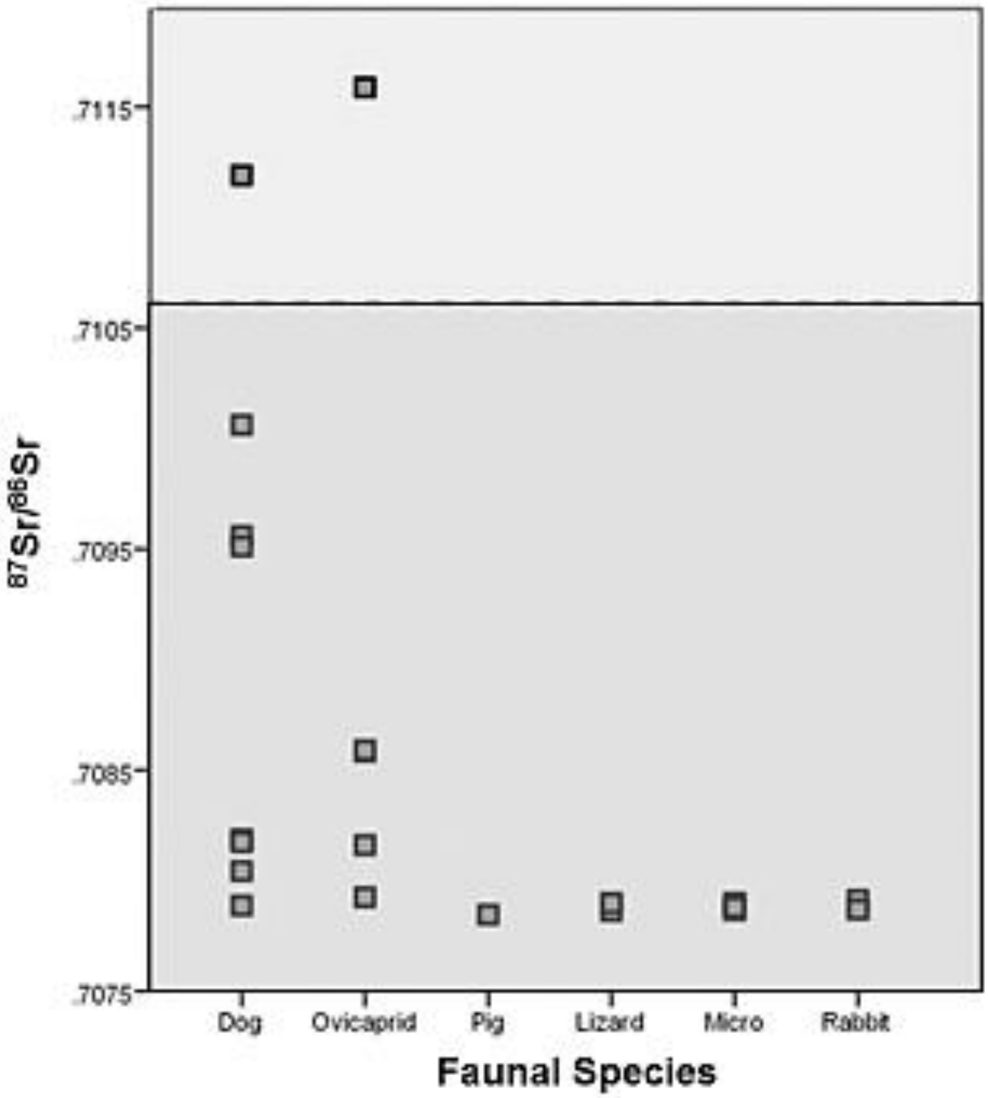

Figure 6.5 Plot of $^{87}Sr/^{86}Sr$ ratio versus faunal species for the Camino del Molino faunal results, including the Sr local limit of 0.706351-0.710610, to demonstrate the identified local and non-local population. Note that two faunal samples, a dog and an ovicaprid, are considered non-local to Camino del Molino.

Two of the Camino del Molino fauna samples were identified as non-local: a dog (CM 115) with a $^{87}Sr/^{86}Sr$ of 0.711190 and an ovicaprid (CM 104) with one of 0.711588 (Table 5.3 & Figure 6.5). These two samples had more radiogenic $^{87}Sr/^{86}Sr$ ratios than the defined bioavailable Sr local limit (0.706351-0.710611) and the estimated geological Sr signature of the region (~0.707-0.709). In addition, the canine and ovicaprid samples produced the highest average $^{87}Sr/^{86}Sr$ ratios of the fauna at 0.709077 and 0.708969, respectively. The evidence of non-local dog and goat/sheep samples could support the presence of shepherding or livestock trade at Camino del Molino. Animals that are part of a mobile herd will have access to different food sources and geological regions that would affect their Sr isotopic values. The small rodent, rabbit, and lizard samples all contained very similar average Sr isotope values (0.707881-0.707885) consistent with the local geological Sr signature and extremely small variances (σ^2 = ~4e-10). These species have smaller home ranges, thereby limiting the geological variation and, as a result, the Sr isotopic values reflect this lack of diversity. The single pig samples also had a Sr ratio consistent with the local geological signature. As pigs are less suitable for long distance migration they are less likely to be involved in mobile pastoralism (Greenfield 2010).

6.4 Non-Local Mobility

6.4.1 Migrant Patterns

The Camino del Molino local strontium limit ranged from 0.706351-0.710611 and identified twelve humans and two fauna as non-local. All of these non-local individuals were found above this range with more radiogenic Sr signatures. The twelve human and two faunal (one dog and one ovicaprid) non-local individuals had $^{87}Sr/^{86}Sr$ ratios between 0.710639-0.720961.

The migrant humans were all adults: three male, three female, and six unsexed. Overall, there is no obvious sex-specific migration pattern. During the earlier stages of the burial (Layers 1110 and 1109), all (n = 2) of the identified non-local individuals were female. Non-local males are only identified in the middle and later stages of the burial. This could indicate females were the primary migrants earlier in the Copper Age, which then switches to a more male-specific mobility in the later Copper Age. However, this claim cannot be substantiated without the sex identification of those six unsexed 'non-locals' or a broader population study of the burial. As the burial progresses, the frequency of migrants increases and half (six of twelve) of the entire migrant population are found in the most recent phase of the site.

The non-local fauna were a dog with an $^{87}Sr/^{86}Sr$ ratio of 0.711190 and an ovicaprid with 0.711588. The other animals with smaller home ranges (the small rodents, rabbits, and lizards) were found between 0.7070-0.7080, which is the approximate expected Sr isotopic range for the geology of marine sedimentary rocks. The sampled fauna were not detailed with a layer number, skeletal analysis or individual burial context. Therefore, it is difficult to discern more specific faunal mobility patterns other than from the different species and the overall time period of when the burial was in use.

Possible places of origin both within and outside southeast Spain are explored in the next section. The $^{87}Sr/^{86}Sr$ ratios of the non-local individuals will be compared to both geological Sr signatures as well as archaeological Sr isotopic studies. Cultural and artifact connections will also be considered to help support these claims.

6.4.2 Potential origins of the non-local individuals

The twelve non-local humans had Sr values ranging from 0.7106-0.7210 and average around 0.7130. In general, the Sr signature of southeast Spain, including the area surrounding Camino del Molino (MacArthur 2007), is dominated by marine sedimentary geology with expected values between ~0.707-0.709 (Gibbons and Moreno 2002; Sealy et al. 1991). The $^{87}Sr/^{86}Sr$ values of the migrants are more consistent with older, more radiogenic geology, such as granites and schists (~0.710-0.740) (Bentley 2004; Bentley 2006; Ericson 1985). However, these are only the broad Sr values from this type of geology and do not reflect the bioavailable Sr. As this is the first southeast Spain Copper Age study of mobility using strontium isotopes, there are no contemporaneous studies to understand the potential bioavailable Sr for other parts of southeast Spain.

The closest comparison in geography and chronology to Camino del Molino is a Sr isotopic study from the Bronze Age site of Las Gatas in southeast Spain (Díaz-Zorita Bonilla et al. 2009; 2012) (Figure 6.6). Eleven human individuals (four male, four female, and three sub-adult) and five rabbit samples were analyzed. Both the human enamel and fauna produced very similar $^{87}Sr/^{86}Sr$ ratios, ranging ~0.7095-0.7102. Therefore, all of the analyzed individuals were identified as local. The Las Gatas local $^{87}Sr/^{86}Sr$ range is too low to be considered as a possible place of origin for non-local individuals buried at Camino del Molino. Therefore, to hypothesize where these migrant individuals may have originated, the results of the Sr analysis are compared with other contemporaneous isotope studies from the Iberian Peninsula but outside of the southeast region.

The first comparison, based on proximity, are three sites in southwest Spain. This region developed similarly to the southeast during the Copper Age (Chapman 2008) and some have proposed the area formed a separate cultural or social group (Nocete Calvo 2001, 2004; Nocete Calvo et al. 2008; Nocete and Peramo 2010). Studies have shown material trade occurring between the two regions as well as similar growth in social hierarchy, animal husbandry, and megalithic funerary structures (García Sanjuán 1999; García Sanjuán and Hurtado Pérez 1997; Hurtado Pérez 1991).

Díaz-Zorita Bonilla (et al. 2009; 2013) analyzed human samples from three Copper Age sites in southwest Iberia: La Pijotilla (Badajoz, Spain) (also within the Ossa-Morena Zone), Valencina-Castilleja (Seville, Spain), and *Tholos* de Palacio III (Seville, Spain) (Figure 6.6). La Pijotilla and Valencina-Castilleja showed material evidence of trade and/or movement from southeast Iberia and beyond. For example, amber from Sicily and ivory or Ostrich egg necklaces from North Africa (Vargas 2004; Costa el al. 2010; Hurtado Pérez & Odriozola 2009). La Pijotilla is situated on Miocene geology, consisting of conglomerates, sandstones, and limestone, and using both the faunal as well as the human enamel Sr values the site was determined to have a local Sr limit of 0.71270-0.715382. Valencina-Castilleja and *Tholos* de Palacio III, found within similar

Lower Pliocene geological substrates, consisting of blue loess and conglomerates, had an estimated local Sr range of 0.70850-0.71050. La Pijotilla and Valencina-Castilleja both contained non-local individuals: five of the seventeen individuals sampled from La Pijotilla and eleven of the thirty-three from Valencina-Castilleja. In comparison, all of the seven human samples from Palacio III were deemed local. Valencina-Castilleja also contained a non-local ovicaprid sample. Díaz-Zorita Bonilla (2013) hypothesized that La Pijotilla and Valencina-Castilleja were connected and all but two of the migrants could be explained as from one of these sites.

Central Iberia 88 samples from singular burials ranging along the tagus river basin from the Neolithic to Bronze Age. Archaeological ties to SE Iberia? Geology was x and x. The local limit was based on the average of the human samples +/-2sd. Local population (mostly) and a slightly higher 0.708-0.712 range with one sample being non local at 0.718. Could be the provenance of some the samples but not the more radiogenic ones.

Western Iberia (the Ossa-Morena Zone) contains geological substrates with expected Sr values ~0.709-0.720 with some areas as high as 0.730 (Azevedo and Nolan 1998; Gibbons and Moreno 2002; Moita et al. 2009) (Figure 6.6). This region is home to the Vila Nova de São Pedro (VNSP) culture that flourished during the Copper Age (Spindler 1981; Paco and Sangmeister 1956; Sangmeister and Schubart 1981; Savory 1972). VNSP shares many similarities to the southeast Spanish Copper Age culture and, in particular, with Los Millares. This culture had agricultural and animal husbandry practices. It is also believed to have contact with the southeast region and other areas of the Iberian Peninsula (Chapman 2008).

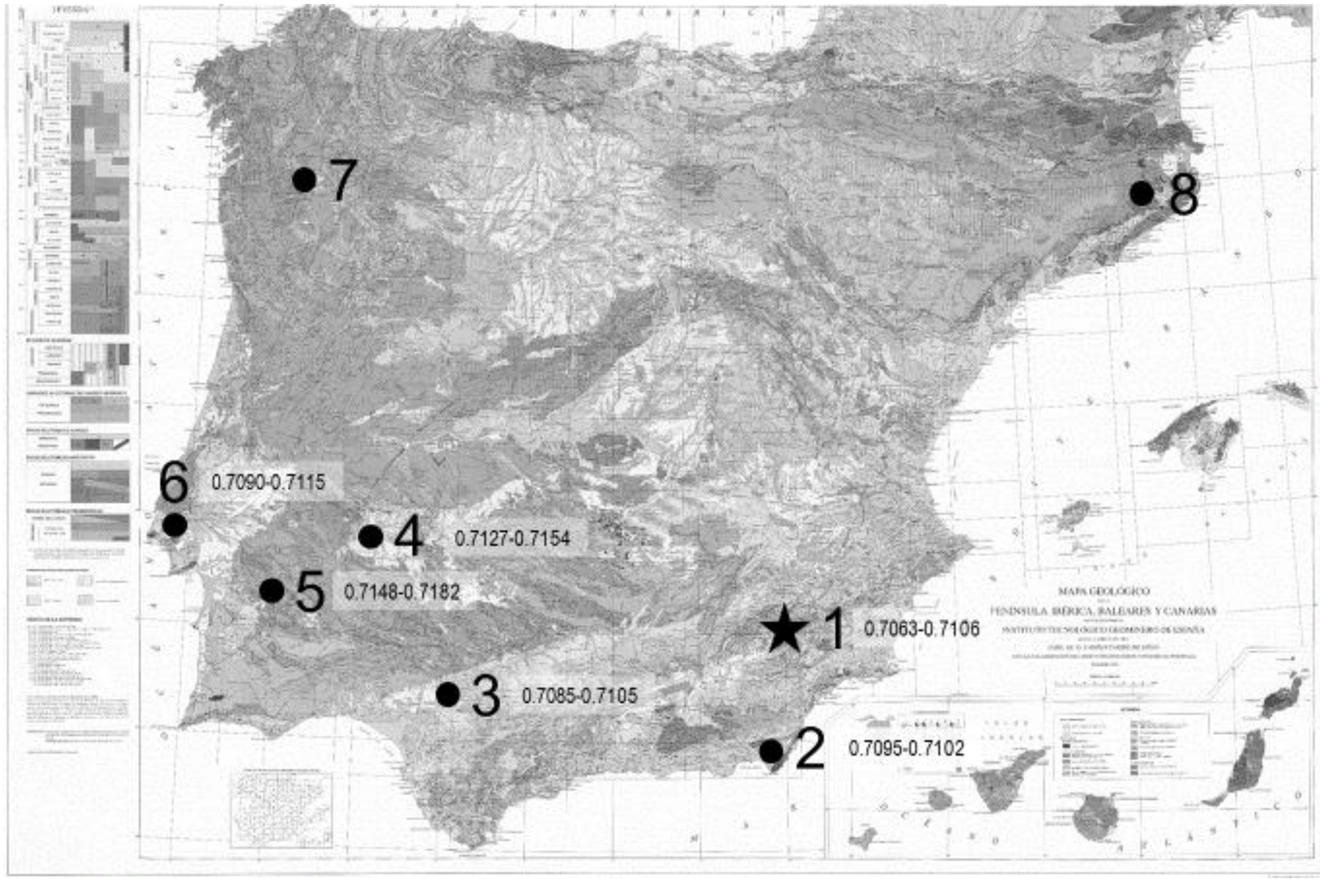

Figure 6.6 Detailed map of Iberian geological substrates to illustrate the potential places of origin for the non-local individuals found at Camino del Molino. Sites with Sr isotope studies have their defined local $^{87}Sr/^{86}Sr$ ranges specified. 1 – Camino del Molino (Lomba et al. 2009); 2 – Las Gatas (Diaz-Zorita Bonilla et al. 2009; 2012); 3 – Tholos de Palacio III and Valencina-Castilleja (Diaz-Zorita Bonilla et al. 2009; 2013); 4 – La Pijotilla (the Ossa-Morena Zone) (Diaz-Zorita Bonilla et al. 2009; 2013); 5 – Perdigoes (the Ossa-Morena Zone) (Hillier et al. 2010); 6 – Seven tombs within the Estremadura region, (Waterman et al. 2014); 7 – Galicia (Carvalho et al. 2012; Mendes and Dias 2004); 8 – Catalan Coastal Range (Navidad et al. 2010).
Adapted from Gibbons and Moreno 2002.

Hillier et al. (2010) analyzed three sites from Portugal: Perdigões, Estria, and Carcavelos (Figure 6.6). Perdigões is located in the region of Alentejo, which consists mainly of Paleozoic granite and schist. Eight human individuals and a small group of fauna (cattle, ovicaprid, pig, and deer) from this site were analysed. The faunal results determined the local Sr limit was 0.7148-0.7182. The majority of the human samples, except for two adult males deemed local, are found to be below the local Sr limit. Estria and Carcavelos are found in the Estemadura region on Cretaceous sedimentary geology, composed mainly of limestone, marl, and sandstone. Eight human samples from Estria and six from Carcavelos were analyzed for Sr analysis. Modern land snails defined the local Sr range for these two sites as 0.7070-0.7081. The majority of the human sample population fell within the local range.

Waterman et al. (2014) collected fifty-five human samples from seven burial sites in the Estremadura region of Portugal: Zambujal, Cova da Moura, Feteira II, Lapa da Rainha II, Bolores, Cabeço de Arruda I, and Paimogo I (Figure 6.6). The sites were all located within 25 km of each other and span the Late Neolithic into the Early Bronze Age. The fauna, in particular the ovicaprid samples, analyzed to determine the local Sr limit produced higher variability than the human results. Therefore, the local range was defined by the mean $^{87}Sr/^{86}Sr$ human enamel isotope ratio ($\pm 2\sigma$), 0.7090-0.7115. Based on this local signature, Cova da Moura and Cabeço da Arruda I were the only two sites that contained non-local individuals. Cova da Moura had four (80% of the sample population) non-locals, including two individuals with enriched $^{87}Sr/^{86}Sr$ isotope ratios of 0.714383 and 0.720730. This burial site is also distinct from the other sites for its relative wealth of foreign goods, such as jet and ivory objects, as well as its long span of use (~ 1000 years) (Cunha et al. 2007; Schuhmacher et al. 2009; Thomas 2011). Waterman et al. (2014) place the origins for the two non-locals with elevated Sr ratios as from the Portuguese interior based on the Hillier et al. (2010) study of Perdigões.

Two other hypothetical Iberian areas for the Camino del Molino migrant individuals are Galicia in the northwest and Catalonia in the northeast (Figure 6.6). However, these areas do not have archaeological Sr studies and greatly reducing their comparative value to the Camino del Molino population. Galicia in northwest Iberia contained a profuse megalithic culture dating from the Neolithic into the early Bronze Age (Gianotti et al. 2011; Valera 2008). The majority of the past work done in this region focused on the ideology of the funerary dolmens and mounds (Criado Boado 1989; Criado Boado and Valcarce 1989; Criado Boado and Villoch Váquez 2000), but recent excavations by commercial archaeology have uncovered domestic settlements and material evidence that shows similarities to other Copper Age Iberian cultures (Bonilla Rodríguez et al. 2006; Criado-Boado and Cabrejas Domínguez 2005; Gianotti et al 2011; Varela 2010; Vilaseco 2009). This region is characterized by granites, schist, and gneiss dating to the early Paleozoic with high expected Sr values ~0.720- 0.750 (Carvalho et al. 2012; Mendes and Dias 2004).

The Catalan Pyrenees also had developed a megalithic culture during the Neolithic and Copper Age that had cultural connections to the rest of the Iberian Peninsula (Aicart Hereu 2006; Geddes 1983; Polo Díaz et al. 2014). However, less archaeological work has been done on the Copper Age sites in this region then the rest of Iberia. As with Galicia, the area has Paleozoic granite and schist geological substrates with high expected Sr isotope values (Navidad et al. 2010).

Southeast Spain as well as other parts of the Iberian Peninsula are shown to have many exotic material goods, such as ivory and precious stones, which originated from Africa and other parts of continental Europe (Chapman 2008; Harrison and Gilman 1977; Harrison and Orozco-Kohler 2001; Hurtado Pérez et al. 2000; Murillo Barroso and García Sanjuán, 2013). For example, Schuhmacher and Banerjee (2012) determined the exact elephant species of some of the Copper Age Iberian ivory artifacts. Southeast Spain was dominated by the Asiatic elephant (*Elephas maximus*), suggesting their trade routes extended into the Middle East. Whereas Portugal and southwest Spanish sites contained almost exclusively African bush elephant (*Loxodonta Africana*), linking these regions to trade with Africa. Interestingly, the ivory found at Los Molinos de Papel, the village associated with Camino del Molino, was from the African bush elephant. This could indicate close connections between Camino del Molino and Portugal, southwest Spain, or, perhaps, even North Africa. It is possible that along with these artifacts people moved to Camino del Molino from North Africa or another part of Europe/the Middle East. However, these are extremely broad areas and without more specific potential origin sites it is currently impractical to explore these migration routes.

Based on the Sr isotopic and geology studies as well as cultural and material connections, there is greater potential that the non-local individuals at Camino del Molino originated from within the broader region surrounding the sites of La Pijotilla in southwest Spain and Perdigões in the Alentejo region of Portugal (Figure 6.6). These two sites are found within the Ossa-Morena Zone, a contact area between cultures of southeast Spain and the Portuguese coast, and contain geological substrates with high expected Sr isotope ratios. La Pijotilla has a local Sr range of 0.71270-0.715382 that fits well with the majority of the Camino del Molino non-local results. Perdigões has a more enriched local Sr signature of 0.7148-0.7182 and could be the initial home for the migrants with higher $^{87}Sr/^{86}Sr$ isotope ratios or as part of a mixed Sr source origin for the less radiogenic migrants.

Both sites, however, did not have Sr local limits that are high enough to be the place of origin for CM 66 (0.720961). The Portuguese coastal site of Cova da Moura contained one individual with a similar $^{87}Sr/^{86}Sr$ isotope ratio of 0.720730. Waterman et al. (2014) explain this radiogenic migrant as from the Portuguese interior based on the older, granitic and schist geology of that region. If not from the Portuguese interior, there is potential that this individual came from Galicia or Catalan based on their geology, or other places on Iberia (see *Fig 6.6*).

6.4.3 'Local' male mobility

The majority (87%) of the Camino del Molino sample population contained $^{87}Sr/^{86}Sr$ ratios within the local Sr limit (between 0.706351-0.710611). These eighty-one individuals were, therefore, considered local to the Camino del Molino area. However, the considerable amount of Sr isotopic variation among the identified local male individuals implies that they were not sedentary and participated in some form of mobility.

Figure 6.2 displays the variation of the local male $^{87}Sr/^{86}Sr$ ratios compared to the sub adult, female, and unsexed individuals within the local population. As stated in the previous section (*6.2.1 Sex-based Mobility Patterns*), the $^{87}Sr/^{86}Sr$ ratios of the local population produced higher variance in identified males than in the females. The local male $^{87}Sr/^{86}Sr$ range (= 0.002716) was over twice that of the local female range (= 0.001342). The local unsexed individuals showed a similar range to the male subset. Three of these unsexed individuals have $^{87}Sr/^{86}Sr$ ratios on the upper limit of the Sr local range. Based on the assumption that males within this local population will produce higher Sr values, these three individuals are more likely to be identified as male.

Similar to the identified non-local individuals, this local mobility pattern contained only adults. There is no obvious correlation between the adult age category and this male-specific Sr isotopic variance. Mature adult, young adult, and adult local male categories showed similar Sr isotope ranges. It is important to remember that these are adult individuals but the Sr values were incorporated during tooth mineralization in childhood. Therefore, the Sr isotopic variation and disparity between the sexes seen in the data represents childhood differences.

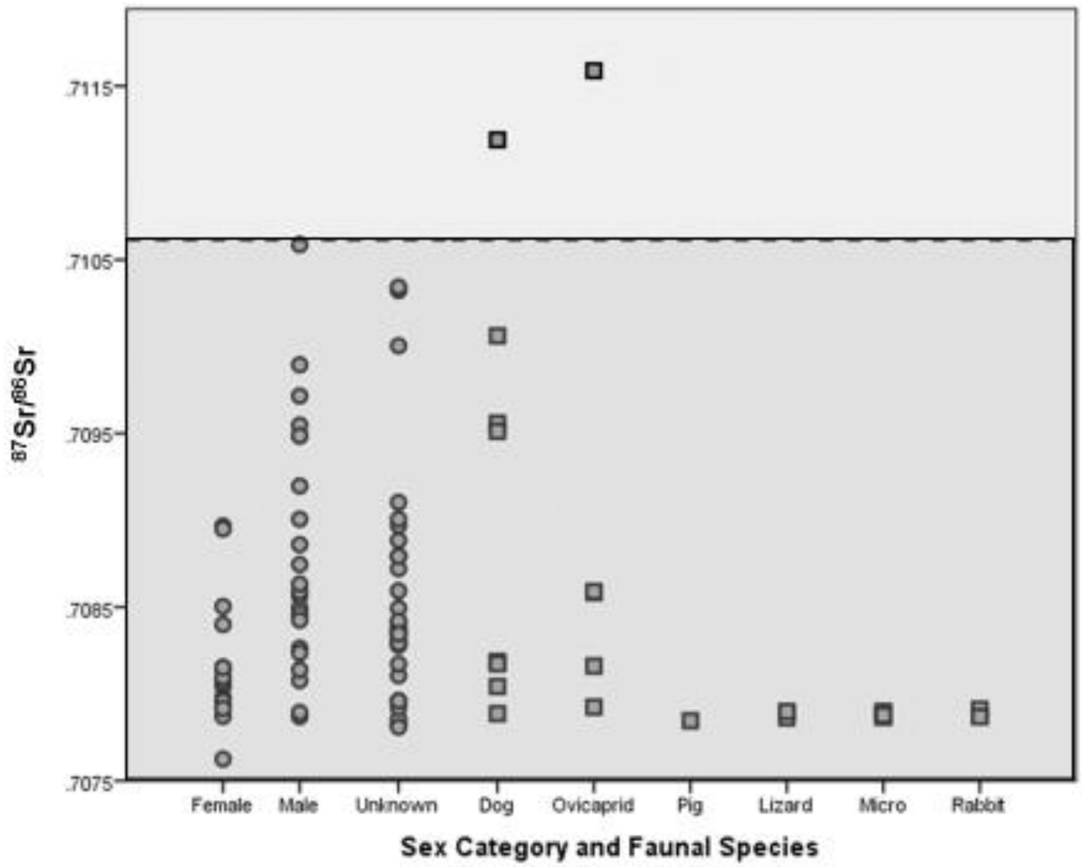

Figure 6.7 Plot of $^{87}Sr/^{86}Sr$ ratio versus sex categories of the local Camino del Molino human population as well as the species categories of the faunal samples from Camino del Molino, including the Sr local limit of 0.706351-0.710610, to demonstrate the $^{87}Sr/^{86}Sr$ ratio variation within all of the categories. Note that males, unknown sex, and dogs contain the highest degree of variation.

Several Iberian archaeological studies have also concluded that male individuals were more mobile than female individuals. In the 1950s, Buikstra and Hoshower (unpublished, cited in Chapman 2003: 202) examined skulls from the El Argar Bronze Age population of southeast Spain. The data showed a greater morphological heterogeneity in male skulls, indicating that there was a greater presence of non-local males at El Argar. This was assumed to be as a result of matrilocality, where husbands would move to their wives' settlements, a practice that was believed to have arisen during the transition to the Bronze Age. Another study from the southeast Spanish Bronze Age (Motilla del Azuer, Daimiel, Spain) found several male skeletons had markings suggestive of intense walking or physical exertion, whereas the females analyzed did not (Jiménez-Brobeil et al. 2004). This was interpreted as evidence for a gendered division of labour; women were involved in domestic centric activities and men engaged in more strenuous duties outside of the home, possibly in foreign regions. Boaventura (2011) discusses the artifact circulation in the Estremadura region of Portugal during the Late Neolithic and claims the travelers who made these exchange journeys were mainly males. His claim is supported by ethnographic accounts of gender division of labour and the above stated studies from southeast Spain, though he provides no new or concrete evidence of male mobility.

The Sr results from Camino del Molino provide direct evidence for male mobility in childhood and support a possible gender division of labour. In theory, females would have participated in more sedentary duties around the settlement and males were found more often in activities external to their home. However, the Sr data also demonstrate that this division was not definite. Female individuals were equally represented in the non-local population and males also contained local $^{87}Sr/^{86}Sr$ signatures.

Local male $^{87}Sr/^{86}Sr$ ratios ranged from 0.707870-0.710586. The Camino del Molino area is comprised primarily of marine sedimentary rock with an expected local strontium signature ranging between ~0.707-0.708 (Bentley 2001; MacArthur 2007; Wright 2005). Therefore, this isotopic variation is only possible through Sr enriched food imported to the Camino del Molino area or by the movement of the male individuals from a more radiogenic geology. Two of the fauna were identified as non-local to Camino del Molino, a dog and a sheep/goat, with $^{87}Sr/^{86}Sr$ ratios higher than the local limit. This indicates that there were animals with more radiogenic Sr signatures but not in high numbers. It is more likely the heterogeneity in the local male Sr values are the result of mobility rather than imported food.

Mobility within the southeast Spanish region could be the source of this local male variation. In general, the Sr signature is dominated by seawater values of 0.7092 along the coast (Hodell et al. 2004; Wright 2005) and marine sedimentary geology inland with expected values up to ~0.709 (Gibbons and Moreno 2005; Sealy et al. 1991). The Bronze Age Sr isotopic study from Las Gatas established the local Sr range to be 0.7095-0.7102 (Díaz-Zorita Bonilla et al. 2009) (Figure 6.6). A childhood residence along the coast could produce Sr values closer to 0.709 or higher as demonstrated at Las Gatas. Another possibility is that these males could be moving from the same region as the migrant population of Camino del Molino. However, due to their lower Sr isotope ratios, these individuals would have had a mixed Sr source, possibly moving to the Camino del Molino area earlier during tooth mineralization.

6.4.4 A transhumance model for Camino del Molino mobility

The presence of ovicaprid and canine fauna within the burial of Camino del Molino, as well as the material evidence for secondary products in the village of Los Molinos de Papel, supported the theory that pastoralism was an important economic practice at these sites (Lomba et al. 2009; Martínez 2005). The discovery of over fifty canid skeletons among the human interments suggested that these individuals were participating in shepherding. Transhumance, a form of shepherding or mobile pastoralism, is defined as the seasonal migration of domesticated herds, usually between different altitudes (Braudel 1966; Geddes 1983). It has historically been an important economic adaption to the Iberian landscape of valleys and mountains, particularly in regions with poor soil for agriculture (Alfaro Giner 2001; Cabo Alonso 1992). Herding routes, or droves, were already well established by the Iron Age and it has been assumed that these pastoral practices began sometime during the Copper Age (Chapman 1979; Criado Boado and Vaquero Lastres 1993; Davidson 1980; Walker 1983). Transhumance provides an explanatory model to frame the mobility patterns seen within the population of Camino del Molino. Animals that are part of a mobile herd and the humans tending to them will have access to different food sources and geological regions that would affect their Sr isotopic values.

The Camino del Molino Sr isotope results identify two non-local fauna, twelve non-local human individuals, and a greater $^{87}Sr/^{86}Sr$ isotope variation among the local male population. The identification of a non-local dog and ovicaprid, as well as these two species containing the most varied Sr isotope ratios among the fauna, establish evidence of shepherding. The canid samples also show a similar $^{87}Sr/^{86}Sr$ spread to the local male and unsexed individuals, indicating a connection between the mobility patterns of dogs and male individuals at Camino del Molino (Figure 6.7). Historically, Iberian transhumance has been a male dominated field, with solitary men and boys tending to the herds, whereas females and non-pastoral males would remain with the family's permanent settlement to look after the agricultural and domestic duties (Braudel 1966; Collantes 2009; Diago 1994; Diago 2002; Moreno 2000; Pérez Romero 1996). Furthermore, southeast Spanish Bronze Age studies have indicated that males exhibit a higher degree of mobility than females (Buikstra and Hoshower; unpublished, cited in Chapman 2003: 202; Jiménez-Brobeil et al. 2004). This sex discrepancy is visible within the Camino del Molino Sr results. Activities of the local males meant access to more diverse geology compared to the females, indicating that shepherding was a gendered practice during the Copper Age.

In exploring potential origins for those non-local individuals, the most probable sources, using the scarce published material on bioavailable Sr from Iberia, were the sites of Perdigões in the Alentejo region of Portugal and La Pijotilla in southwest Spain (Figure 6.6). The broader region surrounding these sites (the Ossa-Morena Zone) is an area unsuitable for wide spread agricultural development and, therefore, shepherding became a central industry (Duque Espino 2005; Fairén Jiménez 2004; Moreno Rey 1998; Rodriguez Vidal et al. 2001; Rodríguez Vidal et al. 2003; Pérez Macías 1983; García Sanjuán 1999). Transhumance allows for the depleted resources to rest and regrow by moving seasonally to new pastures (Manzano and Casas 2010). Copper Age studies in southwest Spain have confirmed that transhumance was not only occurring but was already a prominent socioeconomic activity in the area (Duque Espino 2005; Galán Domingo & Ruíz-Gálvez 2001; Murrieta-Flores 2007, 2011, 2014; Rodríguez Vidal et al. 2001). Shepherds from Perdigões and La Pijotilla, in search of good pastureland, could have found it in the area around Camino del Molino. This region has a strong rainfall seasonality and, as a result, contains a high content of nutrients for grazing herds (Clary 2008; Fryxell and Sinclair 1988; Manzano and Casas 2010). Correspondingly, herds from Camino del Molino could seek new pastureland in the Ossa-Morena Zone. Historically, the Ossa-Morena Zone was the most common winter pasture for the Iberian Peninsula and pastoralists would drive their herd more than 600 km one way to reach it (Collantes 2009). The surrounding area of Camino del Molino, therefore, could have served as a herding station as the animals migrated between the Ossa-Morena Zone and southeast Spain (or other parts of the Iberian Peninsula), creating a seasonal pastoral orbit linking these two regions.

A pastoral orbit is defined as the regular and repetitive movement of herds through a large-scale territory, consisting of settlements, herding stations, and paths (Frachetti 2006). This movement is not aimless; herders migrate on fixed routes to places with known resources and established familial ties (Chapman 1995; Saxe 1970).

Connecting one’s family and ancestry to routes and stations allows herds to acquire and maintain access to needed resources. A shepherd, therefore, belongs to an extended community, which includes the people and places within their pastoral orbit.

Family connections could be formed through marriage between pastoral communities. Marriage between individuals from Camino del Molino and the Ossa-Morena Zone would help guarantee access to the settlements, herding stations, and other resources on both sides of the marriage. Furthermore, it could explain why non-local individuals are interred at Camino del Molino and indistinguishable from the identified local individuals. The foreign partner of a marriage alliance would be accepted as part of the local community and, therefore, buried as one of them. However, these familial connections must extend beyond settlements, for a transhumant herd needs access to resources throughout the network of droves. Murrieta-Flores (2011, 2014) studied the spatial organization of Copper Age transhumance routes and discovered that megalithic tombs were clearly the most common archaeological feature associated with them. It is believed that the tombs acted as a physical and social marker for the migrating shepherds, indicating the group’s territorial boundaries through their ancestors. If this link between droves and burials carries to pastoral communities associated with southwest Spain then it could also explain the presence of non-local individuals interred at Camino del Molino. Despite being isotopically non-local, these individuals would have belonged to this larger pastoral orbit and, as a result, could have been considered a type of local to the Camino del Molino people. Furthermore, the interment of a non-local from the Ossa-Morena Zone would have strengthened the communal and ancestral ties between these distant settlements. In practical terms, this would also be beneficial for the herd if a shepherd were to die during migration. The deceased would have a suitable burial that was connected to their pastoral ancestors and the herd would not need to transport the body back to the individual's birthplace.

The pastoral connection between Camino del Molino and the Ossa-Morena Zone is further supported by the foreign material goods present at Los Molinos de Papel. The ivory artifacts from the village site were identified as from the African bush elephant, which was found almost exclusively in southwest Spain and Portugal, instead of the Asiatic elephant, found only in southeast Spain (Schuhmacher and Banerjee 2012). The lack of ivory from southeast Spain, interestingly, distances Camino del Molino culturally from its geographic region and associates it closer with the Ossa-Morena Zone. This ivory could have been a marriage gift or part of an exchange to solidify the relationship between these pastoral communities. Or these artifacts could have arrived as the result of trade. Historically, pastoralists are known to have engaged in trade because of their chosen employment's requirement to migrate great distances (Collantes 2009).

Over the span of the Camino del Molino burial, there is an increase in the number of non-local individuals. This increase is not seen in the local male population, indicating that it may not just be the result of intensified shepherding but perhaps also a by-product of the practice. As transhumance and the routes used became more established in Iberia, it would improve the social connections between the settlements within the seasonal orbit and reduce the difficulties associated with traveling such distances.

6.5 Conclusion

The Sr isotope results and identified mobility patterns for this study support the presence of transhumance and provide insight into the cultural implications of their movements. Transhumance was an economic and social mobility system, which moved people, animals, and goods to and from Camino del Molino. However, more than that it acted as a central industry that affected gender roles, community inclusion, and foreign relations. Movement from shepherding was a fundamental part of the culture and economy for this site, despite increasing sedentary practices. Through mobility their ecological, economic and social identities were created, shaped, and maintained.

Conclusions

7.1 Summary of Results

The purpose of this study was to explore mobility at the southeast Iberian Copper Age burial site of Camino del Molino using strontium isotope analysis. The large number of interred, the broad demography of the human as well as faunal remains, the temporal span and the contextual preservation of this site made it an advantageous sample population to study. The local Camino del Molino Sr range, defined through faunal Sr isotope ratio results, identified twelve humans and two fauna as non-local or migrants. The two non-local fauna were an ovicaprid and a canid sample. The migrant humans were all adults with sex equally represented: three male, three female, and six unsexed. There does not appear to be a sex-specific migration pattern for the non-local individuals. Migrants are found throughout the site but as the burial progresses the rate of mobility increases with six of the twelve migrants being found in the final layers. The local male population had a greater Sr isotope variation in comparison to the local female population. These results indicate a higher degree of male mobility, despite these individuals being identified as local. Local male mobility occurs throughout the burial sequence and supports a possible gendered division of mobility related to transhumance practices. However, the Sr data also demonstrate that this division was not definite. Female individuals were equally represented in the non-local population and males also contained local $^{87}Sr/^{86}Sr$ signatures.

The Sr isotope results of the migrant individuals as well as the more radiogenic local males were compared with other contemporaneous Iberian Sr isotope studies to determine their possible origins. The non-local $^{87}Sr/^{86}Sr$ ratios were higher than the local Sr limit for Camino del Molino and suggested a childhood spent outside of the southeast Spanish region. The Ossa-Morena Zone sites of La Pijotilla (Díaz-Zorita Bonilla 2013) and Perdigões (Waterman et al. 2014) in the southwest region of the Iberian Peninsula contained local Sr signatures consistent with the majority of the Camino del Molino migrants. One non-local individual, CM 66, had a high $^{87}Sr/^{86}Sr$ ratio that was not comparable to the archaeological Sr isotope studies from the Iberian Peninsula. Using expected geological Sr values, it is possible that this individual originated from a more radiogenic part of the Ossa-Morena Zone, Galicia, the Catalan coastal range, or elsewhere.

The mobility patterns identified through this Sr isotope analysis support already held beliefs of southeast Iberian Copper Age society but also reveal new connections. The Sr isotope results endorse transhumance as an important, perhaps even central, economic practice at Camino del Molino. Pastoralists migrate with their herds between settlements and pastures, constructing and maintaining social and economic connections with distant places through this mobility. The migrant human individuals, as well as the two non-local fauna, had $^{87}Sr/^{86}Sr$ isotope ratios consistent with sites from the Ossa-Morena Zone. This implies that Camino del Molino was potentially connected closely with the Ossa-Morena Zone, most likely through transhumant mobility. This relationship was likely strengthened through alliances as well as burial practices. Additionally, it created a broad communal identity for the people of Camino del Molino that extended to the Ossa-Morena Zone and throughout this pastoral orbit. The seasonal migration of the herds was fundamental to the maintenance of the economic and social identities for those within this pastoral orbit. The gendered division of labour and mobility created gendered spaces. Females remained with the permanent domestic settlement, whereas males had their place in the mobile economy and in foreign relations. This gendered mobility possibly had an impact on the southeast Iberian culture into the Bronze Age (Buikstra and Hoshower unpublished, cited in Chapman 2003: 202; Jiménez-Brobeil et al. 2004).

7.2 Limitations of the Study

This research is the first step towards a better knowledge of Copper Age mobility patterns in southeast Iberia from isotope analysis. The Sr analysis results of this study are significant for understanding the mobility of the individuals interred at Camino del Molino but it was not without its limitations. At the burial site, the human and fauna remains were commingled and damaged in many cases. Samples for this study were chosen from those best preserved and clearly individualized for demographic identification. Sample selection, therefore, limited who was analyzed as well as the number of samples for this study. Furthermore, despite being chosen for their preservation, there is incomplete demographic information on all of the individuals which hindered a complete understanding of the mobility patterns. For example, the sex identification of all the non-local individuals would provide support for a possible shift from female-centric to male-centric migration in the later stages of the burial. With the discovery of non-local fauna at Camino del Molino, the local Sr limit created is potentially too broad and reduces the number of identified migrant individuals. As this is the first Sr isotope study of southeast Iberian Copper Age mobility there was understandably a lack of contemporaneous isotope studies with which to compare the Camino del Molino Sr results or to better understand the region's bioavailable Sr signature. This paucity of comparable data, even from other time periods of southeast Spanish history, has prevented any possible connections to be made between Camino del Molino and other sites within the southeast region. More bioavailable Sr data should be collected from other sites in southeast Iberia to further assess the mobility among Copper Age populations within this region.

7.3 Future Considerations

The results of this research have been a successful first step to reconstructing southeast Iberian Copper Age mobility patterns using Sr isotope analysis. It has shown that movement played an integral role in the ecological, economic, and social management of this region. However, there is still more work to be done.

Beginning with the study site, it is recommended that the unsexed sample individuals be re-examined. If the demographic information can be ascertained from the entire sample population through skeletal morphology or DNA analysis then the already identified, as well as the potential, mobility patterns can be substantiated. Additionally, more human and faunal samples from Camino del Molino should be analyzed for $^{87}Sr/^{86}Sr$ isotope ratios to verify the interpretations presented here. It would also be interesting to obtain tooth samples from the individual burials found at Los Molinos de Papel to observe how they compare to those within the communal burial.

As this is the first Sr isotope analysis of a southeast Iberian Copper Age population, more Sr isotope studies are needed to understand the region's bioavailable Sr signatures. Without this data, it is not possible to do inter-site comparisons and, therefore, inter-regional connections cannot be made. Through the Sr results of this study, Camino del Molino has been connected to the Ossa-Morena Zone. Sr isotope analysis of the human remains from the megalithic tombs along the pastoral routes between these two areas may yield comparative information concerning their relationship and the pastoral orbit.

Transhumance has been interpreted in this study as a central socioeconomic activity that defined the mobility of the individuals from Camino del Molino and their relationship to the Ossa-Morena Zone. To verify this interpretation, it is would be advisable to analyze more ovicaprid and canid samples from Camino del Molino and serial sample those identified as non-local. Serial sampling is a technique that obtains enamel from regular intervals along the length of the tooth (Balasse and Ambrose 2002; Britton et al. 2009). This meticulous technique reveals the seasonal Sr isotope ratios for the fauna and could show a more detailed pattern of herd migration. Additionally, ovicaprid and canid species samples should be included in future Sr analysis of Copper Age sites from southeast Spanish and the Ossa-Morena Zone.

Outside of future Sr isotope analysis, the social interpretations from the Camino del Molino results identify a need for collaborative studies with sites in the Ossa-Morena Zone. The pastoral orbit between the Ossa-Morena Zone and Camino del Molino has opened questions of local and group identity in Copper Age Iberia. Do cultural interpretations from Camino del Molino, such as the gendered division of labour, hold true in the Ossa-Morena Zone? What role does a pastoral orbit play in group social identity? Were the identified non-local individuals considered to be local, or at least a type of local, by the people of Camino del Molino?

The results of this research are the first step to reconstructing past mobility patterns in southeast Iberia during the Copper Age. Future strontium isotope studies in southeast Iberia, the Ossa-Morena Zone, and other Iberian regions will continue to build on this work and expand on the interpretations presented here.

References

Åberg, G. (1995). The use of natural strontium isotopes as tracers in environmental studies. *Water, Air and Soil Pollution, 79*, 309-322.

Aguirre, J., Braga, J. C., & Martín, J. M. (2007). El Mioceno marino del prebético occidental (Cordillera Bética, SE de España): Historia del cierre del estrecho norbético. In J. M. Aguirre, M. Company & F. J. Rodríguez-Tovar (Eds.), *XIII Jornadas de la Sociedad Española de Paleontología: Guía de excursiones. Instituto geológico y minero de España* (pp. 53-66). Granada: Universidad de Granada.

Aicart Hereu, F. (2006). *Agustí casas i l'arqueologia de les gavarres*. Monells: Consorci de les Gavarres.

Alfaro Giner, C. (2001). Vías pecuarias y romanización en la península ibérica. In J. Gomez-Pantoja (Ed.), *Los rebaños de gerión: Pastores y trashumancia en Iberia antigua y medieval* (pp. 215-232). Madrid: Casa de Velázquez.

Almagro Basch, M., & Arribas, A. (1963). *El poblado y la necrópolis megalíticos de Los Millares (Santa Fe de Mondújar, Almería)*. Madrid: Bibliotheca Praehistorica Hispana.

Almagro Gorbea, M. J. (1973). *Los ídolos del bronce I Hispano*. Madrid: CSIC.

Andersson, P., Löfvendahl, R., & Åberg, G. (1990). Major element chemistry, δ^2H, δ^{18}O and ^{87}Sr/^{86}Sr in a snow profile across Scandinavia. *Atmospheric Environment, 24*, 2601-2608.

Anthony, D. (1990). Migration in archaeology: The baby and the bathwater. *American Anthropologist*, *92*, 895-914.

Aranda, G., & Molina, F. (2006). Wealth and power in the bronze age of the south-east of the Iberian Peninsula: The funerary record of Cerro de la Encina. *Oxford Journal of Archaeology, 25*(1), 47-59.

Arribas, A., Pareja, E., Molina, F., Arteaga, O., & Molina Fajardo, F. (1974). *'Excavaciones en el poblado de la Edad del Bronce 'Cerro de la Encina' (Monachil, Granada). el corte estratigráfico nº 3', Excavaciones Arqueológicas en España, 81*. Madrid:

Arsenault, L. R., & Robinson, B. W. (1989). The dentino-enamel junction: A structural and microananalytical study of early mineralization. *Calcified Tissue International, 45*, 111-121.

Aufderheide, A., & Wittmers Jr., L. E. (1992). Selected aspects of the spatial distribution of lead in bone. *Neurotox*, *13*, 809-820.

Aura, J. E., Jordá, J. F., & Fortea, F. J. (2006). La Cueva de Nerja (Málaga, España) y los indicios del solutrense en Andalucía. . *Zephyrus, 59*, 67-88.

Azevedo, M. R., & Nolan, J. (1998). Hercynian late-post-tectonic granitic rocks from the Fornos de Algodres area (northern central Portugal). *Lithos, 44*(1-2), 1-20.

Bacon, J. R., & Bain, D. C. (1995). Characterization of environmental water samples using strontium and lead stable-isotope compositions. *Environmental Geochemistry and Health, 17*, 39-49.

Balasse, M., & Ambrose, S. H. (2002). The seasonal mobility model for prehistoric herders in the south-western cape of South Africa assessed by isotopic analysis of sheep tooth enamel. *Journal of Archaeological Science, 29*, 917-932.

Beard, B. L., & Johnson, C. M. (2000). Strontium isotope composition of skeletal material can determine the birthplace and geographic mobility of humans and animals. *Journal of Forensic Science, 45*(5), 1049-1061.

Beeley, J. G., & Lunt, D. A. (1980). The nature of the biochemical changes in softened dentine from archaeological sites. *Journal of Archaeological Science, 7*, 371-377.

Bentley, R. A. (2006). Strontium isotopes from the earth to the archaeological skeleton: A review. *Journal of Archaeological Method and Theory, 13*(3), 135-187.

Bentley, R. A., Krause, R., Price, T. D., & Kaufmann, B. (2003). Human mobility at the early Neolithic settlement of Vaihingen, Germany: Evidence from strontium isotope analysis. *Archaeometry, 45*(3), 471-486.

Bentley, R. A., Price, T. D., & Stephan, E. (2004). Determining the 'local' $^{87}Sr/^{86}Sr$ range for archaeological skeletons: A case study from Neolithic Europe. *Journal of Archaeological Sciences, 31*, 365-375.

Blum, J. D., Taliaferro, E. H., Weisse, M. T., & Holmes, R. T. (2000). Changes in Sr/Ca, Ba/Ca and $^{87}Sr/^{86}Sr$ ratios between two trophic levels in two forest ecosystems in the northeastern U.S.A. *Biogeochemistry, 49*, 87-101.

Boaventura, R. (2011). Bodies in motion: Implications of gender in long-distance exchange between the Lisbon and Alentejo regions of Portugal in the late Neolithic. In K. T. Lillios (Ed.), *Comparative archaeologies: The American southwest (AD 900-1600) and the Iberian Peninsula (3000-1500 BC)* (pp. 209-220). Oxford: Oxbow Books.

Bocherens, H., Brinkman, D. B., Dauphin, Y., & Mariotti, A. (1994). Microstructural and geochemical investigations on late Cretaceous Archosaur teeth from Alberta, Canada. *Canadian Journal of Earth Sciences, 31*(5), 783-792.

Boivin, G. P., Deloffre, P., Perrat, B., Panczer, G., Boudeulle, M., Mauras, Y., Meunier, P. J. (1996). Strontium distribution and interactions with bone mineral in monkey iliac bone after strontium salt (S 12911) administration. *Journal of Bone and Mineral Research, 11*, 1302-1311.

Bonilla Rodríguez, A., Vila, M. C., & Fábregas Valcarce, R. (2006). Nuevas perspectivas sobre el espacio doméstico en la prehistoria reciente del NO. *Zephyrus, 59*, 257-273.

Boyde, A., Fortelius, M., Lester, K. S., & Martin, L. B. (1988). Basis of the structure and development of mammalian enamel as seen by scanning electron microscopy. *Scanning Microscopy, 2*, 1479-1490.

Braudel, F. (1966). *La Méditerranée et le monde Méditerranéen à l'Epoque de Philippe II: Vol. 1. La part du milieu*. Paris: Librairie Armand Colin.

Britton, K., Grimes, V., Dau, J., & Richards, M. P. (2009). Reconstructing faunal migrations using intra-tooth sampling and strontium and oxygen isotope analyses: A case study of modern caribou (*Rangifer tarandus granti*). *Journal of Archaeological Science, 36*, 1163-1172.

Britton, K., Grimes, V., Niven, L., Steele, T. E., McPherron, S., Soressi, M., Richards, M. P. (2011). Strontium isotope evidence for migration in late Pleistocene *Rangifer*: Implications for Neanderthal hunting strategies at the middle Palaeolithic site of Jonzac, France. *Journal of Human Evolution, 61*, 176-185.

Brudevold, F., Aasenden, R., Srinivasian, B. N., & Bakhos, Y. (1977). Lead in enamel and saliva, dental caries and the use of enamel biopsies for measuring past exposure to lead. *Journal of Dental Research, 56*, 1165-1171.

Brudevold, F., & Söremark, R. (1967). Chemistry of the mineral phase of enamel. In A. E. W. Miles (Ed.), *Structural and chemical organization of teeth Vol. II* (pp. 247-2777). London: Academic Press.

Budd, P., Montgomery, J., Barreiro, B., & Thomas, R. G. (2000). Differential diagenesis of strontium in archaeological human dental tissues. *Applied Geochemistry, 15*, 687-694.

Burmeister, S. (2000). Archaeology and migration. Approaches to an archaeological proof of migration. *Current Anthropology, 41*(4), 539-567.

Burton, J. H., & Price, T. D. (1999). Evaluation of bone strontium as a measure of seafood consumption. *International Journal of Osteoarchaeology, 9*, 233-236.

Cabo Alonso, Á. (1992). Medio natural y transhumancia en la España peninsular. In F. Ruiz Martín, & Á. García Sanz (Eds.), *Meseta, trashumancia y lana en la España moderna* (pp. 11-41). Barcelona: Crítica.

Cacho, C., Papí, C., Sánchez-Barriga, A., & Alonso, F. (1996). La cestería decorada de la Cueva de los Murciélagos (Albuñol, Granada). *Complutum extra (I)* (pp. 105-122). Madrid:

Cámara, J. A. (2001). *El ritual funerario en la prehistoria reciente en el sur de la Penísula Ibérica. BAR International Series 913*. Oxford: Archaeopress.

Capo, R. C., Stewart, B. W., & Chadwick, O. A. (1998). Strontium isotopes as tracers of ecosystems processes: Theory and methods. *Geoderma, 82*, 197-225.

Carvalho, P. C. S., Neiva, A. M. R., Silva, M. M. V. G., & Corfu, F. (2012). A unique sequential melting mechanism for the generation of anatectic granitic rocks from the Penafiel area, northern Portugal. *Lithos*, *155*, 110-124.

Chapman, J. C. (1981). *The Vinča culture of the south-east Europe: Studies in chronology, economy, and society. BAR International Series 117*. Oxford: Archaeopress.

Chapman, R. (1979). Transhumance and megalithic tombs in Iberia. *Antiquity, 53*, 150-152.

Chapman, R. (1990). *Emerging complexity: The later prehistory of south-east Spain, Iberia, and the west Mediterranean*. New York: Cambridge University Press.

Chapman, R. (2003). *Archaeologies of complexity*. London: Routledge.

Chapman, R. (2008). Producing inequalities: Regional sequences in later prehistoric southern Spain. *Journal of World Prehistory*, *21*(3-4), 195-260.

Clary, J. (2008). Rainfall seasonality determines annual/perennial grass balance in vegetation of Mediterranean Iberia. *Plant Ecology*, *195*, 13-20.

Collantes, F. (2009). The demise of European mountain pastoralism: Spain 1500-2000. *Nomadic Peoples, 13*(2), 124-145.

Costa, M. E., Díaz-Zorita Bonilla, M., García Sanjuán, L., & Wheatley, D. (2010). The copper age settlement of Valencina de la Concepcíon (Seville, Spain). *Trabajos De Prehistoria, 67*(1), 85-117.

Criado Boado, F., & Vaquero Lastres, J. (1993). Monumentos, nudos en el Papañuelo: Megalitos, nudos en el espacio: Análisis del emplazamiento de los monumentos tumulares gallegos. *Espacio, Tiempo y Forma, Serie I, Prehistoria y Arqueología, 6*, 205-248.

Criado-Boado, F. (1989). Megalitos, espacio, pensamiento. *Trabajos De Prehistoria, 46*(1), 75-98.

Criado-Boado, F., & Cabrejas Domínguez, E. (Eds.). (2005). *Obras públicas e patrimonio: Estudo arqueolóxico do corredor do morrazo.* Santiago de Compostela: Instituto de Estudios Gallegos Padre Sarmiento, Consejo Superior de Investigaciones Cientificas.

Criado-Boado, F., & Fábregas Valcarce, R. (1989). The megalithic phenomenon of northwest Spain: Main trends. *Antiquity, 63*, 682-696.

Criado-Boado, F., & Villoch Vázquez, V. (1998). La monumentalización del paisaje: Percepción y sentido original en el megalitismo de la Sierra de Barbanza. *Trabajos De Prehistoria, 55*(1), 63-80.

Cunha, E., Umbelino, C., Silva, A. M., & Cardoso, F. (2007). What can pathology say about the Mesolithic and late Neolithic/Chalcolithic communities? The Portuguese case. In M. Cohenm, M. Gillian & M. Crane-Kramer (Eds.), *Ancient health: skeletal indicators of agricultural and economic intensification* (pp. 164-175). Gainesville: University of Florida Press.

Curzon, M. E. J., & Cutress, T. W. (Eds.). (1983). *Trace elements and dental disease*. Boston: PSG Inc.

Davidson, I. (1980). Transhumance, Spain and ethnoarchaeology. *Antiquity, 54*, 144-147.

de la Torre, F., & Sáez, L. (1986). Nuevas excavaciones en el yacimiento de la Edad del Cobre de el Malagón (Cullar Baza, Granada). *Homenaje a luis siret (1934-1984)* (pp. 221-226). Sevilla: Conserjería de Cultura.

Delibes, G., Fernández-Miranda, M., Fernández-Posse, M. D., & Martín, C. (1986). El poblado de Almizaraque. *Homenaje a luis siret (1943-1984)* (pp. 167-177). Sevilla: Conserjería de Cultura.

Diago, M. (1994). Grandes y pequeños ganaderos trashumantes en las Sierras Sorianas en el tránsito de la edad media a la moderna. *Revista De Historia Económica, 12*, 343-364.

Diago, M. (2002). El crédito en el comercio lanero en la región Soriana durante los siglos XVI y XVII.*Revista De Historia Económica*, *20*, 271-299.

Díaz-Zorita Bonilla, M., Costa Caramé, M. E., & García Sanjuán, L. (2012). Funerary practices and demography from the Mesolithic to the Copper Age in southern Spain. In J. F. Gibaja Bao, A. F. Carvalho & P. Chambon (Eds.), *Funerary practices from the Mesolithic to the Chalcolithic of the northwest Mediterranean. BAR.* (pp. 51-65). Oxford: Archaeopress.

Díaz-Zorita Bonilla, M. (2013). *The Copper Age in south-west Spain: A bioarchaeological approach to prehistoric social organisation.* (Unpublished Ph.D.). Durham University,

Díaz-Zorita Bonilla, M., Waterman, A. J., & Knudson, K. J. (2009). Explorando la movilidad y los patrones dietarios en durante la Edad del Cobre en el suroeste de la Península Ibérica: Estudio preliminar bioarqueológico del tholos de palacio III (Almadén de la Plata, Seville). In M. Polo Cerdá, & E. García Prósper (Eds.), *Actas del IX congreso nacional de paleopatología* (pp. 669-674)

Diekwisch, T. G. H., Berman, B. J., Genter, S., & Slavkin, H. C. (1995). Initial enamel crystals are not spatially associated with mineralized dentin. *Cell Tissue Research, 279,* 149-167.

Duque Espino, D. (2005). Resultados antracológicos de los yacimientos de la Coudelaria de Alter do Chão y su integración en las secuencias paleoecológicas y paleoambientales de la prehistoria reciente del suroeste peninsular. *Revista Portuguesa De Arqueología, 8*(1), 21-41.

Elias, R. W., Hirao, Y., & Patterson, C. C. (1982). The circumvention of the natural biopurification of calcium along nutrients pathways by atmospheric inputs of industrial lead. *Geochimica et Cosmochimica Acta, 46*, 2561-2580.

Ericson, J. E. (1985). Strontium isotope characterization in the study of prehistoric human ecology. *Journal of Human Evolution, 14*, 503-514.

Esquivel, J. A., & Navas, E. (2007). Geometric architectural pattern and constructive energy analysis at Los Millares Copper Age settlement (Santa Fé, de Mondújar, Almería, Andalusia). *Journal of Archaeological Science, 34*(6), 894-904.

Evans, J. A., Chenery, C. A., & Fitzpatrick, A. P. (2006). Bronze Age childhood migration of individuals near Stonehenge, revealed by strontium and oxygen isotope tooth enamel analysis. *Archaeometry, 48*, 309-321.

Fairén Jiménez, S. (2004). ¿Se hace camino al andar? Influencia de las variables medioambientales y culturales en el cálculo de caminos óptimos mediante SIG. *Trabajos De Prehistoria, 61*(2), 25-40.

Faure, G., & Mensing, T. M. (2005). *Principles of isotope geology* (3rd ed.). Hoboken, N.J.: Wiley.

Fincham, A. G., Moradian-Oldak, J., & Simmer, J. P. (1999). The structural biology of the developing dental enamel matrix. *Journal of Structural Biology, 126*, 270-299.

Fincham, A. G., & Simmer, J. P. (1997). Amelogenin proteins of developing dental enamel. In D. J. Chadwick, & G. Cardew (Eds.), *Dental enamel: Proceedings of the Ciba foundation symposium 205* (pp. 118-134). Chichester: John Wiley & Sons Inc.

Frachetti, M. D. (2008). Variability and dynamic landscapes of mobile pastoralism in ethnography and prehistory. In H. Barnard, & W. Wendrich (Eds.), *The archaeology of mobility. Old world and new world nomadism* (pp. 366-396). Los Angeles: Cotsen Institute of Archaeology, University of California.

Fryxell, J. M., & Sinclair, A. R. E. (1988). Causes and consequences of migration by large herbivores. *Trends in Ecology and Evolution, 3*, 237-241.

Galán Domingo, E., & Ruíz-Gálvez, M. (2001). Rutas ganaderas, transterminancia y caminos antiguos: El caso del occidente peninsular entre el calcolítico y la edad del hierro. In J. Gómez-Pantoja (Ed.), *Los rebaños de gerión: Pastores y trashumancia en Iberia antigua y medieval,* (pp. 279-311). Madrid: Colección de la Casa de Velázquez.

García Sanjuán L. (2009). Introduction to the megalithic sites and landscapes of Andalusia. In L. García Sanjuán, & B. Ruiz (Eds.), *The large stones of prehistory: Megalithic sites and landscapes of Andalusia* (pp. 12-31). Seville, Spain: Andalusian Government (Junta de Andalucía).

García Sanjuán, L. (1999). *Los orígenes de la estratificación social. patrones de desigualdad en la edad del bronce del suroeste de la Península Ibérica (Sierra*

Morena occidental c. 1700-1100 a.n.e./2100-1300 A.N.E.). BAR International Series 823. Oxford: Archaeopress.

García Sanjuán, L., & Hurtado Pérez, V. (1997). Los inicios de la jerarquización social en el suroeste de la Península Ibérica (c.2500-1700 a.n.e.). Problemas conceptuales empíricos. *Saguntum 30. Homenaje a la dra. milagros gil-mascarell Boscá. la Península Ibérica entre el calcolítico y la edad del bronce. Volumen II.* (pp. 135-152). Valencia: Valencia Universitat de Valencia y Generalitat Valenciana.

Geddes, D. (1983). Neolithic transhumance in the Mediterranean Pyrenees. *World Archaeology*, *15*, 51-66.

Geel, T., Roep, T. B., ten Kate, W., & Smit, J. (1992). Early-middle Miocene stratigraphic turning points in the Alicante region (SE Spain): Reflections of western Mediterranean plate-tectonic reorganizations. *Sedimentary Geology*, *75*, 223-239.

Gianotti, C., Mañana-Borrazás, P., Criado-Boado, F., & López-Romero, E. (2011). Deconstructing Neolithic monumental space: The Montenegro enclosure in Galicia (northwest Iberia). *Cambridge Archaeological Journal*, *21*(3), 391-406.

Gibbons, W., & Moreno, T. (Eds.). (2002). *The geology of Spain*. London: The Geological Society.

Gilman, A. (1987). Unequal development in copper age Iberia. In T. Earle, & E. M. Brumfiel (Eds.), *Specialization, exchange and complex societies* (pp. 22-29). Cambridge: Cambridge University Press.

Gilman, A., & Thornes, J. B. (1985). *Land-use and prehistory in south-east Spain*. Boston: Allen and Unwin.

Graustein, W. C. (1989). $^{87}Sr/^{86}Sr$ ratios measure the sources and flow of strontium in terrestrial ecosystems. In P. W. Rundel, J. R. Ehleringer & K. A. Nagy (Eds.), *Stable isotopes in ecological research: Vol 68, ecological studies* (pp. 491-512). New York: Springer.

Greenfield, H. J. (2010). The secondary product revolution: the past, the present and the future. *World Archaeology, 42*, 29-54.

Grupe, G., Price, T. D., Schröter, P., Söllner, F., Johnson, C. M., & Beard, B. L. (1997). Mobility of Bell Beaker people revealed by strontium isotope ratios of tooth and bone: A study of southern Bavarian skeletal remains. *Applied Geochemistry, 12*, 517-525.

Hanson, D. B., & Buikstra, J. E. (1987). Histomorphological alteration in buried human bone from the lower Illinois Valley: Implications for palaeodietary research. *Journal of Archaeological Science, 14*, 549-563.

Harrison, R. J., & Gilman, A. (1977). Trade in the second and third millennia B.C. between the Magreb and Iberia. In V. Markotic (Ed.), *Ancient Europe and the Mediterranean. Studies presented in honour of Hugh Hencken.* (pp. 90-114). Warminster: Aris and Phillips.

Harrison, R. J., & Orozco Kohler, T. (2001). Beyond charaterisation. Polished stone exchange in the western Mediterranean 5500-2000 BC. *Oxford Journal of Archaeology*, *20*(2), 107-127.

Harrison, R. J. (1977). *The Bell Beaker cultures of Spain and Portugal*. Cambridge, Mass.: Peabody Museum of Archaeology and Ethnology.

Hartman, G., & Richards, M. (2014). Mapping and defining sources of variability in bioavailable strontium isotopes in the eastern Mediterranean. *Geochimica et Cosmochimica Acta*, *126*, 250-264.

Hedges, R. E. M. (2002). Bone diagenesis: An overview of processes. *Archaeometry*, *44*(3), 319-328.

Hillier, M., Boaventura, R., & Grimes, V. (2010). Moving around? Testing mobility with strontium isotopes ($^{87}Sr/^{86}Sr$) in the late Neolithic of south-central Portugal. *Poster presented at the 8th Encontro De Arqueologia do Algarve: A Arqueologia e as Outras Ciências, Silves.*

Hillson, S. (2005). *Teeth* (2nd ed.). New York: Cambridge University Press.

Hodell, D. A., Quinn, R. L., Brenner, M., & Kamenov, G. (2004). Spatial variation of strontium isotopes ($^{87}Sr/^{86}Sr$) in the Maya region: A tool for tracking ancient human migration. *Journal of Archaeological Science, 31*, 585-601.

Hoedemaeker, P. J., & Leereveld, H. (1995). Biostratigraphy and sequence stratigraphy of the Berriasian-lowest Aptian (Lower Cretaceous) of the río Argos succession, Caravaca, SE Spain. *Cretaceous Research, 16*, 195-230.

Horn, P., Höslzl, S., & Storzer, D. (1994). Habitat determination on a fossil stages mandible from the site of Homo erectus heidelbergenius at Mauer by use of $^{87}Sr/^{86}Sr$. *Naturwissenshaten, 81*, 360-362.

Hurtado Pérez, V. (1991). Informe de las excavaciones de urgencia en la Pijotilla. Campaña de 1990. I jornadas de prehistoria y arqueología en Extremadura (1986-1990). *Extremadura Arqueológica, II*, 45-68.

Hurtado Pérez, V. (2002). Intervención arqueológica en San Blas. *Al-Madan, 11*, 206-212.

Hurtado Pérez, V., Mondéjar, P., & Pecero, J. C. (2000). Excavaciones en la tumba 3 en La Pijotilla. In J. J. Jiménez, & J. J. Enríquez (Eds.), *El megalitismo en Extremadura. Homenaje a elías diéguez luengo. Extremadura arqueológica VIII* (pp. 249-266). Mérida: Regional Government of Extremadura.

Hurtado Pérez, V., & Odriozola, C. P. (2009). Landscape, identity, and material culture in "Tierra de Barros" (Badajoz, Spain) during the 3rd millenium BC. In R. B. Salisbury, & T. Thurston (Eds.), *Reimagining regional analyses: The archaeology of spatial and social dynamics* (pp. 265-290). New York: Cambridge Scholar Press.

Jiménez Brobeil, S. A., Oumaoui, I., & Esquivel, J. A. (2004). Actividad fisica según sexo en la cultura Argárica. una aproximación desde los restos humanos. *Trabajos De Prehistoria, 61*(2), 141-153.

Jordá, J. F., & Aura, J. E. (2008). 70 fechas para una cueva: Revisión crítica de 70 dataciones C14 del Pleistoceno Superior y Holoceno de la Cueva de Perja (Málaga, Andalucía, España). *Espacio, tiempo y forma. serie I, Prehistoria y arqueología. Homenaje al profesor Eduardo Ripoll Berelló* (pp. 239-256)

Knudson, K. J., & Price, T. D. (2007). Utility of multiple chemical techniques in archaeological residential mobility studies: Case studies from Tiwanku and Chiribaya affiliated sites in the Andes. *American Journal of Physical Anthropology, 132*, 25-39.

Koch, P. L., Halliday, L. M., Walter, L. M., Stearley, R. F., Huston, T. J., & Smith, G. R. (1992). Sr-isotopic composition of hydroxyapatite from recent and fossil salmon: The record of lifetime migration and diagenesis. *Earth and Planetary Science Letters, 108*, 277-287.

Koch, P. L., Tuross, N., & Fogel, M. (1997). The effects of sample treatment and diagenesis on the isotopic integrity of carbonate in biogenic hydroxylapatite. *Journal of Archaeological Science, 24*, 417-429.

Kohn, M. J., Schoeninger, M. J., & Barker, W. W. (1999). Altered states: Effects of diagenesis on fossil tooth chemistry. *Geochimica et Cosmochimica Acta, 63*, 2737-2747.

Land, M., Ingri, J., Andersson, P. S., & Öhlander, B. (2000). Ba/Sr, Ca/Sr and $^{87}Sr/^{86}Sr$ ratios in soil water and groundwater: Implications for relative contributions to stream water discharge. *Applied Geochemistry, 15*, 311-325.

Lee-Thorp, J. A., & van der Merwe, N. J. (1991). Aspects of the chemistry of modern and fossil biological apatites. *Journal of Archaeological Science, 18*, 343-354.

LeGeros, R. Z. (1991). *Calcium phosphates in oral biology and medicine*. New York: Karger.

Leisner, V., & Leisner, G. (1943). *Die megalithgräber der iberischen halbinsel: Erster teil, der süden*. Berlin: Gruyter.

Lomba, J., López, M., Ramos, F., & Avilés, A. (2009). El enterramiento múltiple calcolítico de Camino del Molino (Caravaca, Murcia): Metodología y primeros resultados de un yacimiento excepcional. *Trabajos De Prehistoria, 66*(2), 99-116.

Losee, F. L., Curzon, M. E. J., & Little, M. F. (1974). Trace element concentrations in human enamel. *Archaeological Oral Biology, 19*, 467-470.

Lull, V. (2000). Argaric society: Death at home. *Antiquity, 74*, 581-590.

Mann, S. (1997). The biomimetics of enamel: A paradigm for organized biomaterials synthesis. In D. J. Chadwick, & G. Cardew (Eds.), *Dental enamel. Ciba symposium 205* (pp. 261-274). Chichester: John Wiley.

Manzano Baena, P., & Casas, R. (2010). Past, present and future of trashumancia in Spain: Nomadism in a developed country. *Pastoralism, 1*(1), 72-90.

Martín, J. M., Braga, J. C., Auirre, J., & Puga-Bernabéu, Á. (2009). History and evolution of the north-Betic strait (Prebetic zone, Betic Cordillera): A narrow, early tortonian, tidal-dominated, Atlantic-Mediterranean marine passage. *Sedimentary Geology, 216*, 80-90.

Martínez, A. P. (2005). El yacimiento prehistórico de los Molinos de Papel (Caravaca de la Cruz, Murcia). Intervención arqueológica vinculada a las obras de infraestructura del plan parcial scr 2, 1999-2000. *Memorias De Arqueología*, (14), 133-172.

Mathers, C. (1984). Beyond the grave: The context and wider implications of mortuary practices in south-east Spain. *BAR International Series, 193*, 13-46.

McArthur, J. M., Janssen, N. M. M., Reboulet, S., Leng, M. J., Thirlwall, M. F., & van de Schootbrugge, B. (2007). Palaeotemperatures, polar ice-volume, and isotope stratigraphy (Mg/Ca, $\delta^{18}O$, $\delta^{13}C$, $^{87}Sr/^{86}Sr$): The early Cretaceous (Berriasian, Valanginian, Hauterivian). *Palaeogeography, Palaeoclimatology, Palaeoecology*, *248*, 391-430.

Mendes, A. C., & Dias, G. (2004). Mantle-like Sr–Nd isotope composition of Fe–K subalkaline granites: The Peneda–Gere’s Variscan massif (NW Iberian peninsula). *Terra Nova*, *16*(3), 109-115.

Micó, R. (1991). Objeto y discurso arqueológico. El calcolítico del sudeste peninsular. *Revista d'Arqueologia De Ponent*, 51-70.

Micó, R. (1993). *Pensamientos y prácticas en la arqueologías contemporáneas. Normatividad y exclusión en los grupos arqueológicos del III y II milenios cal ANE en el subeste de la Península Ibérica.* (Unpublished Ph.D.). Universitat Autònoma de Barcelona,

Millard, A. R., & Hedges, R. E. M. (1996). A diffusion-absorption model of uranium uptake by archaeological bone. *Geochimica et Cosmochimica Acta*, *60*(12), 2139-2152.

Miller, E. K., Blum, J. D., & Friedland, A. J. (1993). Determination of soil exchangeable-cation loss and weathering rates using Sr isotopes. *Nature*, *362*, 438-441.

Moiroud, M., Martínez, M., Deconinck, J., Monna, F., Pellenard, P., Riquier, L., & Company, M. (2012). High-resolution clay minerology as a proxy for orbital tuning:

Example of the Hauterivian-Barremian transition in the Betic Cordillera (SE Spain). *Sedimentary Geology, 282*, 336-346.

Moita, P., Santos, J. F., & Francisco Pereira, M. (2009). Layered granitoids: Interaction between continental crust recycling processes and mantle derived magmatism. Examples from the Évora Massif (Ossa-Morena Zone, southwest Iberia, Portugal). *Lithos, 11*, 125-141.

Molina, F., & Cámara, J. A. (2002). *El calcolítico y la cultura de los Millares, en nueva historia de España. La historia en su lugar. T.I. los Albores de la historia (desde los orígenes hasta el siglo III a.c.).* Barcelona: Planeta.

Montero Ruiz, I., Rihuete Herrada, C., & Ruiz Taboada, A. (1999). Precisiones sobre el enterramiento colectivo neolítico de Cerro Virtud (Cuevas de Almanzora, (Almería)). *Trabajos De Prehistoria, 56*(1), 119-130.

Montero, I. (1993). Bronze Age metallurgy in south-east Spain. *Antiquity, 67*, 46-57.

Montgomery, J. (2002). *Lead and strontium isotope compositions of human dental tissues as an indicator of ancient exposure and population dynamics.* (Unpublished Ph.D.). University of Bradford,

Montgomery, J., Budd, P., & Evans, J. (2000). Reconstructing the lifetime movements of ancient people: A Neolithic case study from southern England. *European Journal of Archaeology, 3*, 407-422.

Moreno Rey, A. (1998). La estribacion occidental de Sierra Morena. Introducción al medio físico y humano. In L. García Sanjuán (Ed.), *La traviesa. Ritual funerario y jerarquización social en una comunidad de la Edad del Bronce de Sierra Morena occidental* (pp. 17-34). Sevilla: Universidad de Sevilla.

Moreno, J. R. (2000). Entre el padre y el patrón. La organización del trabajo trashumante en la Montaña Riojana (s. XVIII). *Historia Agraria*, *22*, 131-158.

Murillo Barroso, M., & García Sanjuán, L. (2013). El pomo de ámbar de la estructura 10.042- 10.049 del sector PP4-montelirio del asentamiento de Valencina de la Concepción (Seville). In L. García Sanjuán, V. Hurtado Pérez, J. M. Vargas Jiménez, T. Ruiz Moreno & R. Cruz-Auñón Briones (Eds.), *Valencina prehistórica. Actas del congreso conmemorativo del descubrimiento de la pastora (1860-2010).* (pp. 511-520). Sevilla: Universidad de Sevilla.

Murrieta-Flores, P. (2007). *Mobility, transhumance and prehistoric landscape: A GIS approach to the archaeological landscape of Almadén de la Plata in Andalucía, Spain.* (Unpublished M.Sc.). University of Southampton.

Murrieta-Flores, P. (2011). *Travelling through past landscapes: Analysing the dynamics of movement during late prehistory in southern Iberia with spatial technologies.* (Unpublished Ph.D.). University of Southampton.

Murrieta-Flores, P. (2014). Space and temporality in herding societies: Exploring the dynamics of movement during the Iberian late prehistory. In S. Souvatzi, & A. Hadji

(Eds.), *Space and time in Mediterranean prehistory* (pp. 196-213). New York: Routledge Taylor & Francis Group.

Navidad, M., Castiñeiras, P., Casas, J. M., Liesa, M., Fernández Suárez, J., Barnolas, A., Gil-Peña, I. (2010). Geochemical characterization and isotopic age of Caradocian magmatism in the northeastern Iberian peninsula: Insights into the late Ordovician evolution of the northern Gondwana margin. *Gondwana Research, 17*, 325-337.

Nehlich, O., Montgomery, J., Evans, J., Schade-Lindig, S., Pichler, S. L., Richards, M. P., & Alt, K. W. (2009). Mobility or migration: A case study from the Neolithic settlement of Nieder-mörlen (Hessen, Germany). *Journal of Archaeological Science*, *36*, 1791-1799.

Neuman, W. F., & Neuman, M. W. (1953). The nature of the mineral phase of bone. *Chemical Reviews, 53*, 4.

Nielsen-Marsh, C. M., & Hedges, R. E. M. (2000). Patterns of diagenesis in bone II: effects of acetic acid treatment and the removal of diagenetic CO32-. *Journal of Archaeological Science, 27*, 1151-1159.

Nocete Calvo, F. (2001). *Tercer milenio antes de nuestra era. relaciones y contradicciones centro/periferia en el valle del Guadalquivir*. Barcelona: Ediciones Bellaterra.

Nocete Calvo, F. (Ed.). (2004). *Odiel: Proyecto de investigación arqueológica para el análisis del origen de la desigualdad social en el suroeste de la península ibérica.* Seville: Junta de Andalucía. Consejería de Cultura. Arqueología Monografías.

Nocete Calvo, F., Queipo de Llano, G., Sáenz, R., Nieto, J. M., Inácio, N., Rodríguez Bayona, M., Santos, J. F. (2008). The smelting quarter of Valencina de la Concepción (Seville, Spain): the specialised copper industry in a political centre of the Guadalquivir valley during the third millenium BC (2750-2500 BC). *Journal of Archaeological Science, 35*, 717-732.

Nocete, F., & Peramo, A. (2010). More than big stones! Peripheral and confined or resistant lineage societies in the pristine class-society territorial framework of the south-west Iberian Peninsula (2900-2000 BC). In D. Calado, M. Baldia & M. Boulanger (Eds.), *Monumental questions: Prehistoric megalithic, mound, and enclosures. BAR International Series 2122* (pp. 71-82). Oxford: Archaeopress.

Paço, A. D., & Sangmeister, E. (1956). Vila Nova de São Pedro, eine befestigte siedlung der kupferzeit in Portugal. *Germania, 34*, 211-230.

Parker, R. B., & Toots, H. (1980). Trace elements in bones as paleobiological indicators. In A. K. Behrensmeyer, & A. P. Hill (Eds.), *Fossils in the making: Vertebrate taphonomy and paleoecology* (pp. 197-207). London: University of Chicago Press.

Pate, F. D., & Brown, K. A. (1985). The stability of bone strontium in the geochemical environment. *Journal of Human Evolution, 14*, 483-491.

Pate, F. D., & Hutton, J. T. (1988). The use of soil chemistry data to address post-mortem diagenesis in bone mineral. *Journal of Archaeological Science, 15*, 729-739.

Pellegrini, M., Donahue, R. E., Chenery, C., Evans, J., Lee-Thorp, J., Montgomery, J., & Mussi, M. (2008). Faunal migration in late-glacial central Italy: Implications for human resource exploitation. *Rapid Communication Mass Spectrometry, 22*, 1714-1726.

Pérez Macías, J. A. (1983). Introducción al bronce final en el noroeste de la provincia de Huelva. *Habis, 14*, 207-238.

Pérez Romero, E. (1996). Trashumancia y pastos de agostadero en las sierras sorianas durante el siglo XVIII. *Revista De Historia Económica, 14*, 91-124.

Pollard, A., Batt, C., & Stern, B. (2007). *Analytical chemistry in archaeology*. Cambridge: Cambridge University Press.

Polo-Díaz, A., Martínez-Moreno, J., Benito-Calvo, A., & Mora, R. (2014). Prehistoric herding facilities: Site formation processes and archaeological dynamics in Cova Gran de Santa Linya (southeastern Prepyrenees, Iberia). *Journal of Archaeological Science, 41*, 784-800.

Price, T. D. (1989). *The chemistry of prehistoric human bone*. Cambridge: Cambridge University Press.

Price, T. D., Bentley, R. A., Gronenborn, D., Lüning, J., & Wahl, J. (2001). Human migration in the Linearbandkeramik of central Europe. *Antiquity, 75*, 593-603.

Price, T. D., Blitz, J., Burton, J. H., & Ezzo, J. A. (1992). Diagenesis in prehistoric bone: Problems and solutions. *Journal of Archaeological Science, 19*, 513-529.

Price, T. D., Burton, J. H., & Bentley, R. A. (2002). The characterization of biologically available strontium isotope ratios for the study of prehistoric migration. *Archaeometry, 44*, 117-135.

Price, T. D., Grupe, G., & Schröter, P. (1994a). Reconstruction of migration patterns in the Bell Beaker period by stable strontium isotope analysis. *Applied Geochemistry, 9*, 413-417.

Price, T. D., Johnson, C. M., Ezzo, J. A., Burton, J. H., & Ericson, J. A. (1994b). Residential mobility in the prehistoric southwest united states. A preliminary study using strontium isotope analysis. *Journal of Archaeological Science*, *24*(315), 330.

Price, T. D., Knipper, C., Grupe, G., & Smrcka, V. (2004). Strontium isotopes and prehistoric human migration: The Bell Beaker period in central Europe. *European Journal of Archaeology, 7*, 9-40.

Priest, N. D., & Van de Vyver, F. L. (1990). *Trace metals and fluoride in bones and teeth*. Boca Raton, Florida: CRC Press Inc.

Robinson, C., Kirkham, J., Brookes, S. J., & Shore, R. C. (1995). Chemistry of mature enamel. In C. Robinson, J. Kirkham & R. C. Shore (Eds.), *Dental enamel: Formation to destruction* (pp. 167-191). Boca Raton, Florida: CRC Press Inc.

Robinson, C. J., Kirkham, J., Weatherell, J. A., & Strong, M. (1986). Dental enamel - A living fossil. In E. Cruwya, & R. A. Foley (Eds.), *Teeth and anthropology, BAR International Series 291* (pp. 31-54). Oxford, England: Archaeopress.

Rodriguez Vidal, J., Alvarez Garcia, G., Alcaraz Pelegrina, J. M., Martínez Aguirre, A., Caceres Puro, L. M., Cantano Martin, M., & Caro Gomez, J. A. (2001). Episodios cuaternarios de sedimentación quimica en la Cueva de los Covachos (Almaden de la Plata, Sevilla). *Geogaceta, 21*, 107-110.

Rodríguez Vidal, J., Alvarez García, G., Cáceres, L. M., Martínez Aguirre, A., Alcaraz, J. M., Lòpez Sàez, J. A., Moreno, A. B. (2003). Registro sedimentario del cuaternario reciente en la Cueva de la Sima, Sierra Norte de Sevilla. *Boletín Sedeck. Sociedad Española De Espeleología y Ciencias Del Karst,* (80), 87.

Sangmeister, E., & Schubart, H. (1981). *Zambujal. die grabungen 1964 bis 1973.* Mainz and Rhein: Philip von Zabem.

Sanz de Galdeano, C. (2000). Evolution of Iberia during the Cenozoic with special emphasis on the formation of the Betic Cordillera and its relation with the western Mediterranean. *Ciências De Terra, 14*, 9-24.

Sasaki, T., Takagi, M., & Yanagisawa, T. (1997). Structure and function of secretory ameloblasts in enamel formation. In D. J. Chadwick, & G. Cardew (Eds.), *Dental enamel. Proceedings of the Ciba foundation symposium 205* (pp. 32-50). Chichester: John Wiley.

Savory, H. N. (1972). The culture sequence at Vila Nova de Sâo Pedro. *Madrider Mitteilungen, 13*, 23-37.

Schuhmacher, T. X., Cardoso, J. L., & Banerjee, A. (2009). Sourcing African ivory in Chalcolithic Portugal. *Antiquity, 83*, 983-997.

Schuhmacher, T. X., & Banerjee, A. (2012). Procendenia e intercambio de marfil en el calcolítico de la Península Ibérica. *Congrés Internacional Xarxes Al Neolític – Neolithic Networks Rubricatum.* Revista del Museu de Gavà. *, 5* 289-298.

Schwarcz, H., White, C., & Longstaffe, F. (2010). Stable and radiogenic isotopes in biological archaeology: Some applications. In J. West, G. Bowen & T. Dawson (Eds.), *Isoscapes: Understanding movement, pattern, and process on earth through isotope mapping.* (pp. 335-356). New York: Springer.

Sealy, J. C. (1989). *Reconstruction of later Stone Age diets in the south-western cape, South Africa: evaluation and application of five isotopic and trace element techniques.* (Unpublished Ph.D.). University of Cape Town.

Sealy, J. C., van der Merwe, N. J., Sillen, A., Kruger, F. J., & Krueger, H. W. (1991). $^{87}Sr/^{86}Sr$ as a dietary indicator in modern and archaeological bone. *Journal of Archaeological Science, 18*, 399-416.

Shemesh, A. (1990). Crystallinity and diagenesis of sedimentary apatites. *Geochimica et Cosmochimica Acta, 54*, 2433-2438.

Sillen, A. (1989). Diagenesis of the inorganic phase of the cortical bone. In T. D. Price (Ed.), *The chemistry of prehistoric human bone* (pp. 211-229). Cambridge: Cambridge University Press.

Sillen, A., & LeGeros, R. (1991). Solubility profiles of synthetic apatites and of modern and fossil bones. *Journal of Archaeological Science, 19*, 385-397.

Sillen, A., & Sealy, J. C. (1995). Diagenesis of strontium in fossil bone: A reconsideration of Nelson et al. (1986). *Journal of Archaeological Science, 22*, 313-320.

Simmer, J. P., & Fincham, A. G. (1995). Molecular mechanisms of dental enamel formation. *Critical Review of Oral Biological Medicine, 6*(2), 84-108.

Siret, H., & Siret, L. (1887). *Les Premiers âges du métal dans le sud-est de l'Espagne* Anvers.

Spindler, K. (1981). *Cova da Moura. die besiedlung des atlantischen küstengebietes mittel Portugals vom neolithikum bis an das ende der bronzezeit.* Mainz and Rhein: Philip von Zabern.

Sponheimer, M., & Lee-Thorp, J. A. (1999). Alteration of enamel carbonate environments during fossilization. *Journal of Archaeological Science, 26*, 143-150.

Stamoulis, K. C., Assimakopoulos, P. A., Ioannides, K. G., Johnson, E., & Soucacos, P. N. (1999). Strontium-90 concentration measurements in human bones and teeth in Greece. *Science of the Total Environment, 229*(3), 166-182.

Thomas, J. T. (2011). Fashioning identities, forging inequalities: Late Neolithic/Copper age personal ornaments of the Portuguese Estremadura. *European Journal of Archaeology, 14*(1-2), 29-59.

Thornton, E. K. (2011). Reconstructing ancient Maya animal trade through strontium isotope ($^{87}Sr/^{86}Sr$) analysis. *Journal of Archaeological Science, 38*(3254), 3263.

Towers, J., Montgomery, J., Evans, J., Jay, M., & Pearson, M. P. (2010). An investigation of the origins of cattle and aurochs deposited in the early Bronze Age barrows at Gayhurst and Irthlingborouch. *Journal of Archaeological Science, 37*, 508-515.

Trickett, Mark A., Budd, Paul, Montgomery, Janet, & Evans, Jane. (2003). An assessment of solubility profiling as a decontamination procedure for the $^{87}Sr/^{86}Sr$ analysis of archaeological human skeletal tissue. *Applied Geochemistry, 18*, 653-658.

Tuross, N., Behrensmeyer, A. K., & Eanes, E. D. (1989). Strontium increases and crystallinity changes in taphonomic and archaeological bone. *Journal of Archaeological Science, 16*, 661-672.

Underwood, E. J., & Mertz, W. (1977). *Trace elements in human and animal nutrition* (4th ed.). New York: Academic Press.

Valera, M. P. (Ed.). (2008). *Actuacións arqueolóxicas*. *Ano 2007.* Santiago de Compostela: Xunta de Galicia, Consellería de Cultura e Deporte, Dirección Xeral de Patrimonio Cultural.

Vargas Jiménez, J. M. (2004). Elementos para la definición territorial del yacimiento prehistórico de Valencina de la Concepción (Seville). *Revista De Prehistoria y Arqueología, 12*, 127-146.

Vegas, J. I. (2007). *San juan ante portam latinam. una inhumación colectiva prehistórica en el valle medio del ebro. memoria de las excavaciones arqueológicas 1985, 1990 y 1991.* Vitoria: Fundación José Miguel de Barandiarán, Diputación Foral de Álava.

Veis, A. (1989). Studies of vertebrate tooth mineralization. Insights from studies of dentinogenesis. *Northwestern Dental Research, 1*(2), 3-5.

Vera, J.A. (Ed.). (2004). *Geología de España*. Madrid: SGE-IGME.

Vilaseco, I. (2009). O círculo que foi: A mourela no seu contexto histórico. In A. Bonilla Rodríguez, & R. Fábregas Valcarce (Eds.), *Círculo de engaños: Excavación de A mourela (as pontes de garcía rodríguez, A coruña)* (pp. 37-58)

Vuorinen, H. S., Pihlman, S., Mussalo-Rauhamaa, H., Tapper, U., & Varrela, T. (1996). Trace and heavy metal analyses of a skeletal population representing the town people in Turku (Abo), Finland in the 16th-17th centuries: With special reference to sex, age, and social background. *Science Total Environment*, *177*, 145-160.

Wadleigh, M. A., Veizer, J., & Brooks, C. (1985). Strontium and its isotopes in Canadian rivers - fluxes and global implications. *Geochimica et Cosmochimica Acta*, *8*(1), 1727-1736.

Walker, M. J. (1983). Laying a mega-mith: Dolmens and drovers in prehistoric Spain. *World Archaeology 1: Transhumance and Pastoralism, 15*, 37-50.

Waterman, A. J., Peate, D. W., Silva, A. M., & Thomas, J. T. (2014). In search of homelands: Using strontium isotopes to identify biological markers of mobility in late prehistoric Portugal. *Journal of Archaeological Science*, *42*, 119-127.

White, C. D., Price, T. D., & Longstaffe, F. J. (2007). Residential histories of the human sacrifices at the moon pyramid, Teotihuacan: Evidence from oxygen and strontium isotopes. *Ancient Mesoamerica, 18*(1), 159-172.

Wright, L. E. (2005). Identifying immigrants to Tikal, Guatemala: Defining local variability in strontium isotope ratios of human tooth enamel. *Journal of Archaeological Science, 32*(4), 555-566.

Wright, L. E., & Schwarcz, H. P. (1996). Infrared and isotopic evidence for diagenesis of bone apatite at dos Pilas, Guatemala: paleodietary implications. *Journal of Archaeological Science, 23*(6), 933-944.

Appendix I

Data Tables

A1 Original Camino del Molino data table

A2 MC-ICP-MS sample sequence and run results

A3 Table of the corrected $^{87}Sr/^{86}Sr$ sample ratios and the calibrated sample Sr concentrations

A4 Table of $^{87}Sr/^{86}Sr$ ratio and Sr conc differences between the first run and the rerun

A1 Original Camino del Molino data table

The original Camino del Molino human and fauna data given with the samples and the MARC number assigned to each of the sample enamel and dentine samples taken. Note the underlined MARC Dentine numbers denote the ten samples randomly chosen for Sr analysis.

Sample no	Site	Period	Local Code	Sex	Age	Tooth	Radio Carbon Dates	MARC Dentine	MARC Enamel
1	CMol	Calcolithic	Sujeto 3 Cuadro 71	N	Adult	P2 upper left		558	559
2	CMol	Calcolithic	Sujeto 4 Cuadro 112	N	Adult	P1 lower right		562	563
3	CMol	Calcolithic	Sujeto 6 Cuadro 194	F	20-28	P1 upper right	3910 +/-40BP	566	567
4	CMol	Calcolithic	Sujeto 7 Cuadro 320	M	20-23	I2 upper left	3910 +/-40BP	570	571
5	CMol	Calcolithic	Sujeto 8 Cuadro 216	N	Adult	M1 upper left		574	575
6	CMol	Calcolithic	Sujeto 9 Cuadro 210	N	Adult	P1 upper right		578	579
7	CMol	Calcolithic	Sujeto 10 Cuadro 209	Alofiso	14-18	M1 lower right		582	583
8	CMol	Calcolithic	Sujeto 11 Cuadro 219	N	Adult	P2 upper right		586	587
9	CMol	Calcolithic	Sujeto 12 Cuadro 273	M	33-24	C upper left	3970 +/-40BP	590	591
10	CMol	Calcolithic	Sujeto 16 Cuadro 280	F	20-35	P1 upper left		594	595
11	CMol	Calcolithic	Sujeto 17 Cuadro 318	M	43-55	I2 lower left		598	599
12	CMol	Calcolithic	Sujeto 20 Cuadro 338	N	Adult	P1 upper left		602	603
13	CMol	Calcolithic	Sujeto 21 Cuadro 361	M	30-40	P2 upper left	3920 +/-BP	606	607
14	CMol	Calcolithic	Sujeto 24 Cuadro 384	N	Adult	P2 upper right		610	611
15	CMol	Calcolithic	Sujeto 25 Cuadro 399	N	Adult	P2 upper right		614	615
16	CMol	Calcolithic	Sujeto 26 Cuadro 401	N	Adult	M1 lower left		618	619
17	CMol	Calcolithic	Sujeto 27 Cuadro 412	N	Adult	P1 upper left		622	623
18	CMol	Calcolithic	Sujeto 28 Cuadro 358bis	M	20-24	I2 upper left		626	627
19	CMol	Calcolithic	Sujeto 29 Cuadro 440	Indet.	(9-10)	P1 upper left		630	631
20	CMol	Calcolithic	Sujeto 30 Cuadro 455	N	Adult	P1 lower left		634	635
21	CMol	Calcolithic	Sujeto 35 Cuadro 513	N	Adult	P2 upper right		638	639
22	CMol	Calcolithic	Sujeto 40 Cuadro 551	N	Adult	P1 upper left		642	643
23	CMol	Calcolithic	Sujeto 41 Cuadro 543	N	Adult	P1 lower left		646	647
24	CMol	Calcolithic	Sujeto 43 Cuadro 577	N	Adult	dM1 upper left		650	651
25	CMol	Calcolithic	Sujeto 44 Cuadro 575	M	24-28	P2 upper left		654	655
26	CMol	Calcolithic	Sujeto 49 Cuadro 590	N	Adult	P1 upper right		658	659
27	CMol	Calcolithic	Sujeto 53 Cuadro 634	N	Adult	P2 upper right		662	663
28	CMol	Calcolithic	Sujeto 54 Cuadro 643	N	Adult	dM1 lower right		666	667
29	CMol	Calcolithic	Sujeto 55 Cuadro 657	N	Adult	P2 upper right		670	671
30	CMol	Calcolithic	Sujeto 56 Cuadro 658	N	Adult	P1 upper right		674	675
31	CMol	Calcolithic	Sujeto 59 Cuadro 676	N	Adult	P1 upper left		678	679
32	CMol	Calcolithic	Sujeto 60 Cuadro 680	N	Adult	P2 upper left		682	683
33	CMol	Calcolithic	Sujeto 61 Cuadro 690	N	Adult	P1 upper left		686	687
34	CMol	Calcolithic	Sujeto 63 Cuadro 753	N	Adult	C upper left		690	691
35	CMol	Calcolithic	Sujeto 67 Cuadro 723	N	Adult	P1 upper right		694	695
36	CMol	Calcolithic	Sujeto 68 Cuadro 734	N	Adult	P1 upper left		698	699
37	CMol	Calcolithic	Sujeto 71 Cuadro 800	M	>45	P1 upper right		702	703
38	CMol	Calcolithic	Sujeto 72 Cuadro 817	N	Adult	P1 upper right		706	707
39	CMol	Calcolithic	Sujeto 79 Cuadro 857	M	35-45	P1 upper left	3730 +/-40BP	710	711
40	CMol	Calcolithic	Sujeto 81 Cuadro 887	F	25-30	P1 lower left		714	715

Sample no	Site	Period	Local Code	Sex	Age	Tooth	Radio Carbon Dates	MARC Dentine	MARC Enamel
41	CMol	Calcolithic	Sujeto 83 Cuadro 894	N	Adult	P1 upper left		718	719
42	CMol	Calcolithic	Sujeto 84 Cuadro 915	M	20-28	P1 upper left		722	723
43	CMol	Calcolithic	Sujeto 87 Cuadro 959	N	Adult	M1 upper left		726	727
44	CMol	Calcolithic	Sujeto 88 Cuadro 992	N	Adult	I1 upper left		730	731
45	CMol	Calcolithic	Sujeto 92 Cuadro 965	N	Adult	dI1 upper right		734	735
46	CMol	Calcolithic	Sujeto 100 Cuadro 1031	M	20-23	P1 upper left	4140 +/-BP	738	739
47	CMol	Calcolithic	Sujeto 101 Cuadro 1031	Alofiso	10	dM1 upper right		742	743
48	CMol	Calcolithic	Sujeto 103 Cuadro 1039	N	Juvenile	dM1 upper left		746	747
49	CMol	Calcolithic	Sujeto 104 Cuadro 1041	M	Adult	P1 upper left		750	751
50	CMol	Calcolithic	Sujeto 105 Cuadro 1043	M	33-35	P1 upper left	4130 +/-BP	754	755
51	CMol	Calcolithic	Sujeto 106 Cuadro 1082	N	Adult	P1 upper left		758	759
52	CMol	Calcolithic	Sujeto 108 Cuadro 1072	M	35-39	P1 upper right	4160 +/-BP	762	763
53	CMol	Calcolithic	Sujeto 109 Cuadro 1068	F	33-42	P2 upper right		766	767
54	CMol	Calcolithic	Sujeto 110 Cuadro 1077	F	20-45	P2 upper right		770	771
55	CMol	Calcolithic	Sujeto 112 Cuadro 1094	F	20-25	P1 upper right		774	775
56	CMol	Calcolithic	Sujeto 113 Cuadro 1095	F	24-28	P1 lower right		778	779
57	CMol	Calcolithic	Sujeto 117 Cuadro 1119	N	Adult	P1 upper right		782	783
58	CMol	Calcolithic	Sujeto 119 Cuadro 1127	M	55	P1 lower left		786	787
59	CMol	Calcolithic	Sujeto 122 Cuadro 1132	F	20-21	P1 upper right		790	791
60	CMol	Calcolithic	Sujeto 123 Cuadro 1568	M	25-30	M3 upper left	4210 +/-BP	794	795
61	CMol	Calcolithic	Sujeto 124 Cuadro 1160	N	Adult	C upper right		798	799
62	CMol	Calcolithic	Sujeto 125 Cuadro 1205	N	Adult	P2 upper left		802	803
63	CMol	Calcolithic	Sujeto 126 Cuadro 1184	Alofiso	14-18	P1 upper left		806	807
64	CMol	Calcolithic	Sujeto 127 Cuadro 1192	Alofiso	(3-4)	M1 lower left		810	811
65	CMol	Calcolithic	Sujeto 129 Cuadro 1228	F	20-22	P1 lower right		814	815
66	CMol	Calcolithic	Sujeto 131 Cuadro 1248	F	20-23	P2 upper right		818	819
67	CMol	Calcolithic	Sujeto 132 Cuadro 1258	M	33-45	M3 upper right		822	823
68	CMol	Calcolithic	Sujeto 133 Cuadro 1255	F	25-30	M3 upper left		826	827
69	CMol	Calcolithic	Sujeto 136 Cuadro 1269	M	20-30	P1 upper left		830	831
70	CMol	Calcolithic	Sujeto 137 Cuadro 1272	M	20-25	C upper left		834	835
71	CMol	Calcolithic	Sujeto 138 Cuadro 1283	F	15-22	P1 upper left		838	839
72	CMol	Calcolithic	Sujeto 139 Cuadro 1289	F	25	P1 lower left		842	843
73	CMol	Calcolithic	Sujeto 140 Cuadro 1298	M	35-45	P1 upper left		846	847
74	CMol	Calcolithic	Sujeto 142 Cuadro 1323	Indet.	(3-4)	M1 upper left		850	851
75	CMol	Calcolithic	Sujeto 143 Cuadro 1346	N	Adult	P2 upper right		854	855
76	CMol	Calcolithic	Sujeto 151 Cuadro 1460	M	30-35	P1 lower right		858	859
77	CMol	Calcolithic	Sujeto 145 Cuadro 1374	M	24-30	I1 upper right		862	863
78	CMol	Calcolithic	Sujeto 150 Cuadro 1423	M	22-24	P1 upper left		866	867
79	CMol	Calcolithic	Sujeto 154 Cuadro 1447	F	33-42	P1 upper left		870	871
80	CMol	Calcolithic	Sujeto 155 Cuadro 1475	Alofiso	11	P1 upper left		874	875

Sample no	Site	Period	Local Code	Sex	Age	Tooth	Radio Carbon Dates	MARC Dentine	MARC Enamel
81	CMol	Calcolithic	Sujeto 158 Cuadro 1533	*	*	P1 upper left		878	879
82	CMol	Calcolithic	Sujeto 161 Cuadro 1552	F	25-35	P2 upper left		882	883
83	CMol	Calcolithic	Sujeto 162 Cuadro 1577	N	Adult	dM2 lower left		886	887
84	CMol	Calcolithic	Sujeto 164 Cuadro 1599	M	45-55	P2 upper right		890	891
85	CMol	Calcolithic	Sujeto 165 Cuadro 1598	M	25-30	P2 upper right		894	895
86	CMol	Calcolithic	Sujeto 166 Cuadro 1614	M	17-21	P2 upper right		898	899
87	CMol	Calcolithic	Sujeto 167 Cuadro 1640	N	Adult	M1 upper right		902	903
88	CMol	Calcolithic	Sujeto 168 Cuadro 1657	F	14-18	M2 upper right		906	907
89	CMol	Calcolithic	Sujeto 169 Cuadro 1674	F	40-55	P1 upper left		910	911
90	CMol	Calcolithic	Sujeto 170 Cuadro 1678	M	43-55	P2 upper right		914	915
91	CMol	Calcolithic	Sujeto 173 Cuadro 1696	F	15-18	P1 upper left		918	919
92	CMol	Calcolithic	Sujeto 172 Cuadro 1682	Indet.	(7-9)	M2 lower right		922	923
93	CMol	Calcolithic	Sujeto 13 Cuadro 292	Alophys	>45yo	M1 lower right		926	927
94	CMol	Calcolithic	Conejo Criba Cuadr 1672	*	*	Many teeth		1144	
95	CMol	Calcolithic	Micro Criba Cuadro 1135	*	*	Many teeth		1146	
96	CMol	Calcolithic	Conejo Criba Cuadr 1666	*	*	Many teeth		1147	
97	CMol	Calcolithic	Micro Criba Cuadro 1408	*	*	Many teeth		N/A	
98	CMol	Calcolithic	Conejo Cuadro 1093	*	*	Many teeth		1150	
99	CMol	Calcolithic	Micro Criba Cuadro 1340	*	*	1 Tooth		1152	
100	CMol	Calcolithic	Micro Criba Cuadro 1052	*	*	Many teeth		1153	
101	CMol	Calcolithic	Lagarto Crib Limpiez sol	*	*	Many teeth		1154	
102	CMol	Calcolithic	Micro Criba Cuadro 1150	*	*	Many teeth		1155	
103	CMol	Calcolithic	Micro Criba Cuadro 1142	*	*	1 Tooth		1156	
104	CMol	Calcolithic	Ovicaprido Cuadro 388	*	*	1 Tooth		1157	
105	CMol	Calcolithic	Ovicaprido Cuadro 550	*	*	2 Teeth		1159	
106	CMol	Calcolithic	Ovicaprido Cuadro 316	*	*	2 Teeth		1161	
107	CMol	Calcolithic	Ovicaprido Cuadro 1042	*	*	1 Tooth		1163	
108	CMol	Calcolithic	Canido Cuadro 308	*	*	1 Tooth		1165	
109	CMol	Calcolithic	Canido Cuadro 360	*	*	1 Tooth		1167	
110	CMol	Calcolithic	Canido Cuadro 600	*	*	1 Tooth		1169	
111	CMol	Calcolithic	Ovicaprido Cuadro 323	*	*	2 Teeth		1171	
112	CMol	Calcolithic	Canido Criba Sector Nort	*	*	2 Teeth		1173	
113	CMol	Calcolithic	Canido Cuadro 511	*	*	2 Teeth		1175	
114	CMol	Calcolithic	Canido Cuadro 471	*	*	1 Tooth		1177	
115	CMol	Calcolithic	Canido Cuadro 394	*	*	1 Tooth		1179	
116	CMol	Calcolithic	Lagarto Crib Cuadr 1052	*	*	Many teeth		1181	
117	CMol	Calcolithic	Lagarto Crib Cuadr 1150	*	*	2 Teeth		1182	
118	CMol	Calcolithic	Canido Crib Cuadr 1142	*	*	1 Tooth		1183	
119	CMol	Calcolithic	Cerdo Criba Cuadro 1142	*	*	1 Tooth		1184	

A2 MC-ICP-MS sample sequence and results

The data table shows the sample sequence, including standards and procedural blanks, and the sample Sr results data from the first Neptune mass spectrometer run of the Camino del Molino samples.

Date	02-Feb-12	**Operator**	C. Merner
Nebulizer	100µl PFA neb	**Start Time**	10:15am
Spray chamber	ESI SIS	**End Time**	6:50am (03-Feb-12)
Method		**No. Standards**	13
Tune file		**No. Samples**	
Acquisition	1 block of 50 cycles; 2 sec integration		

Run no.	Standard/Sample	Name	^{88}Sr int (V)	^{85}Rb Int (V)	Rb/Sr (%)	^{84}Sr/^{86}Sr	^{87}Sr/^{86}Sr	1SE	Comments
1	Std	MAF-11C 987	11.5	0.000138	0.0012	0.05648	0.710291	0.000011	200ppb
2	Std	MAF-11C 987	11	0.000044	0.0004	0.056503	0.710263	0.000012	200ppb
3	Std	MAF-11C 987	10.9	0.000025	0.0002	0.056561	0.71026	0.000011	200ppb
4	Sample	MARC 558	16.6	0.000509	0.0031	0.056493	0.707869	0.000008	
5	Sample	MARC 562	9	0.000695	0.0077	0.056481	0.708923	0.000016	
6	Sample	MARC 563	7.5	0.000891	0.0118	0.056518	0.708113	0.000012	
7	Sample	MARC 566	6	0.001343	0.0223	0.056437	0.712976	0.000015	
8	Sample	MARC 570	18.4	1.523268	8.2823	0.056502	0.708304	0.000007	
9	Sample	MARC 574	6.4	0.000539	0.0084	0.05646	0.708633	0.000012	
10	Sample	MARC 578	8.5	0.00049	0.0058	0.056424	0.710678	0.000013	
11	Sample	MARC 582	9.1	0.000446	0.0049	0.05647	0.708769	0.000013	
12	Sample	MARC 586	11.7	0.000316	0.0027	0.056484	0.713174	0.000009	
13	Sample	MARC 590	4.6	0.000401	0.0087	0.056443	0.713066	0.00002	
14	Std	MAF-11C 987	10.7	0.000028	0.0003	0.056493	0.710281	0.000013	200ppb
15	Blk	AB1	0	0.000124	2.692	-0.088087	0.76529	0.010409	
16	Sample	MARC 594	5.9	0.00042	0.0071	0.056513	0.709006	0.000014	
17	Sample	MARC 598	7.2	0.000576	0.008	0.056463	0.709935	0.000013	
18	Sample	MARC 602	6	0.00136	0.0228	0.056614	0.715051	0.000014	
19	Sample	MARC 606	14	0.000719	0.0051	0.056501	0.709754	0.000008	
20	Sample	MARC 607	3.2	0.000505	0.0158	0.056379	0.708309	0.000027	
21	Sample	MARC 610	15.6	0.000317	0.002	0.056538	0.70838	0.000008	
22	Sample	MARC 614	7.5	0.001558	0.0209	0.05652	0.707896	0.000015	
23	Sample	MARC 618	8.6	0.000268	0.0031	0.056531	0.708347	0.000016	
24	Sample	MARC 622	2.9	0.000762	0.0262	0.05683	0.708533	0.000025	
25	Sample	MARC 626	10	0.005858	0.0588	0.056506	0.71334	0.00001	
26	Std	MAF-11C 987	10.9	0.000044	0.0004	0.056477	0.710272	0.000011	200ppb
27	Blk	AB2	0	0.000098	3.2479	0.048442	0.731092	0.014057	
28	Sample	MARC 630	7.3	0.007157	0.0976	0.056553	0.708403	0.000014	
29	Sample	MARC 634	15.2	0.000501	0.0033	0.056528	0.707961	0.001444	
30	Sample	MARC 638	5.2	0.000462	0.0088	0.05652	0.708001	0.000019	
31	Sample	MARC 642	3.6	0.000411	0.0114	0.056479	0.709142	0.000026	
32	Sample	MARC 646	13.5	0.000429	0.0032	0.056513	0.712315	0.000011	
33	Sample	MARC 650	5.3	0.00097	0.0183	0.056601	0.707944	0.000016	

Run no.	Standard/Sample	Name	^{88}Sr int (V)	^{85}Rb Int (V)	Rb/Sr (%)	^{84}Sr/^{86}Sr	^{87}Sr/^{86}Sr	1SE	Comments
34	Sample	MARC 654	19	0.000672	0.0035	0.056491	0.708527	0.000007	
35	Sample	MARC 655	11.8	0.000325	0.0028	0.056509	0.70804	0.00001	
36	Sample	MARC 658	8.2	0.000469	0.0057	0.056498	0.708448	0.000014	
37	Sample	MARC 662	16	0.000586	0.0037	0.056509	0.707849	0.000009	
38	Std	MAF-11C 987	10.8	0.000035	0.0003	0.056545	0.710281	0.00001	200ppb
39	Blk	AB3	0	0.000237	4.8687	0.115971	0.742234	0.009531	
40	Sample	MARC 666	3.6	0.000559	0.0156	0.056578	0.708099	0.000021	
41	Sample	MARC 670	12.6	0.000256	0.002	0.056525	0.708	0.00001	
42	Sample	MARC 674	6.9	0.000253	0.0037	0.05648	0.70832	0.000014	
43	Sample	MARC 678	4.1	0.000812	0.0199	0.05658	0.709009	0.00002	
44	Sample	MARC 682	6.2	0.009772	0.1575	0.056554	0.708833	0.000015	
45	Sample	MARC 686	6.9	0.016569	0.2394	0.056508	0.710363	0.000014	
46	Sample	MARC 690	8.5	0.000606	0.0072	0.056486	0.710044	0.000013	
47	Sample	MARC 694	9	0.000303	0.0034	0.056446	0.713522	0.000012	
48	Sample	MARC 698	16.8	0.000457	0.0027	0.056479	0.708333	0.000009	
49	Sample	MARC 702	4.1	0.003691	0.0908	0.056488	0.712852	0.000017	
50	Std	MAF-11C 987	11	0.000036	0.0003	0.056522	0.710307	0.000011	200ppb
51	Blk	AB4	0	0.000191	4.5646	0.160345	0.753421	0.012588	
52	Sample	MARC 706	5.8	0.00035	0.006	0.05649	0.711251	0.000016	
53	Sample	MARC 707	12.2	0.000369	0.003	0.056497	0.708522	0.000011	
54	Sample	MARC 710	11.4	0.000462	0.004	0.056484	0.708117	0.000011	
55	Sample	MARC 714	5	0.001498	0.0301	0.056458	0.708192	0.000022	
56	Sample	MARC 718	10.7	0.000923	0.0086	0.05649	0.708408	0.00001	
57	Sample	MARC 722	5.3	0.000508	0.0096	0.056442	0.709525	0.000015	
58	Sample	MARC 723	27.4	0.000592	0.0022	0.056493	0.708025	0.000007	
59	Sample	MARC 726	2.8	0.000373	0.0131	0.056502	0.709046	0.000022	
60	Sample	MARC 730	9.7	0.000422	0.0043	0.056474	0.708144	0.00001	
61	Sample	MARC 734	4.1	0.000533	0.013	0.056516	0.707985	0.000019	
62	Std	MAF-11C 987	10.9	0.000018	0.0002	0.056539	0.710261	0.00001	200ppb
63	Blk	AB5	0	0.000602	4.5068	0.119539	0.712753	0.00369	
64	Sample	MARC 738	17.6	0.001144	0.0065	0.056483	0.708536	0.00001	
65	Sample	MARC 742	5.2	0.000494	0.0094	0.056537	0.708502	0.000018	
66	Sample	MARC 746	5	0.000482	0.0096	0.056708	0.707904	0.000014	
67	Sample	MARC 750	29.1	0.000238	0.0008	0.05648	0.708498	0.000006	
68	Sample	MARC 754	10.8	0.000418	0.0039	0.056515	0.708275	0.000009	
69	Std	MAF-11C 987	10.9	0.000029	0.0003	0.056555	0.710251	0.000013	200ppb
70	Std	MAF-11C 987	10.8	0.000027	0.0003	0.056523	0.710269	0.000011	200ppb
71	Std	MAF-11C 987	10.6	0.000033	0.0003	0.05651	0.710256	0.000011	200ppb
72	Sample	MARC 758	10.3	0.000338	0.0033	0.05656	0.710382	0.00001	
73	Sample	MARC 762	8.7	0.000549	0.0063	0.056534	0.70818	0.000014	
74	Sample	MARC 766	4.5	0.000457	0.0103	0.056667	0.708081	0.000017	
75	Sample	MARC 767	24.1	0.000856	0.0035	0.056521	0.707947	0.000008	
76	Sample	MARC 770	3.1	0.013438	0.4372	0.05665	0.708113	0.000023	
77	Sample	MARC 774	5.7	0.000389	0.0068	0.056502	0.708439	0.000015	
78	Sample	MARC 778	1.3	0.0015	0.1155	0.056335	0.708989	0.000044	

Run no.	Standard/Sample	Name	^{88}Sr int (V)	^{85}Rb Int (V)	Rb/Sr (%)	$^{84}Sr/^{86}Sr$	$^{87}Sr/^{86}Sr$	1SE	Comments
79	Sample	MARC 782	5.7	0.001155	0.0203	0.056611	0.708416	0.000016	
80	Sample	MARC 786	2.1	0.002044	0.0991	0.056537	0.708605	0.000034	
81	Sample	MARC 790	18.7	0.002592	0.0138	0.056496	0.707664	0.000009	
82	Std	MAF-11C 987	11.2	0.000016	0.0001	0.05657	0.710263	0.000012	200ppb
83	Blk	AB6	0	0.001984	19.9515	0.124658	0.754058	0.006121	
84	Sample	MARC 794	14.4	0.000389	0.0027	0.056529	0.709586	0.000009	
85	Sample	MARC 798	2.5	0.000656	0.0266	0.056659	0.70846	0.000022	
86	Sample	MARC 802	2.3	0.000647	0.0284	0.056572	0.70876	0.000029	
87	Sample	MARC 806	11.2	0.000657	0.0058	0.056487	0.708469	0.000012	
88	Sample	MARC 807	29.7	0.000261	0.0009	0.056522	0.708005	0.000006	
89	Sample	MARC 810	4.8	0.000504	0.0106	0.056535	0.708049	0.000017	
90	Sample	MARC 814	3.7	0.00088	0.0241	0.056521	0.708018	0.000022	
91	Sample	MARC 818	5.5	0.000277	0.005	0.0566	0.721	0.000017	
92	Sample	MARC 822	9	0.000521	0.0058	0.056532	0.707909	0.000013	
93	Sample	MARC 826	10.2	0.000638	0.0063	0.056526	0.708007	0.000011	
94	Blk	AB7	0	0.00025	3.1732	0.092657	0.736497	0.00542	
95	Sample	MARC 830	4.9	0.001074	0.022	0.056623	0.709527	0.000016	
96	Sample	MARC 834	2.3	0.000454	0.0202	0.056376	0.708899	0.000024	
97	Sample	MARC 838	17	0.001079	0.0063	0.05651	0.708187	0.000008	
98	Sample	MARC 842	4.3	0.000678	0.0159	0.056496	0.708137	0.000022	
99	Sample	MARC 846	9.5	0.00024	0.0025	0.05649	0.707933	0.000015	
100	Sample	MARC 850	8.4	0.000735	0.0087	0.056492	0.708011	0.000014	
101	Sample	MARC 854	13.5	0.000529	0.0039	0.05648	0.708212	0.000012	
102	Sample	MARC 858	4.7	0.000462	0.0098	0.056418	0.708629	0.000018	
103	Sample	MARC 862	6.8	0.001178	0.0173	0.056389	0.708465	0.000016	
104	Sample	MARC 866	3.3	0.000526	0.0158	0.056627	0.708237	0.000025	
105	Std	MAF-11C 987	11.5	0.00001	0.0001	0.056493	0.710263	0.000011	200ppb
106	Blk	AB8	0	0.000461	5.6902	0.102109	0.727617	0.004622	
107	Sample	MARC 867	8.5	0.000394	0.0046	0.056456	0.708051	0.000014	
108	Sample	MARC 870	1.8	0.000358	0.0199	0.05664	0.712953	0.000035	
109	Sample	MARC 874	1.2	0.000418	0.0337	0.056101	0.708269	0.000048	
110	Sample	MARC 878	1.8	0.000247	0.0135	0.056463	0.708385	0.000039	
111	Sample	MARC 882	3.3	0.000184	0.0055	0.056545	0.708544	0.000023	
112	Sample	MARC 886	2.6	0.000194	0.0074	0.05659	0.708234	0.000029	
113	Sample	MARC 887	6.4	0.000368	0.0057	0.05643	0.707962	0.000013	
114	Sample	MARC 890	4.2	0.000199	0.0048	0.056553	0.709046	0.000023	
115	Sample	MARC 894	2.1	0.000213	0.0099	0.056545	0.710626	0.00003	
116	Sample	MARC 898	0.5	0.000113	0.0213	0.05576	0.709076	0.000096	
117	Blk	AB9	0	0.00053	10.7295	-0.143944	0.816486	0.011915	
118	Sample	MARC 902	1.8	0.00019	0.0105	0.056351	0.708832	0.000041	
119	Sample	MARC 906	5.9	0.000179	0.003	0.056522	0.707998	0.000014	
120	Sample	MARC 910	5.5	0.003054	0.0554	0.056497	0.70791	0.000016	

Run no.	Standard/Sample	Name	^{88}Sr int (V)	^{85}Rb Int (V)	Rb/Sr (%)	$^{84}Sr/^{86}Sr$	$^{87}Sr/^{86}Sr$	1SE	Comments
121	Sample	MARC 911	1.3	0.000864	0.0644	0.056625	0.708047	0.000031	
122	Sample	MARC 914	4.6	0.000636	0.0137	0.056693	0.708673	0.000021	
123	Sample	MARC 918	8.2	0.000329	0.004	0.056509	0.707956	0.000014	
124	Sample	MARC 922	4.1	0.000351	0.0085	0.056323	0.708022	0.000021	
125	Sample	MARC 926	5.4	0.000362	0.0067	0.056541	0.708193	0.000018	
126	Sample	MARC 1146	34.6	0.000668	0.0019	0.056493	0.707909	0.000005	
127	Sample	MARC 1147	22.5	0.000383	0.0017	0.056512	0.707911	0.000009	

A3 Table of the corrected $^{87}Sr/^{86}Sr$ sample ratios and the calibrated sample Sr concentrations

The Sr ratio correction and Sr concentration calibration methods and corresponding tables follow the corrected $^{87}Sr/^{86}Sr$ and calibrated Sr concentration (ppm) results table.

Sample MARC No	$^{87}Sr/^{86}Sr$ Corr	Sr conc (ppm)
558	0.707830	242
562	0.708884	162
563	0.708074	208
566	0.712937	122
570	0.708264	348
574	0.708594	125
578	0.710639	148
582	0.708730	98
586	0.713135	296
590	0.713027	103
594	0.708967	115
602	0.709895	117
602	0.715012	74
606	0.709715	214
607	0.708269	145
610	0.708340	305
614	0.707857	102
618	0.708307	114
622	0.708494	52
626	0.713301	107
630	0.708364	98
634	0.707922	244
638	0.707961	55
642	0.709103	52
646	0.712275	231
650	0.707904	109
654	0.708487	293
655	0.708000	273
658	0.708409	128
662	0.707810	326
666	0.708060	68
670	0.707960	154
674	0.708280	86
678	0.708970	59
682	0.708794	133
686	0.710323	88
690	0.710004	75

Sample MARC No	$^{87}Sr/^{86}Sr$ Corr	Sr conc (ppm)
694	0.713483	98
698	0.708293	184
702	0.712812	59
706	0.711212	86
707	0.708483	223
710	0.708077	154
714	0.708153	97
718	0.708369	203
722	0.709486	87
723	0.707986	466
726	0.709007	48
730	0.708105	220
734	0.707946	151
738	0.708497	397
742	0.708463	120
746	0.707865	96
750	0.708459	371
754	0.708236	330
758	0.710343	104
762	0.708140	197
766	0.708042	123
767	0.707908	368
770	0.708074	62
774	0.708400	104
778	0.708950	24
782	0.708376	132
786	0.708565	34
790	0.707625	311
794	0.709547	271
798	0.708421	31
802	0.708721	30
806	0.708430	164
807	0.707966	360
810	0.708009	80
814	0.707979	95
818	0.720961	117
822	0.707870	117

Sample MARC No	$^{87}Sr/^{86}Sr$ Corr	Sr conc (ppm)
826	0.707967	108
830	0.709487	63
834	0.708860	45
838	0.708148	184
842	0.708098	58
846	0.707894	214
850	0.707972	163
854	0.708173	269
858	0.708590	86
862	0.708425	99
866	0.708198	47
867	0.708012	140
870	0.712914	44
874	0.708229	50
878	0.708346	43
882	0.708504	69
886	0.708195	62
887	0.707922	217
890	0.709007	91
894	0.710586	40
898	0.709037	13
902	0.708793	42
906	0.707959	147
910	0.707871	115
911	0.708007	27
914	0.708634	78
918	0.707917	143
922	0.707982	96
926	0.708153	107
1146	0.707870	540
1147	0.707871	538
1150	0.707913	438
1152	0.707897	380
1153	0.707897	574
1154	0.707898	415
1155	0.707867	789

Sample $^{87}Sr/^{86}Sr$ ratios were corrected to the standard SRM 987. Each sample's $^{87}Sr/^{86}Sr$ result was subtracted by 0.000039, the average difference between the SRM 987 $^{87}Sr/^{86}Sr$ results and their real value (0.710240).

	$^{87}Sr/^{86}Sr$	**Real Value**	**Difference**
SRM987	0.710291	0.710240	0.000051
	0.710263	0.710240	0.000023
	0.710260	0.710240	0.000020
	0.710281	0.710240	0.000041
	0.710272	0.710240	0.000032
	0.710281	0.710240	0.000041
	0.710307	0.710240	0.000067
	0.710261	0.710240	0.000021
	0.710251	0.710240	0.000011
	0.710269	0.710240	0.000029
	0.710256	0.710240	0.000016
	0.710263	0.710240	0.000023
	0.710263	0.710240	0.000023
Ave	**0.710279**	**0.710240**	**0.000039**

Sample concentrations were calibrated by:

1. Find the average SRM 987 sample ^{88}Sr (V) signal intensity (= 11 V).
2. Divide the SRM 987 Sr standard concentration (200 ppb) by this SRM 987 ^{88}Sr (V) average (11 V) to obtain a Factor (= 18.2).
3. Correct each sample using this Factor.
4. Multiply each sample's ^{88}Sr (V) by the Factor to obtain the concentration of the analyte.
5. Divide each sample's concentration of the analyte by its dilution factor to obtain the Off column concentration.
   (The dilution factor is the same across the run = 0.125)
6. Divide each sample's Off column concentration by the sample's mass to obtain the calibrated sample concentration (ppm).
   (The mass of each sample was weighed and recorded at the radiogenic lab prior to its column chemistry.)

Sample MARC No	Int ^{88}Sr (V)	Conc of Analyte	Dilution Factor	Off column conc	Mass of sample (mg)	Sample conc (ppm)	Corr Sr conc (ppm)
558	16.6	302	0.125	2418	16.65	145	242
562	9.0	164	0.125	1311	13.46	97	162
563	7.5	137	0.125	1095	8.76	125	208
566	6.0	110	0.125	877	11.98	73	122
570	18.4	335	0.125	2676	12.82	209	348
574	6.4	117	0.125	935	12.51	75	125
578	8.5	155	0.125	1238	13.98	89	148
582	9.1	166	0.125	1328	22.66	59	98
586	11.7	213	0.125	1705	9.61	177	296
590	4.6	84	0.125	673	10.89	62	103
594	5.9	107	0.125	859	12.4	69	115
602	7.2	131	0.125	1049	14.93	70	117
602	6.0	108	0.125	867	19.59	44	74
606	14.0	255	0.125	2038	15.87	128	214
607	3.2	58	0.125	463	5.33	87	145
610	15.6	284	0.125	2271	12.4	183	305
614	7.5	136	0.125	1086	17.7	61	102
618	8.6	156	0.125	1252	18.3	68	114
622	2.9	53	0.125	423	13.66	31	52
626	10.0	181	0.125	1449	22.66	64	107
630	7.3	133	0.125	1067	18.22	59	98
634	15.2	277	0.125	2212	15.11	146	244
638	5.2	95	0.125	760	22.93	33	55
642	3.6	66	0.125	524	16.86	31	52
646	13.5	245	0.125	1962	14.17	138	231
650	5.3	96	0.125	770	11.72	66	109
654	19.0	345	0.125	2762	15.72	176	293
655	11.8	214	0.125	1712	10.45	164	273

Sample MARC No	Int ^{88}Sr (V)	Conc of Analyte	Dilution Factor	Off column conc	Mass of sample (mg)	Sample conc (ppm)	Corr Sr conc (ppm)
658	8.2	150	0.125	1199	15.55	77	128
662	16.0	291	0.125	2329	11.9	196	326
666	3.6	65	0.125	521	12.73	41	68
670	12.6	230	0.125	1840	19.93	92	154
674	6.9	126	0.125	1006	19.38	52	86
678	4.1	74	0.125	593	16.72	35	59
682	6.2	113	0.125	903	11.31	80	133
686	6.9	126	0.125	1007	19.12	53	88
690	8.5	154	0.125	1232	27.52	45	75
694	9.0	164	0.125	1309	22.16	59	98
698	16.8	305	0.125	2442	22.12	110	184
702	4.1	74	0.125	591	16.81	35	59
706	5.8	106	0.125	845	16.38	52	86
707	12.2	221	0.125	1769	13.23	134	223
710	11.4	208	0.125	1663	18.05	92	154
714	5.0	91	0.125	725	12.51	58	97
718	10.7	195	0.125	1563	12.82	122	203
722	5.3	97	0.125	772	14.87	52	87
723	27.4	498	0.125	3982	14.23	280	466
726	2.8	52	0.125	414	14.48	29	48
730	9.7	177	0.125	1416	10.74	132	220
734	4.1	74	0.125	596	6.56	91	151
738	17.6	320	0.125	2563	10.76	238	397
742	5.2	95	0.125	762	10.6	72	120
746	5.0	91	0.125	730	12.69	57	96
750	29.1	529	0.125	4229	19.02	222	371
754	10.8	196	0.125	1572	7.94	198	330
758	10.3	187	0.125	1497	24.03	62	104
762	8.7	158	0.125	1260	10.64	118	197
766	4.5	81	0.125	648	8.75	74	123
767	24.1	439	0.125	3512	15.9	221	368
770	3.1	56	0.125	447	12.03	37	62
774	5.7	104	0.125	831	13.31	62	104
778	1.3	24	0.125	189	13.2	14	24
782	5.7	103	0.125	827	10.44	79	132
786	2.1	38	0.125	300	14.86	20	34
790	18.7	341	0.125	2728	14.62	187	311
794	14.4	261	0.125	2090	12.83	163	271
798	2.5	45	0.125	359	19.33	19	31
802	2.3	41	0.125	332	18.35	18	30
806	11.2	204	0.125	1635	16.64	98	164
807	29.7	540	0.125	4318	19.98	216	360
810	4.8	87	0.125	692	14.48	48	80
814	3.7	66	0.125	531	9.33	57	95
818	5.5	100	0.125	802	11.46	70	117
822	9.0	164	0.125	1311	18.63	70	117
826	10.2	185	0.125	1483	22.82	65	108

Sample MARC No	Int ^{88}Sr (V)	Conc of Analyte	Dilution Factor	Off column conc	Mass of sample (mg)	Sample conc (ppm)	Corr Sr conc (ppm)
830	4.9	89	0.125	710	18.73	38	63
834	2.3	41	0.125	328	12.04	27	45
838	17.0	310	0.125	2479	22.5	110	184
842	4.3	78	0.125	620	17.97	35	58
846	9.5	172	0.125	1379	10.74	128	214
850	8.4	153	0.125	1224	12.49	98	163
854	13.5	246	0.125	1965	12.19	161	269
858	4.7	86	0.125	688	13.4	51	86
862	6.8	124	0.125	989	16.69	59	99
866	3.3	61	0.125	485	17.35	28	47
867	8.5	155	0.125	1240	14.77	84	140
870	1.8	33	0.125	261	9.81	27	44
874	1.2	23	0.125	180	6.04	30	50
878	1.8	33	0.125	265	10.34	26	43
882	3.3	61	0.125	486	11.73	41	69
886	2.6	48	0.125	383	10.35	37	62
887	6.4	116	0.125	932	7.14	130	217
890	4.2	76	0.125	605	11.03	55	91
894	2.1	39	0.125	313	12.88	24	40
898	0.5	10	0.125	77	10.17	8	13
902	1.8	33	0.125	262	10.31	25	42
906	5.9	108	0.125	864	9.78	88	147
910	5.5	100	0.125	802	11.67	69	115
911	1.3	24	0.125	195	11.91	16	27
914	4.6	84	0.125	675	14.5	47	78
918	8.2	149	0.125	1195	13.91	86	143
922	4.1	75	0.125	604	10.53	57	96
926	5.4	99	0.125	791	12.37	64	107
1146	34.6	630	0.125	5039	15.56	324	540
1147	22.5	409	0.125	3269	10.12	323	538
1150	13.0	236	0.125	1888	7.19	263	438
1152	20.3	369	0.125	2953	12.96	228	380
1153	27.4	498	0.125	3981	11.55	345	574
1154	13.1	239	0.125	1913	7.68	249	415
1155	40.7	740	0.125	5923	12.51	473	789

A4 Table of $^{87}Sr/^{86}Sr$ ratio and Sr conc differences between the first run and the rerun

The samples chosen for the second run were those that had less than 5V signal intensity. The average $^{87}Sr/^{86}Sr$ ratio and Sr concentration difference between the two runs was -0.000010 and 25 ppm.

	Rerun		First Run			
Sample MARC No	Corr $^{87}Sr/^{86}Sr$	Sr conc (ppm)	Corr $^{87}Sr/^{86}Sr$	Sr conc (ppm)	$^{87}Sr/^{86}Sr$ Difference	Sr conc (ppm) Difference
570	0.708251	271	0.708264	348	0.000013	77
590	0.713019	88	0.713027	103	0.000008	15
607	0.708356	133	0.708269	145	-0.000087	12
614	0.707856	30	0.707857	102	0.000001	72
618	0.708301	32	0.708307	114	0.000006	82
622	0.708550	45	0.708494	52	-0.000056	7
642	0.709237	45	0.709103	52	-0.000134	7
666	0.708207	62	0.708060	68	-0.000147	6
678	0.709021	50	0.708970	59	-0.000051	9
702	0.712861	50	0.712812	59	-0.000049	9
726	0.709044	44	0.709007	48	-0.000037	4
734	0.708027	141	0.707946	151	-0.000081	10
766	0.708093	117	0.708042	123	-0.000051	6
770	0.707992	57	0.708074	62	0.000082	5
778	0.708908	22	0.708950	24	0.000042	2
798	0.708460	28	0.708421	31	-0.000039	3
802	0.708857	27	0.708721	30	-0.000136	3
814	0.708081	85	0.707979	95	-0.000102	10
818	0.721132	30	0.720961	117	-0.000171	87
830	0.709574	59	0.709487	63	-0.000087	4
834	0.708961	422	0.708860	45	-0.000101	-377
842	0.708156	51	0.708098	58	-0.000058	7
858	0.708569	71	0.708590	86	0.000021	15
866	0.708152	41	0.709198	47	0.001046	6
870	0.712978	52	0.712914	44	-0.000064	-8
874	0.708111	70	0.708229	50	0.000118	-20
878	0.708441	37	0.708346	43	-0.000095	6
882	0.708583	92	0.708504	69	-0.000079	-23
886	0.708294	87	0.708195	62	-0.000099	-25
890	0.709092	113	0.709007	91	-0.000085	-22
894	0.710653	50	0.710586	40	-0.000067	-10
898	0.708746	16	0.709037	13	0.000291	-3
902	0.708748	55	0.708793	42	0.000045	-13
911	0.708056	28	0.708007	27	-0.000049	-1
914	0.708739	69	0.708634	78	-0.000105	9
922	0.708001	80	0.707982	996	-0.000019	916